Accurate Determination of pH by Use of Ionic Liquid Salt Bridge

Manabu Shibata

2012

Contents

General introduction

Background of this work

The definition of pH

pH is the most widely used measure for the acidity of solutions. Accurate pH measurements are indispensable in many facets of our life and environments. The notional definition[1,2] of pH, which is widely accepted nowadays, is

$$\mathrm{pH} = -\log a_{\mathrm{H^+}} \tag{1}$$

where $a_{\mathrm{H^+}}$ is the activity of hydrogen ions. However, the single ion activity can not be measured without an extrathermodynamic assumption. The reason for the necessity of an extrathermodynamic assumption is illustrated in the following example.[3]

Suppose that we have a cell,

	I	II	III	
Pt	H_2, aq. H^+, Cl^-	SB	aq. H^+, Cl^-, H_2	Pt′

(A)

where SB denotes a salt bridge. The cell voltage, E, is given by,

$$E = \Delta E_{\mathrm{SB}} + \frac{RT}{F} \ln \frac{a^{\mathrm{III}}_{\mathrm{H^+}}}{a^{\mathrm{I}}_{\mathrm{H^+}}} \tag{2}$$

where ΔE_{SB} is the difference between the two liquid junction potentials formed on both sides of the salt bridge and $a^{\alpha}_{\mathrm{H^+}}$ is the activity of H^+ in phase α (α is either phase I or III). If ΔE_{SB}

is negligibly small, it is possible to know the ratio of the activities of H^+ from E. Conversely, if the ratio of the activities of H^+ on both side of the aqueous solutions is determined, it is possible to know the difference in the liquid junction potentials from eq (2).

When the concentration of H^+ in one of the phases is lower than 0.1 mmol dm^{-3}, the following Debye-Hückel limiting law[4] is applicable to calculate the activity coefficient of ions

$$\log \gamma_i = -0.511 z_i^2 \sqrt{I} \tag{3}$$

where z_i is the charge on the ion i and I is the ionic strength. Once the value of $a^{\alpha}_{H^+}$ in either phase I or III is known, the $a^{\alpha}_{H^+}$ in the other phase can be calculated from the measured E value. For this procedure of the estimate of the single-ion activity, the liquid junction potential (LJP) between the salt bridge and an aqueous phase, I or III, is required to be constant. The single-ion activity can thus be estimated resorting to two extrathermodynamic assumptions, that is, the constant LJP and the Debye-Hückel limiting law.

The single-ion activity can also be estimated by use of a Harned cell[2,5] that is believed to be a cell without a liquid junction. The Harned cell is represented as

I	II	III	IV	
Pt	H_2, standard buffer, Cl^-	AgCl	Ag	(B)

Even the Harned cell, the composition of the electrolyte solution in the vicinity of the Pt electrode and that in the Ag/AgCl electrode is not strictly the same[6] because the solution on the left-hand side is saturated with H_2, while the solution around the right is not with H_2 but with AgCl. In pH determination by use of a Harned cell, it is assumed that the LJP does not exist. The activity coefficient of chloride ions is needed to determine the activity of hydrogen ions in a sample solution in the pH determination by use of a Harned cell. To date, the Bates-Guggenheim convention[7] that is an extrathermodynamic assumption is adopted for the estimation of the activity coefficient of Cl^- in a solution (see below).

In practice, the unknown pH value (pH_X) of a sample solution is determined in the following manner.[7]

$$pH_X = pH_S - \frac{F}{RT \ln 10}(E_X - E_S) \tag{4}$$

where pH_S is the assigned pH value of the standard buffer solution, F is the Faraday constant, R is the gas constant, and T is the absolute temperature. In equation (4), E_X and E_S are the values of cell voltages of the following pH cell with the electrodes immersed in the unknown sample solution (X) and the standard buffer solution (S), respectively.

I	II	III	IV	V	VI	
Pt	standard buffer (S) or H_2, sample solution (X)	salt bridge	KCl(sat. or 3.5 M)	AgCl	Ag	(C)

In eq 4, it is assumed that the LJP between a salt bride and a sample solution (X) is the same as that between a salt bridge and a standard buffer (S). Moreover, it is assumed that the leakage of substances constituting the salt bridge from junction part causes no change in pH of the sample solution (X).

Determination of pH values of primary standard buffers

To determine pH values of buffer solutions used as primary pH standards, IUPAC recommends the method based on a Harned cell which consists of a hydrogen electrode and a silver-silver chloride electrode as a primary method.[2] The standard potential of E° of the cell (B) where phase II containing only HCl is determined separately from a Harned cell. The molality of chloride ions is known from the composition of the cell solution. Hence unambiguous values of the quantity $p(a_{H^+}\gamma_{Cl^-})$, that is, $-\log(a_{H^+}\gamma_{Cl^-})$ are obtainable by use of cell (B).

$$p(a_{H^+}\gamma_{Cl^-}) \equiv p(\gamma_{H^+}m_{H^+}\gamma_{Cl^-}) = -\log(\gamma_{H^+}m_{H^+}\gamma_{Cl^-}) = \frac{(E - E^\circ)F}{RT \ln 10} + \log m_{Cl^-} \tag{5}$$

where γ_{H^+} and γ_{Cl^-} are the activity coefficients of hydrogen and chloride ions, respectively, and m_{H^+} and m_{Cl^-} are the molalities of hydrogen and chloride ions, respectively. The value of $\log(a_{H^+}\gamma_{Cl^-})^\circ$, that is, $\log(a_{H^+}\gamma_{Cl^-})$ at zero chloride molality is determined by linear extrapolation of measurements by use of a Harned cell with at least three added molalities of sodium or potassium chloride. For the solutions of low ionic strength ($I < 0.1$ mol kg^{-1}), the activity coefficient of chloride ions may be calculated with reasonable accuracy from Debye-Hückel (D-H) equation.[4]

$$\log \gamma_{Cl^-} = -\frac{A\sqrt{I}}{1 + B\text{å}\sqrt{I}} \tag{6}$$

where A and B are constants which vary with the temperature and dielectric constant of the solvent and å is the ion size parameter introduced to take account of the mean distance of closest approach of the ions. Bates and Guggenheim suggested that γ_{Cl^-} at ionic strengths not exceeding 0.1 mol kg^{-1} can be calculated by equation (6) with Bå = 1.5 kg$^{1/2}$ mol$^{-1/2}$, which is called as Bates-Guggenheim convention.[7] By use of $\gamma^\circ_{Cl^-}$, that is, γ_{Cl^-} at zero chloride molality calculated by adopting Bates-Guggenheim convention, pH (= pa_{H^+}) of a buffer solution is obtained from

$$\text{pH} \equiv \text{p}a_{H^+} = \text{p}(a_{H^+}\gamma_{Cl^-})^\circ + \log \gamma^\circ_{Cl^-} \tag{7}$$

Table 1 lists the typical values of pH determined by use of a Harned cell for seven primary standard buffers at 0 ~ 50 °C.[2]

In IUPAC Recommendations 2002,[2] the sources of uncertainty in the use of the Harned cell are mentioned. The assumptions based on electrolyte theories are used in the method for determination of pH by use of a Harned cell at the following three points:

i. The Debye-Hückel theory is the basis of the extrapolation procedure to calculate the value for the standard potential of the silver-silver chloride electrode

ii. Specific ion interaction theory is the basis for using a linear extrapolation to zero chloride

iii. The Bates-Guggenheim convention sets the value of Bå in Debye-Hückel equation used for the calculation of $\gamma^\circ_{Cl^-}$ as 1.5 kg$^{1/2}$ mol$^{-1/2}$ for any electrolytes.

Table 1: Typical values of pH for primary standards at 0 ~ 50 °C.[2]

	Temperature, °C										
Primary standards	0	5	10	15	20	25	30	35	37	40	50
Sat. potassium hydrogen tartrate (at 25 °C)						3.557	3.552	3.549	3.548	3.547	3.549
0.05 mol kg^{-1} potassium dihydrogen citrate	3.863	3.840	3.820	3.802	3.788	3.776	3.766	3.759	3.756	3.754	3.749
0.05 mol kg^{-1} potassium hydrogen phthalate	4.000	3.998	3.997	3.998	4.000	4.005	4.011	4.018	4.022	4.027	4.050
0.025 mol kg^{-1} disodium hydrogen phosphate + 0.025 mol kg^{-1} potassium dihydrogen phosphate	6.984	6.951	6.923	6.900	6.881	6.865	6.853	6.844	6.841	6.838	6.833
0.03043 mol kg^{-1} disodium hydrogen phosphate + 0.008695 mol kg^{-1} potassium dihydrogen phosphate	7.534	7.500	7.472	7.448	7.429	7.413	7.400	7.389	7.386	7.380	7.367
0.01 mol kg^{-1} disodium tetraborate	9.464	9.395	9.332	9.276	9.225	9.180	9.139	9.102	9.088	9.068	9.011
0.025 mol kg^{-1} sodium carbonate	10.317	10.245	10.179	10.118	10.062	10.012	9.966	9.926	9.910	9.889	9.828

These assumptions are sources of uncertainty in the estimation of the activity of hydrogen ions by use of a Harned cell. IUPAC recommends an estimate of the uncertainty of 0.01 (95 % confidence interval) in pH associated with the Bates-Guggenheim convention. In addition, the experimental uncertainty for pH measurement by use of a Harned cell is of the order of 0.004. We need to consider these uncertainties for an accurate determination of pH.

The roles of KCl salt bridge

The validity of eq (4) rests on the assumption that replacement of the standard buffer solution by a sample solution causes no change in both the magnitude and sign of the LJP between the salt bridge and the sample solution in contact with it. Tower[8] demonstrated in 1895 that a concentrated KCl solution (up to 0.1 mol dm^{-3}) nearly canceled out the LJP between two electrolyte solutions of different compositions. Since then, a concentrated KCl solution

has been used as a salt bridge that eliminates the LJP in electrochemical measurements. However, a concentrated KCl salt bridge (KClSB) does not always work satisfactorily. There are intrinsic problems in a KClSB that hamper accurate measurements of pH, which have remained unsolved to date.

The limitations of KCl salt bridge

The problems in a KClSB are (1) the imperfect elimination of the LJP (for example of sample solution, low ionic strength solutions, the strong acid and alkaline solutions, blood, and sea water), (2) the contamination of a sample solution due to the dissolution of the KCl solution from the junction part, (3) clogging of the junction, and (4) the difficulty of the miniaturization of the reference electrode equipped with a KClSB. The problems in pH determination of low ionic strength solutions, the strong acid and alkaline solutions, blood, and sea water are summarized below.

The pH determination of low ionic strength solutions

The accurate pH measurements of rain water and fresh water are of decisive importance for geochemistry and environmental science. From the 1970s to the 1990s, intensive studies were conducted to accurately determine pH values of low ionic strength solutions. However it turned out to be difficult to estimate accurately pH values of low ionic strength solutions with potentiometric pH measurement based on the KClSB. The main reason of the difficulty is the LJP between a KClSB and low ionic strength sample solutions.[9–24] The LJPs between a saturated KCl solution and low ionic strength solutions estimated by Picknett[25] are listed in Table 2. The LJPs at 10^{-6} mol dm^{-3} of all solutions listed in Table 2 are about 6 mV which equal to about 0.1 pH.

Whereas an LJP is not thermodynamically measurable and so is pH, it is possible to estimate pH values of dilute mineral acid solutions because in sufficiently dilute solutions mineral acids are fully dissociated and D-H theory is applicable to estimate their activity coefficients.

Metcalf showed that the error in pH determination of 50 μmol dm^{-3} sulfuric acid solutions using a glass electrode in combination with a reference electrode with a concentrated

Table 2: Liquid junction potentials between dilute solutions and a saturated KCl solution at 25 °C in millivolts.[25]

Molarity	Equimolar Na acetate + acetic acid	Potassium hydrogen phthalate	Sodium acetate	HCl	KOH	KCl
10^{-2}	3.20	3.49	3.23	2.85	1.92	2.78
10^{-3}	4.15	4.06	4.21	3.97	3.22	3.93
10^{-4}	5.00	4.87	5.27	4.77	4.48	5.02
10^{-5}	5.80	5.78	6.29	5.69	5.75	6.10
10^{-6}	6.72	6.71	7.23	6.70	6.88	7.07

KClSB was 0.055 ± 0.05 pH (positive bias ± two standard deviations).[20] Metcalf concluded that the source of the difference between the experimental and theoretical pH values was the LJP between a concentrated KClSB and dilute solutions and put out, “Further progress in this field seems limited by the non-availability of technological innovations which provide highly reproducible liquid junction errors or minimize temperature equilibration errors in pH probes”.[20]

In addition, the clogging of the junction part of the reference electrode due to the precipitate as AgCl causes errors in the measured pH values.[12,23] The clogging more readily occurs and the performance of a salt bridge is interfered more seriously as the ionic strength of sample solutions becomes low. It is reported that the errors of measured pH values because of ill-behaved KClSBs can amount to the level ranging from 0.1 to 0.8 pH unit.[9,11,26]

Another source of the error in pH is an increase in the ionic strength of a sample solution due to the leakage of the concentrated KCl solution from the liquid junction part of the KClSB. Though the degree of the change in pH depends on the type of the junction, the sample volume, and the time of the contact of the sample solution through the junction, the effect of the leakage of KCl should be more appreciable in the case of a glass combination elec-

trode, in which the junction is positioned in close proximity of the hydrogen ion-responsive glass membrane. Such errors resulting from the LJP and the change in the ionic strength due to the dissolution of the concentrated KCl are inescapable problems, as long as a KClSB is used.

The LJP between a KClSB and strongly acidic and alkaline solutions

The LJPs between a KClSB and strongly acidic and alkaline solutions are large to give rise to an uncertainty in the interpretation of measured pH values. Bates et al.[27] reported that the residual liquid junction potential (RLJP) amounted to 1.8 mV (equal to 0.03 pH unit) and 3.6 mV (equal to 0.06 pH unit) at pH value below 2 and above 10. It is expected from the following simple qualitative considerations that the high mobility of hydrogen and hydroxyl ions are responsible for the LJPs at alkaline and acidic ends of the pH scale. The LJPs at various solutions | a saturated KCl solution interfaces calculated from the Henderson equation[28] are large in the solutions having the great difference between the mobility of the cation and anion, e.g., 1 mol dm^{-3} KOH : -6.9 mV and 1 mol dm^{-3} HCl : 14.1 mV[29] (The LJP is inner potential of a saturated KCl solution referred to that of an aqueous solution). Table 3 summarizes the values of LJPs between a saturated KCl solution and a variety of aqueous solutions calculated by Bates.[29]

Table 3: Liquid junction potentials, E_j, between solution X and saturated KCl solution calculated from limiting ionic mobility values by the Henderson equation at 25 °C.[29]

Solution X, concentration (mol dm^{-3})	E_j (mV)
HCl, 1	14.1
HCl, 0.1	4.6
HCl, 0.01	3.0
HCl, 0.01; NaCl, 0.09	1.9
HCl, 0.01; KCl, 0.09	2.1
KCl, 0.1	1.8
$KH_3(C_2O_4)_2$, 0.1	3.8
$KH_3(C_2O_4)_2$, 0.05	3.3
$KH_3(C_2O_4)_2$, 0.01	3.0
KHC_2O_4, 0.1	2.5
KH phthalate, 0.05	2.6
KH_2 citrate, 0.1	2.7
KH_2 citrate, 0.02	2.9
CH_3COOH, 0.05; CH_3COONa, 0.05	2.4
CH_3COOH, 0.01; CH_3COONa, 0.01	3.1
KH_2PO_4, 0.025; Na_2HPO_4, 0.025	1.9
$NaHCO_3$, 0.025; Na_2CO_3, 0.025	1.8
Na_2CO_3, 0.025	2.0
Na_2CO_3, 0.01	2.4
Na_3PO_4, 0.01	1.8
NaOH, 0.01	2.3
NaOH, 0.05	0.7
NaOH, 0.1	-0.4
NaOH, 1	-8.6
KOH, 0.1	-0.1
KOH, 1	-6.9

The pH determination of blood

The accurate pH measurements of blood and plasma are an indispensable part of clinical diagnosis. In the potentiometric pH measurement of an isotonic saline media of ionic strength, I = 0.16 mol kg^{-1}, such as blood plasma, with a glass combination electrode equipped with a KClSB, the LJP between a KClSB and the isotonic saline media causes errors amounting to 0.03 - 0.05 pH unit.[30] Bates reported that the RLJP, that is the difference of two LJPs at the interface between primary standard buffers and KClSB and that at the isotonic saline media and KClSB, can be nearly eliminated by matching the ionic strength of the standard buffer solution to that of the clinical sample.[30] However, there still seems to remain unknown contributions due to the RLJP to measured pH values.

The concentrated KCl solution leaked from junction part contaminates the blood samples and bring about the precipitate of blood protein. To avoid this problem, Semple[31] and Maas[32,33] studied the use of 0.16 mol dm^{-3} NaCl as a salt bridge. Maas et al.[32–34] showed that pH values determined by use of 0.16 mol dm^{-3} NaCl salt bridge were lower by 0.1 pH unit than that by use of a saturated KClSB.

The pH determination of sea water

Although pH of sea water is an important parameter for oceanographic science,[35–37] there are the problems on the procedure of measurement and the question for the interpretation of measured pH.[38] The main problem is the uncertainty of LJP between a concentrated KClSB and sea water.[39] The ionic strength of sea water is about 0.7 mol dm^{-3}. Butler et al. reported the error caused by the LJP in the pH scale based on dilute standard buffer solution amounted to ca. 0.1 pH.[40] The error is eliminated by use of the reference buffer solutions whose composition and ionic strength are similar to those of sea water.[41,42] However, Bates-Guggenheim convention is not reliable but no methods except a complicated and less accurate Pitzer equation[43–45] for activity coefficients evaluation have been available at high ionic strength solutions. Moreover, the reference buffers with the different ionic strength are needed because the ionic strength of sea water in estuarine region has a gradient. However, in practice, the procedure becomes unacceptively complicate.[42]

Ionic liquid salt bridge

A new type of salt bridge made of a moderately hydrophobic ionic liquid (ILSB) recently proposed[46–50] is superior to KClSBs, in that the solubility of the ionic liquid (IL) employed for ILSBs is less than 1 mmol dm^{-3} and the principle of cancelling out the LJP between a sample solution and the inner solution of the reference electrode is based on the partition of the IL into the sample side.[47] The principles and performance of the ILSB are summarized below.

The principles of ionic liquid salt bridge

If the distribution equilibrium is established at the interface between an IL composed of the moderately hydrophobic cation and anion and an aqueous solution (W), the LJP between IL and W is governed by the distribution potential determined by the standard Gibbs energy of transfer of each ion between IL and W. When the transfer of ions in W to the IL is negligibly small, the distribution potential determined by the partition of the IL between the IL and the aqueous solution (W) is described by[46,51,52]

$$\Delta_{\mathrm{IL}}^{\mathrm{W}}\phi = \frac{1}{2F}(\Delta_{\mathrm{IL}}^{\mathrm{W}}G_{\mathrm{tr,A^-}}^{\mathrm{IL}\rightarrow\mathrm{W},0} - \Delta_{\mathrm{IL}}^{\mathrm{W}}G_{\mathrm{tr,C^+}}^{\mathrm{IL}\rightarrow\mathrm{W},0}) + \frac{RT}{2F}\ln\frac{\gamma_{\mathrm{C^+}}^{\mathrm{IL}}\gamma_{\mathrm{A^-}}^{\mathrm{W}}}{\gamma_{\mathrm{C^+}}^{\mathrm{W}}\gamma_{\mathrm{A^-}}^{\mathrm{IL}}} \tag{8}$$

where $\Delta_{\mathrm{IL}}^{\mathrm{W}}\phi$ is the inner potential of W referred to that of the IL, and $\Delta_{\mathrm{IL}}^{\mathrm{W}}G_{\mathrm{tr,C^+}}^{\mathrm{IL}\rightarrow\mathrm{W},0}$ and $\Delta_{\mathrm{IL}}^{\mathrm{W}}G_{\mathrm{tr,A^-}}^{\mathrm{IL}\rightarrow\mathrm{W},0}$ are the standard Gibbs energy of transfer of the cation (C^+) and the anion (A^-) constituting the IL from IL to W, respectively, and $\gamma_{\mathrm{i}}^{\mathrm{IL}}$ and $\gamma_{\mathrm{i}}^{\mathrm{W}}$ are the activity coefficients of the ions (i = C^+ and A^-) in the phases IL and W. The standard ion-transfer potential between IL and W is defined by

$$\Delta_{\mathrm{IL}}^{\mathrm{W}}\phi_i^0 = -\frac{1}{z_iF}\Delta_{\mathrm{IL}}^{\mathrm{W}}G_{\mathrm{tr},i}^{\mathrm{IL}\rightarrow\mathrm{W},0} \tag{9}$$

where z_i is the valence of the ionic species i. If the second term on the right side of the equation(8) is negligible, the distribution potential is represented in terms of $\Delta_{\mathrm{IL}}^{\mathrm{W}}\phi_i^0$ by

$$\Delta_{\mathrm{IL}}^{\mathrm{W}}\phi = \frac{1}{2}(\Delta_{\mathrm{IL}}^{\mathrm{W}}\phi_{\mathrm{C^+}}^0 + \Delta_{\mathrm{IL}}^{\mathrm{W}}\phi_{\mathrm{A^-}}^0) \tag{10}$$

The LJP between IL and W is thus determined by partition of ions constituting the IL and independent of the composition and concentration of electrolytes in W, provided that

the dissolution of the electrolytes in W into to the IL is negligible. If such an IL is inserted two electrolyte solutions of different compositions, the LJP between these two electrolyte solutions would be effectively canceled out because $\Delta_{\mathrm{IL}}^{\mathrm{W}}\phi$ values at both sides of the ILSB have the same magnitudes but with opposite signs. Therefore, an IL can be used as a salt bridge.

However, it dose not mean that any IL can be used as a salt bridge. First, to avoid interference by hydrophilic cations and anions likely to be present in the aqueous solutions, $\Delta_{\mathrm{IL}}^{\mathrm{W}}\phi$ must be away from $\Delta_{\mathrm{IL}}^{\mathrm{W}}\phi_i^0$ of those ions, that is, be close to zero. Second, the IL has a certain but not excessive solubility in water. When the interface between an IL and an aqueous phase (W) is polarized, the phase boundary potential between IL and W is easy to shift due to the interference of ions in W. The charge-transfer resistance at zero current, $R_{I=0}$, is represented by[53]

$$R \propto \exp\left[\frac{F}{2RT}\left(\Delta_{\mathrm{IL}}^{\mathrm{W}}\phi_{\mathrm{A}^-}^0 - \Delta_{\mathrm{IL}}^{\mathrm{W}}\phi_{\mathrm{C}^+}^0\right)\right] = \frac{1}{\sqrt{K_{\mathrm{s}}^{\mathrm{W}}}} \tag{11}$$

where $K_{\mathrm{s}}^{\mathrm{W}}$ is the solubility product of CA in W. The polarizability is, thus, inversely proportional to the square root of $K_{\mathrm{s}}^{\mathrm{W}}$ or to the solubility of the IL. The phase boundary potential is susceptible to the interference due to the ions in W as the solubility of IL to W becomes low. On the other hand, in practice, the low solubility of IL to W has advantage in terms of life time of ILSB and contamination of sample solution due to the dissolution of an ILSB. Therefore, we need to set the solubility of IL to W up as 0.1 - a few mmol dm^{-3}.[53]

The performance of ionic liquid salt bridge

Kakiuchi and Yoshimatsu showed the LJP between 1-methyl-3-octylimidazolium bis(trifluoromethanesulfonyl)amide ($\mathrm{C_8mimC_1C_1N}$) and aqueous solutions was stable at the 0.001 - 0.5 mol dm^{-3} aqueous solutions.[47] The structure of $\mathrm{C_8mimC_1C_1N}$ is given in Fig. 1. The $\mathrm{C_8mimC_1C_1N}$ salt bridge showed a stable LJP upon contact with 50 μmol dm^{-3} aqueous solution.[48] However, when the ionic strength of the sample solution is lower than 0.1 mmol dm^{-3}, the junction potential between $\mathrm{C_8mimC_1C_1N}$ and an aqueous solution of either HCl, LiCl, NaCl, or KCl deviates from the value determined by the partition of $\mathrm{C_8mimC_1C_1N}$ in W.[48] This deviation is mainly ascribable to the diffusion potential in W that accompa-

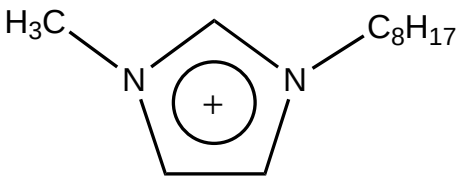

1-Methyl-3-octylimidazolium (C_8mim^+)

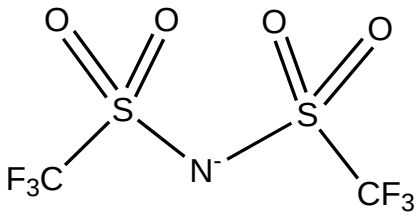

Bis(trifluoromethanesulfonyl)amide ($C_1C_1N^-$)

Figure 1: Structure of $C_8mimC_1C_1N$

nies the dissolution of $C_8mimC_1C_1N$. The magnitude of the diffusion potential becomes non-negligible when the ionic strength is significantly lower than the solubility of the IL. Sakaida et al. recently proposed an IL that consists of tributyl(2-methoxyethyl)phosphonium ($TBMOEP^+$) and bis(pentafluoroethanesulfonyl)amide ($C_2C_2N^-$) for an ILSB suitable to low ionic strength samples.[49] The structure of $TBMOEPC_2C_2N$ is given in Fig. 2. Sakaida and Kakiuchi determined the single-ion activities of H^+ and Cl^- independently up to 0.5 mol dm^{-1} HCl by inserting $TBMOEPC_2C_2N$ salt bridge in the middle of a Harned cell.[54] The geometric mean of the single-ion activities of H^+ and Cl^- agreed with thermodynamically reliable mean activity values of HCl determined with a Harned cell.

An ILSB may give a solution of the problems in miniaturization of the reference electrode. An ILSB is readily gelled by use of poly (vinylidene fluoride-co-hexafluoropropylene) (PVdF-HFP).[55] The structure of PVdF-HFP is given in Fig 3. The all solid-state reference electrode is realized by the gelled IL including AgCl coated directly with Ag/AgCl electrode which works also as an inner solution.[56]

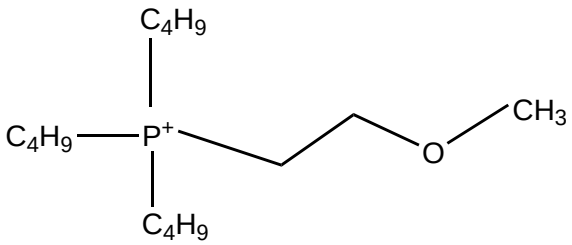

Tributyl(2-methoxyethyl)phosphonium ($TBMOEP^+$)

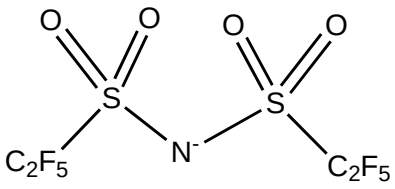

Bis(pentafluoroethanesulfonyl)amide ($C_2C_2N^-$)

Figure 2: Structure of $TBMOEPC_2C_2N$

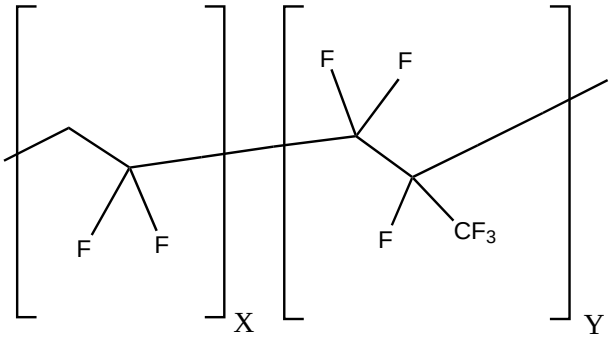

Poly(vinylidene fluoride-co-hexafluoropropylene) (PVdF-HFP)

Figure 3: Structure of PVdF-HFP

The contribution of ILSB to the pH determination

The basis of KClSB which has formed the backbone of the pH determination over a century is not necessarily well-established. Many problems remain unresolved because of non-availability of a devise alternative to a KClSB. The ILSB the one that can give solutions to

those problems. It is expected that a new basis of pH determination is constructed by the ILSB. Reexamination of pH data accumulated for nature water may lead to a new horizon in environmental science. The accurate determination of single-ion activities can bring about new developments in electrochemistry and solution chemistry.

However, no systematic study of pH determination of low ionic strength solutions has been made by use of an ILSB. It is not known how accurately pH, that is, single-ion activity of H^+, in low ionic strength solutions can be estimated by use of an ILSB. In addition, the LJPs between an ILSB and standard buffer solutions, blood, or sea water and the influence of buffer substances or electrolytes in blood and sea water on the LJP have not been investigated.

Outline of this work

In chapter 1, it is shown that values of the activity of hydrogen ions in 20 - 200 μmol dm^{-3} H_2SO_4 solution are accurately estimated by use of the ionic liquid salt bridge (ILSB), made of $TBMOEPC_2C_2N$, sandwiched by two hydrogen electrodes. The experimental pH values were in good agreement within 0.01 pH with those calculated with the Pitzer model.[57] The source of the small difference between measured and calculated pH values can be explained by the residual diffusion potential due to the dissolution of $TBMOEPC_2C_2N$ in the H_2SO_4 solution (W) and the resultant increase in the ionic strength of W.

However, this type of cell based on the hydrogen electrode is inconvenient in practical use. In chapter 2, the author showed the activities of the hydrogen ions in the 20 - 200 μmol dm^{-3} H_2SO_4 solution could be estimated accurately and reliably by use of glass combination electrodes equipped with $TBMOEPC_2C_2N$ salt bridge-type reference electrode. A glass combination electrode equipped with an ILSB gives a solution to the problem intrinsic to the pH measurement of low ionic strength samples based on a KClSB.

The pH values assigned to standard buffer solutions by use of Harned cells include an uncertainty[2] associated with the Bates-Guggenheim convention.[7] In chapter 3, the author proposed a new method to determine the activity of hydrogen ions in phosphate standard buffer solutions by use of an electrochemical cell[58] with an ILSB[46,47,49,50] sandwiched by two hydrogen electrodes. In this method, pH determination is made based on the activity of

hydrogen ions in sufficient dilute sulfuric acid solutions to apply the Debye-Hückel limiting law.[4] Therefore, this pH determination is more reliable than the pH determination by use of a Harned cell in combination with Bates-Guggenheim convention. The experimental pH values at 0.01 - 0.05 mol kg^{-1} phosphate buffers were in good agreement within 0.013 pH with those calculated with the Pitzer model.[59] The difference between the experimental and theoretical pH values at 0.01 - 0.075 mol kg^{-1} was smaller than that obtained using a Harned cell. The pH determination by use of an ILSB has potential to be a better alternative to that by use of Harned cell in estimating the activity of hydrogen ions in phosphate buffer solutions.

In earlier studies conducted to examine the performance of ILSBs, temperature was always 25 °C. What is required for application of an ILSB to potentiometric pH measurement is an ILSB that maintains the LJP constant over a wide range of temperature. In chapter 4, the author investigated the performance of TBMOEPC_2C_2N salt bridge at 5 - 60 °C. The activities of hydrogen ions in 0.025 mol kg^{-1} equimolal phosphate buffer solutions containing potassium dihydrogen phosphate and disodium hydrogen phosphate were estimated by use of the TBMOEPC_2C_2N salt bridge, sandwiched by two hydrogen electrodes at 5 - 60 °C. The experimental pH values at 5 - 60 °C were in agreement within 0.02 pH with those determined by use of a Harned cell. The results confirm that a pH combination electrode equipped with the TBMOEPC_2C_2N salt bridge is applicable to pH determination in the temperature range between 5 and 60 °C.

In chapter 5, the author showed the interference by ions in aqueous solution (W) of the LJP between an ILSB and W. The stability of a Ag/AgCl reference electrode equipped with a gelled ionic liquid, C_8mimC_1C_1N, as a salt bridge, was examined by the potentiometry of pH standard solutions. The reproducible and systematic deviation of the potential of the IL-type reference electrode in the phthalate pH standard amounted to 5 mV. The deviation is ascribed to the partition of the hydrogen phthalate in the C_8mimC_1C_1N.

The solubility of TBMOEPC_2C_2N is lower than C_8mimC_1C_1N. Therefore, it is expected that TBMOEPC_2C_2N salt bridge is susceptible to the interference by ions in W. The buffer solutions[30,60–69] of the ionic strength, I = 0.16, which has compatibility with biological fluids, for the potentiometric pH measurement of blood and biological fluids have been em-

ployed. In such high ionic strength, Bates-Guggenheim convention is no longer applicable. In chapter 6, the author investigated the stability of TBMOEPC_2C_2N salt bridge in reference buffer solutions that have been used for pH measurement of physiological solutions. The experimental pH values determined by the ILSB were closer to the pH values determined by an Harned cell than by use of KClSB at 1:3.5 phosphate and 1:3 Tris buffer solutions. However, experimental pH values of 1:2 HEPES and 1:2 TES were greater than that of KClSB. In cyclic voltammograms for 1:2 HEPES and 1:2 TES in contact with a TBMOEPC_2C_2N, the negative end of polarized potential window (ppw) shifted to more positive potentials than that of ppw in the cyclic voltammogram for NaCl in contact with the TBMOEPC_2C_2N. From the results of voltammograms, the PBP between the IL and 1:2 HEPES or 1:2 TES is expected to shift to the positive direction and then the measured pH values will decrease. The expected direction of the shift of pH values at 1:2 HEPES and 1:2 TES is consistent with the results obtained from potentiometric measurement. The shift of measured pH values by use of a TBMOEPC_2C_2N salt bridge at 1:2 HEPES and 1:2 TES seems to be due to the interference by the anions in buffer solutions.

Chapter 7 concludes my study on application of ionic liquid salt bridge to accurate determination of pH and summarizes the remained problems and scope for future studies.

References

(1) Sørensen, S. P. L.; Linderstrøm-Lang, K.; Lund, E. *Compt. Rend. Trav. Lab. Carlsberg* **1924**, *15*, 1–40.

(2) Buck, R. P.; Rondinini, S.; Covington, A. K.; Baucke, F. G. K.; Brett, C. M. A.; Camoes, M. F.; Milton, M. J. T.; Mussini, T.; Naumann, R.; Pratt, K. W.; Spitzer, P.; Wilson, G. S. *Pure Appl. Chem.* **2002**, *74*, 2169–2200.

(3) Kakiuchi, T. *J. Solid State Electrochem.* **2011**, *15*, 1661–1671.

(4) Debye, P.; Hückel, E. *Physik. Z.* **1923**, *24*, 185–206.

(5) Bates, R. G. *Chem. Rev.* **1948**, *42*, 1–61.

(6) MacInnes, D. A. In *The principles of electrochemistry.*; Dover: New York, 1961.

(7) Bates, R. G.; Guggenheim, E. A. *Pure Appl. Chem.* **1960**, *1*, 163–168.

(8) Tower, O. F. *Z. Phys. Chem.* **1895**, *18*, 17–50.

(9) Galloway, J. N.; Cosby, B. J.; Likens, G. E. *Limnol. Oceanogr.* **1979**, *24*, 1161–1165.

(10) Midgley, D.; Torrance, K. *Analyst* **1979**, *104*, 63–72.

(11) Tyree, S. Y. *Atmos. Environ.* **1981**, *15*, 57–60.

(12) Brezinski, D. P. *Anal. Chim. Acta* **1982**, *134*, 247–262.

(13) Brezinski, D. P. *Analyst* **1983**, *108*, 425–442.

(14) Mcquaker, N. R.; Kluckner, P. D.; Sandberg, D. K. *Environ. Sci. Technol.* **1983**, *17*, 431–435.

(15) Johnson, C. A.; Sigg, L. *Chimia* **1985**, *39*, 59–61.

(16) Covington, A. K.; Whalley, P. D.; Davison, W. *Pure Appl. Chem.* **1985**, *57*, 877–886.

(17) Davison, W.; Woof, C. *Anal. Chem.* **1985**, *57*, 2567–2570.

(18) Davison, W.; Gardner, M. J. *Anal. Chim. Acta* **1986**, *182*, 17–31.

(19) Koch, W. F.; Marinenko, G.; Paule, R. C. *J. Res. Natl. Bur. Stand (U.S.)* **1986**, *91*, 23–32.

(20) Metcalf, R. C. *Analyst* **1987**, *112*, 1573–1577.

(21) Davison, W.; Covington, A. K.; Whalley, P. D. *Anal. Chim. Acta* **1989**, *223*, 441–447.

(22) Durst, R. A.; Davison, W.; Koch, W. F. *Pure Appl. Chem.* **1994**, *66*, 649–658.

(23) Ozeki, T.; Tsubosaka, Y.; Nakayama, S.; Ogawa, N.; Kimoto, T. *Anal. Sci.* **1998**, *14*, 749–756.

(24) Kadis, R.; Leito, I.; v. o. Leito, I. *Anal. Chim. Acta* **2010**, *664*, 129–135.

(25) Picknett, R. G. *Trans. Faraday Soc.* **1968**, *64*, 1059–1069.

(26) Metcalf, R. C. *Z. Gletscher. Glazial* **1984**, *20*, 41–51.

(27) Bates, R. G.; Pinching, G. D.; Smith, E. R. *J. Res. Nat. Bur. Stand.* **1950**, *45*, 418–429.

(28) Henderson, P. *Z. Phys. Chem.* **1908**, *63*, 325–345.

(29) Bates, R. G. In *Determination of pH*; Wiley: New York, 1973.

(30) Bates, R. G.; Vega, C. A.; D. R. White, J. *Anal. Chem.* **1978**, *50*, 1295–1300.

(31) Semple, S. J. *J. Appl. Physiol.* **1961**, *16*, 576–577.

(32) Maas, A. H. J. *J. Appl. Physiol.* **1971**, *30*, 248–250.

(33) Maas, A. H. J. *Clin. Chim. Acta* **1970**, *28*, 373–390.

(34) Khuri, R. N.; Merril, C. R. *Phys. Med. Biol.* **1964**, *9*, 541–550.

(35) Millero, F. J. In *The Physical Chemistry of Natural Waters.*; Wiley-Interscience: New York, 2001.

(36) Marion, G. M.; Millero, F. J.; Feistel, R. *Ocean Sci.* **2009**, *5*, 285–291.

(37) Millero, F. J.; Woosley, R.; DiTrolio, B.; Waters, J. *Oceanography* **2009**, *22*, 72–85.

(38) Dickson, A. G. *Deep Sea Res* **1993**, *40*, 107–118.

(39) Dickson, A. G. *Mar. Chem.* **1993**, *44*, 131–142.

(40) Butler, R. A.; Covington, A. K.; Whitfield, M. *Oceanol. Acta* **1985**, *8*, 433–439.

(41) Hansson, I. *Deep-sea res* **1973**, *20*, 479–491.

(42) Covington, A. K.; Whitfield, M. *Pure Appl. Chem.* **1988**, *60*, 865–870.

(43) Hardege, J. D.; Rotchell, J. M.; Terschak, J.; Greenway, G. M. *TrAC Trends in Analytical Chemistry* **2011**, *30*, 1320–1326.

(44) Tishchenko, P. Y.; Kang, D. J.; Chichkin, R. V.; Lazaryuk, A. Y.; Wong, C. S.; Johnson, W. K. *Deep Sea Research Part I: Oceanographic Research Papers* **2011**, *58*, 778–786.

(45) Prenesti, E.; Ferrara, E.; Berto, S.; Fisicaro, P.; Daniele, P. G. *Anal. Baioanal. Chem.* **2007**, *388*, 1877–1883.

(46) Kakiuchi, T.; Tsujioka, N.; Kurita, S.; Iwami, Y. *Electrochem. Commun.* **2003**, *5*, 159–164.

(47) Kakiuchi, T.; Yoshimatsu, T. *Bull. Chem. Soc. Jpn.* **2006**, *79*, 1017–1024.

(48) Yoshimatsu, T.; Kakiuchi, T. *Anal. Sci.* **2007**, *23*, 1049–1052.

(49) Sakaida, H.; Kitazumi, Y.; Kakiuchi, T. *Talanta* **2010**, *83*, 663–666.

(50) Fujino, Y.; Kakiuchi, T. *J. Electroanal. Chem.* **2011**, *651*, 61–66.

(51) Hung, L. Q. *J. Electroanal. Chem.* **1980**, *115*, 159–174.

(52) Kakiuchi, T.; Senda, M. *Bull. Chem. Soc. Jpn.* **1987**, *60*, 3099–3107.

(53) Kakiuchi, T.; Tsujioka, N. *J. Electroanal. Chem.* **2007**, *599*, 209–212.

(54) Sakaida, H.; Kakiuchi, T. *J. Phys. Chem. B* **2011**, *115*, 13222–13226.

(55) Fuller, J.; Breda, A. C.; Carlin, R. T. *J. Electroanal. Chem.* **1998**, *459*, 29–34.

(56) Kakiuchi, T.; Yoshimatsu, T.; Nishi, N. *Anal. Chem.* **2007**, *79*, 7187–7191.

(57) Pitzer, K. S.; Roy, R. N.; Silvester, L. F. *J. Am. Chem. Soc.* **1977**, *99*, 4930–4936.

(58) Shibata, M.; Sakaida, H.; Kakiuchi, T. *Anal. Chem.* **2011**, *83*, 164–168.

(59) Partanen, J. I.; Minkkinen, P. O. *J. Solution Chem.* **1997**, *26*, 709–727.

(60) Durst, R. A.; Staples, B. R. *Clin. Chem.* **1972**, *18*, 206–208.

(61) Bower, V. E.; Paabo, M.; Bates, R. G. *J. Res. Natl. Bur. Stand* **1961**, *65A*, 267–270.

(62) Roy, R. N.; Roy, L. N.; Denton, C. E.; LeNoue, S. R.; Fuge, M. S.; Dunseth, C. D.; Durden, J. L.; Roy, C. N.; Bwashi, A.; Wollen, J. T.; DeArmon, S. J. *J. Chem. Eng. Data* **2009**, *54*, 428–435.

(63) Wu, Y. C.; Berezansky, P. A.; Feng, D.; Koch, W. F. *Anal. Chem.* **1993**, *65*, 1084–1087.

(64) Roy, R. N.; Mrad, D. R.; Lord, P. A.; Carlsten, J. A.; Good, W.; Allsup, P.; Roy, L. N.; Kuhler, K. M.; Koch, W. F.; Wu, Y. C. *J. Solution Chem.* **1998**, *27*, 73–87.

(65) Roy, R. N.; Roy, L. N.; Tabor, B. J.; Richards, C. A.; Simon, A. N.; Moore, A. C.; Seing, L. A.; Craig, H. D.; Robinson, K. T. *J. Solution Chem.* **2004**, *33*, 1199–1211.

(66) Roy, R. N.; Roy, L. N.; Denton, C. E.; LeNoue, S. R.; Roy, C. N.; Ashkenazi, S.; Williams, T. R.; Church, D. R.; Fuge, M. S.; Sreepada, K. N. *J. Solution Chem.* **2006**, *35*, 605–624.

(67) Bates, R. G.; Roy, R. N.; Robinson, R. A. *Anal. Chem.* **1973**, *45*, 1663–1666.

(68) Roy, R. N.; Roy, L. N.; Stegner, J. M.; A.Sechler, S.; Jenkins, A. L.; Krishchenko, R.; Henson, I. B. *J. Electroanal. Chem.* **2011**, *663*, 8–13.

(69) Roy, R. N.; Roy, L. N.; Ashkenazi, S.; Wollen, J. T.; Dunseth, C. D.; Fuge, M. S.; Durden, J. L.; Roy, C. N.; ; Hughes, H. M.; Morris, B. T.; Cline, K. L. *J. Solution Chem.* **2009**, *38*, 449–458.

Chapter 1

Determination of the Activity of Hydrogen Ions in Dilute Sulfuric Acids Using an Ionic Liquid Salt Bridge Sandwiched by Two Hydrogen Electrodes

1.1 Introduction

pH is the most widely used measure for the acidity of solutions, whose notional definition[1,2] is

$$\mathrm{pH} = -\log a_{\mathrm{H^+}} \tag{1.1}$$

where $a_{\mathrm{H^+}}$ is the activity of hydrogen ions. Accurate pH measurements are indispensable in many facets of our life and environments. For geochemistry and environmental science, it is of decisive importance to measure accurate pH values of fresh waters. However, it is difficult to measure pH of dilute aqueous solutions such as rain water and surface water with potentiometry using a glass electrode and a reference electrode with a concentrated KCl salt bridge (KClSB).[3–22] Many studies conducted in 1970s-1990s ascribed this difficulty to the reference electrode.[3,4,9,11,12,16,19,21,22] In these foregoing studies, it has been established that the best way of verifying the accuracy of pH measuring systems is to measure the pH values

of aqueous dilute mineral acids, whose pH can be accurately calculated by the Debye-Hückel (D-H) limiting law.[23]

Metcalf showed that the error in pH determination of 50 μmol dm^{-3} sulfuric acid solutions using a glass electrode in combination with a reference electrode with a concentrated KClSB was 0.06 ± 0.05 pH (positive bias ± two standard deviations).[16] The major source of the error was ascribed to the non-negligible liquid junction potential (LJP) at the contact of the concentrated KCl solution with the sample solution.[24] Another possible source of the error in pH is an increase in the ionic strength of a sample solution due to the leakage of the concentrated KCl solution from the liquid junction part of the KClSB. Though the degree of the change in pH depends on the type of the junction, the sample volume, and the time of the contact of the sample solution through the junction, the effect of the leakage of KCl should be more appreciable in the case of a combination type glass pH electrode, in which the junction is positioned in close proximity of the glass membrane. Such errors resulting from the LJP and the change in the ionic strength due to the dissolution of the concentrated KCl are unescapable problems, as long as a concentrated KClSB is used.

A new type of salt bridge made of a moderately hydrophobic ionic liquid (ILSB) recently proposed[25–27] is superior to KClSBs, in that the solubility of the ionic liquid (IL) employed for ILSBs is less than 1 mmol dm^{-3} and the principle of cancelling out the LJP between a sample solution and the inner solution of the reference electrode is based on the partition of the IL into the sample side.[26] However, when the ionic strength of the sample solution is lower than 0.1 mmol dm^{-3}, the junction potential between the ILSB that consists of 1-methyl-3-octylimidazolium bis(trifluoromethanesulfonyl)amide ($C_8mimC_1C_1N$) and an aqueous solution of either HCl, LiCl, NaCl, or KCl deviates from the value determined by the partition of $C_8mimC_1C_1N$ in W.[27] This deviation is mainly ascribable to the diffusion potential in W that accompanies the dissolution of $C_8mimC_1C_1N$. The magnitude of the diffusion potential becomes non-negligible when the ionic strength is significantly lower than the solubility of the IL. Sakaida et al. recently proposed an IL that consists of tributyl(2-methoxyethyl)phosphonium ($TBMOEP^+$) and bis(pentafluoroethanesulfonyl)amide ($C_2C_2N^-$) for an ILSB suitable to low ionic strength samples.[28]

This chapter describes that the activity of the hydrogen ions in dilute sulfuric acids can be accurately estimated using a TBMOEPC_2C_2N salt bridge sandwiched by two hydrogen electrodes and that the TBMOEPC_2C_2N ILSB can effectively cancel out the LJP between the two dilute sulfuric acid solutions of different concentrations. The results is encouraging in that the use of the ILSB sandwiched by a proper reference electrode and a glass electrode opens the way for accurate determination of pH of low ionic strength samples and single ion activities in aqueous solutions, in general.

1.2 Experimental

1.2.1 Reagents

Tributyl(2-methoxyethyl)phosphonium chloride (TBMOEPCl) was synthesized by adding tributylphosphine (Kanto Chemical Co., Inc. 98 %) to chloroethylmethylether (Tokyo Chemical Industry Co., Ltd. 98 %) at 70 °C with stirring the mixture for 7 days under nitrogen atmosphere.[29] The mixture was then washed five times with hexane and vacuum stripped to remove any volatiles.

TBMOEPC_2C_2N was prepared by mixing equimolar amounts of TBMOEPCl and hydrogen bis(pentafluoroethanesulfonyl)amide (Central Glass Co., Ltd. 70 % aqueous solution) in methanol. TBMOEPC_2C_2N was washed 25 times with MilliQ water to remove halide impurities. After the 15th washing, Cl^- was not detected when a few drops of a $AgNO_3$ solution were added to the supernatant solution. TBMOEPC_2C_2N was then purified by column chromatography.[30] TBMOEPC_2C_2N was saturated with MilliQ water before potentiometric pH measurements using the TBMOEPC_2C_2N salt bridge. Because the acidity of hydrogen bis(trifluoromethanesulfonyl)amide is stronger than HNO_3,[31] $C_2C_2N^-$ is presumably not protonated in contact with aqueous dilute sulfuric acid solutions employed in the present study.

Aqueous sulfuric acid solutions of six different concentrations, 20, 50, 100, 150, 200, and 500×10^{-6} mol dm^{-3} were prepared by diluting with MilliQ water a standardized sulfuric acid solution, which was certified to be $(5.00 \pm 0.01) \times 10^{-2}$ mol dm^{-3} by coulometric titration with the NaOH solution (Nacalai Tesque, Inc., Japan). A $(500 \pm 3) \times 10^{-6}$ mol dm^{-3}

H_2SO_4 solution was prepared by adding 5.00 ± 0.03 ml of (5.00 ± 0.01) × 10^{-2} mol dm^{-3} H_2SO_4 to a 500.00 ± 0.25 ml flask and diluting to a final volume of 500 ± 0.25 ml with MilliQ water at 20.0 °C. (20.0 ± 0.12), (50.0 ± 0.3), (100 ± 0.6), (150 ± 0.9), and (200 ± 1.2) × 10^{-6} mol dm^{-3} H_2SO_4 were prepared by adding 20.00 ± 0.02, 50.00 ± 0.03, 100.00 ± 0.05, 150.00 ± 0.06, and 200.00 ± 0.07 ml of (500 ± 3) × 10^{-6} mol dm^{-3} H_2SO_4 to a 500.00 ± 0.25 ml flask and diluting to a final volume of 500 ± 0.25 ml with MilliQ water at 20.0 °C, respectively.

The hydrogen electrodes were prepared by electrolysis of platinum foils of about 10 mm square for about 5 min at 30 mA cm^{-2} in a 3.5 % (g/L) solution of chloroplatinic acid (Nacalai Tesque, Inc.) containing 0.005 % (g/L) lead acetate trihydrate (Nacalai Tesque, Inc.)[32]

1.2.2 Methods

The electrochemical cell employed is represented as

I	II	III	IV	V	
	H_2,		H_2,		
Pt	500 μmol dm^{-3}	$TBMOEPC_2C_2N$	x μmol dm^{-3}	Pt	
	H_2SO_4		H_2SO_4		(A)

The single dashed vertical bars indicate the interfaces between the ILSB and the aqueous solutions (II and IV). Figure 1.1 illustrates the structure of the U-type glass cell used for potentiometry. It consists of the two hydrogen electrode compartments and the $TBMOEPC_2C_2N$ salt bridge.

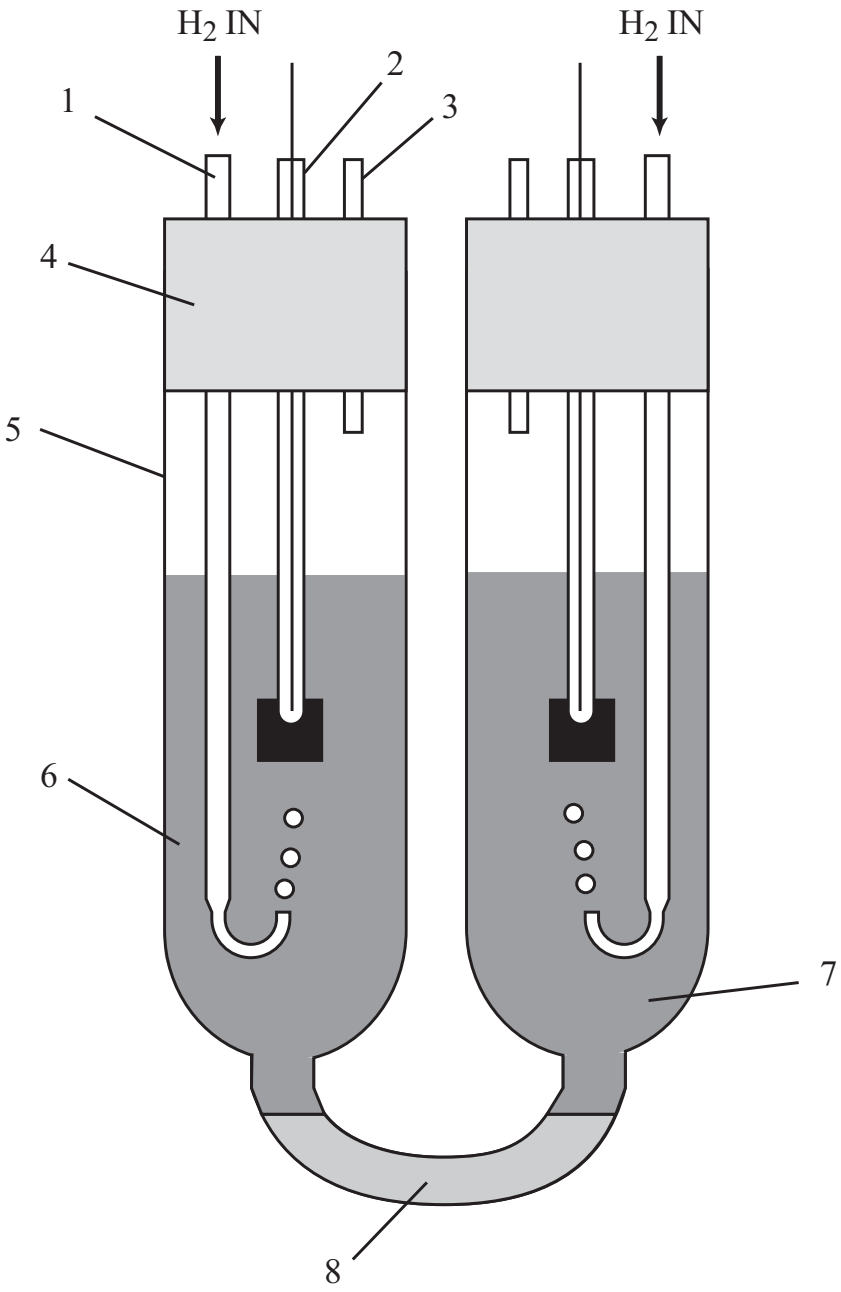

Figure 1.1: Illustration of the electrochemical cell using a ILSB sandwiched by two hydrogen electrodes. 1: glass tube for introducing hydrogen gas; 2: hydrogen electrode; 3: glass tube for exhausting hydrogen gas; 4: silicon rubber stopper; 5: U-type glass cell; 6: 500 μmol dm^{-3} H_2SO_4; 7: x μmol dm^{-3} H_2SO_4; 8: TBMOEPC_2C_2N

The cell voltage, E, i.e., the potential of the right-hand-side terminal referred to that of the left in the cell (A), was measured with an electrometer (Advantest, R8240) with a GPIB interface. The sampling interval was 1 min. The cell was immersed in a water bath maintained at 25.0 ± 0.1 °C. Each of the two hydrogen electrodes was supplied with hydrogen gas (99.9995 %), which was generated by a hydrogen gas generator (Horiba Stec, OPGU-7100), at the rate of two to three bubbles per second from a jet about 1 mm in diameter during measurements. The gas was passed through a saturator containing the same solution as the one in the hydrogen electrode compartment before it entered the cell.

The value of E was measured at 20, 50, 100, 150, and 200 μmol dm^{-3} H_2SO_4 in phase IV in cell (A). The measurement at each concentration of H_2SO_4 was repeated three times. After each measurement, both H_2SO_4 solutions in phases II and IV in cell (A) was drained and the U-type glass cell and two platinum electrodes were washed with MilliQ water three times. The measurement for each concentration of H_2SO_4 was completed in a day and it took 5 days to complete all measurements. The E was recorded for 1 h after the hydrogen gas was passed in cell (A) for 1 h. The average of E values recorded in the last ten min at each measurement was employed to estimate the pH value.

1.2.3 Experimental pH Values of Dilute Sulfuric Acids

An unknown pH value of sulfuric acids (pH_x) in IV in cell (A) is written by

$$pH_x = pH_s - \frac{F}{RT \ln 10}(E - E_j) \tag{1.2}$$

where pH_s is the pH value of the 500 μmol dm^{-3} H_2SO_4 solution in II in cell (A), and E_j is the sum of two LJPs on both sides of the ILSB in cell (A), F is the Faraday constant, R is the gas constant, and T is the absolute temperature. The value of pH_s is calculated by the following procedure. The values of $\ln(\gamma_{H^+}^2 \gamma_{SO_4^{2-}})$ and $\ln(\frac{\gamma_{H^+}\gamma_{SO_4^{2-}}}{\gamma_{HSO_4^-}})$ at a given value of m_{H^+} were calculated using the method proposed by Pitzer et al.,[33] where γ_{H^+}, $\gamma_{HSO_4^-}$, and $\gamma_{SO_4^{2-}}$ are the activity coefficients of hydrogen ion, hydrogensulfate, and sulfate, respectively, and m_{H^+} is the molality of hydrogen ion. When the ionic strength of a solution is so low that the D-H limiting law[23] is valid, γ_{H^+} is equal to $\gamma_{HSO_4^-}$. Then from the values of $\ln(\gamma_{H^+}^2 \gamma_{SO_4^{2-}})$

and $\ln(\frac{\gamma_{H^+}\gamma_{SO_4^{2-}}}{\gamma_{HSO_4^-}})$ given by the Pitzer model, it is possible to calculate γ_{H^+}. Although 500 μmol dm^{-3} is too high to apply this approximation, we calculated γ_{H^+} based on the assumption that γ_{H^+} is equal to $\gamma_{HSO_4^-}$ and obtained 0.9584. Then, the value of $pH_s = -\log \gamma_{H^+} m_{H^+}$ is 3.033. Instead, if we use the D-H limiting law, $\gamma_{H^+} = 0.9566$ and $pH_s = 3.034$. The difference, 0.0018 in γ_{H^+}, corresponds to −0.05 mV in E, which is within the experimental error in the present E measurements. To calculate the activity of hydrogen ions, the molarities of sulfuric acids at 20.0 °C were converted to the molalities using the densities obtained by the extrapolation of the known densities of sulfuric acids at 20.0 °C as a function of the molarity. [34] If the ILSB works ideally, E_j is null and the equation (1.2) reduces to

$$pH_x = pH_s - \frac{FE}{RT \ln 10} \tag{1.3}$$

The pH_x value obtained by the equation (1.3) is hereafter denoted as pH_{ex}.

1.3 Results and Discussion

1.3.1 Comparison of Experimental pH Values with Theoretical Values Based on Pitzer and D-H Models

Figures 1.2 - 1.6 show the time dependence of E for 1h at 20 - 200 μmol dm^{-3} H_2SO_4 in IV in cell (A), respectively. The excursion of E in 1 h was within 0.30 mV (equal to about 0.005 pH) in each run and the standard deviation of E was 0.05 mV for all measurements. However, three independent runs fluctuated around their own values and the pooled standard deviation of the average values was 0.67 mV.

Table 1.1 lists the concentration of H_2SO_4 in molality, the molality of H^+, m_{H^+}, the corresponding ionic activity coefficient, γ_{H^+}, the experimental pH value, pH_{ex}, and calculated pH value, pH_{cal}, for 20, 50, 100, 150, and 200 μmol dm^{-3} H_2SO_4. The value of pH_{ex} was obtained from the average E value for each measurement. The ± 95 % confidence interval of pH_{ex} for the triplicate measurements at each concentration is also given in Table 1.1. The pH_{cal} values were calculated from the molal concentration of H^+ and the corresponding ionic activity coefficient as is the case of pH_s. The average pH_{ex} values were in good agreement

with the pH_{cal} for all concentrations of H_2SO_4 examined, but the average pH_{ex} values were always higher than the corresponding pH_{cal} values by 0.001 to 0.009 pH unit or 0.06 to 0.5 mV in E. The difference between the experimental and theoretical pH values determined using $TBMOEPC_2C_2N$ salt bridge is smaller by one order of magnitude than KClSB[16,22] and the standard deviation of the experimental pH values using $TBMOEPC_2C_2N$ salt bridge is also smaller than those obtained with KClSB.[16] The ILSB thus measures more accurately the activity of hydrogen ions in a dilute sulfuric acid than KClSB. However, the experimental pH values are still higher than the corresponding theoretical values by 0.001 to 0.009 pH unit; the experimental pH values are positively biased by this amount. Two possible reasons for the difference between measured and theoretical values in Table 1.1 are the diffusion potential due to the different mobilities of $TBMOEP^+$ and $C_2C_2N^-$ in the H_2SO_4 solution and the increase in the ionic liquid strength of the H_2SO_4 solution due to the dissolution of $TBMOEPC_2C_2N$.

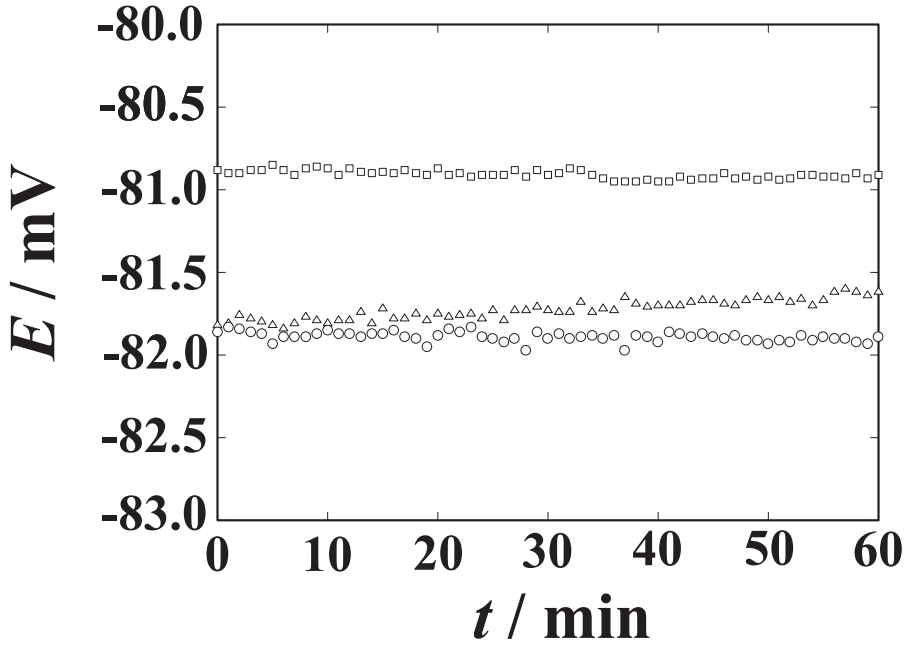

Figure 1.2: Time dependence of E for 1 h at 20 μmol dm^{-3} H_2SO_4 solution in cell (A). Open circle : first measurement, open triangle : second measurement, open square: third measurement.

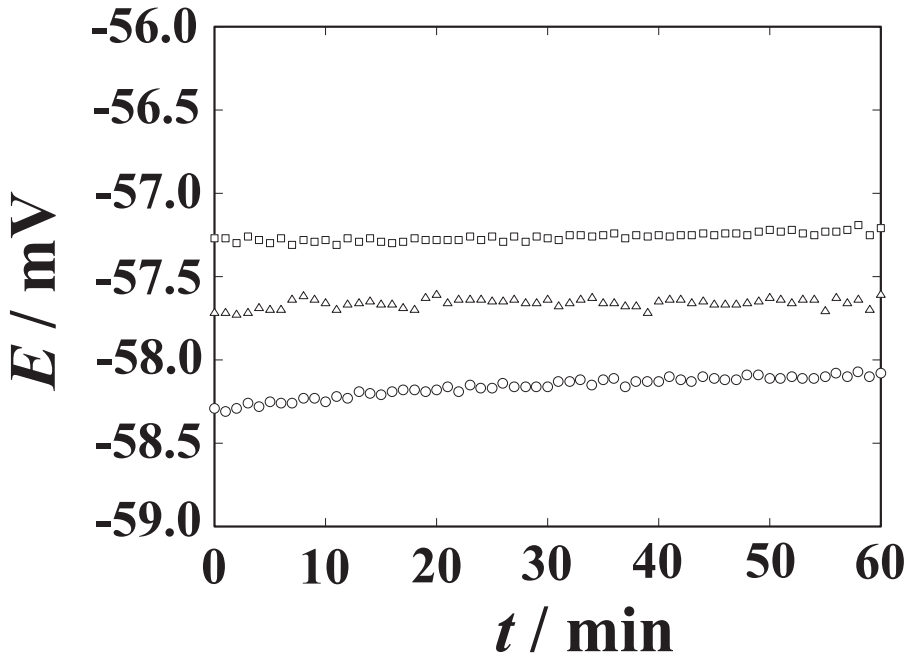

Figure 1.3: Time dependence of E for 1 h at 50 μmol dm^{-3} H_2SO_4 solution in cell (A). Open circle : first measurement, open triangle : second measurement, open square: third measurement.

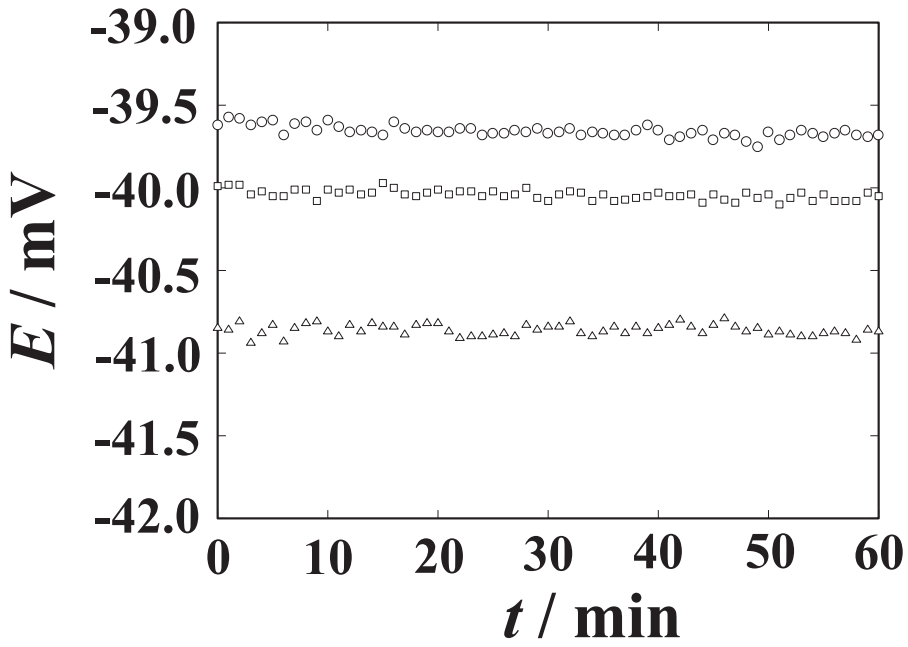

Figure 1.4: Time dependence of E for 1 h at 100 μmol dm^{-3} H_2SO_4 solution in cell (A). Open circle : first measurement, open triangle : second measurement, open square: third measurement.

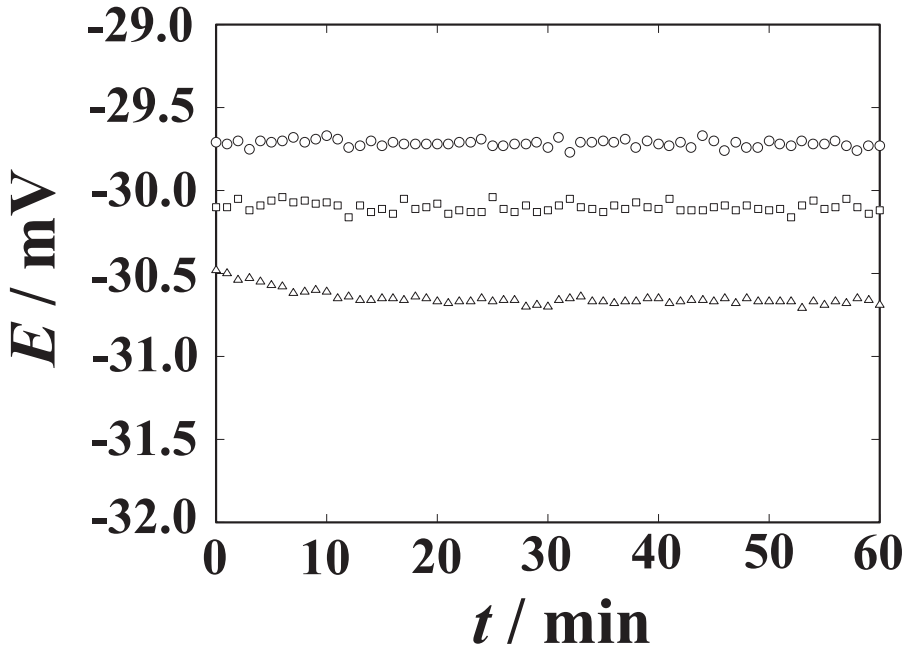

Figure 1.5: Time dependence of E for 1 h at 150 μmol dm^{-3} H_2SO_4 solution in cell (A). Open circle : first measurement, open triangle : second measurement, open square: third measurement.

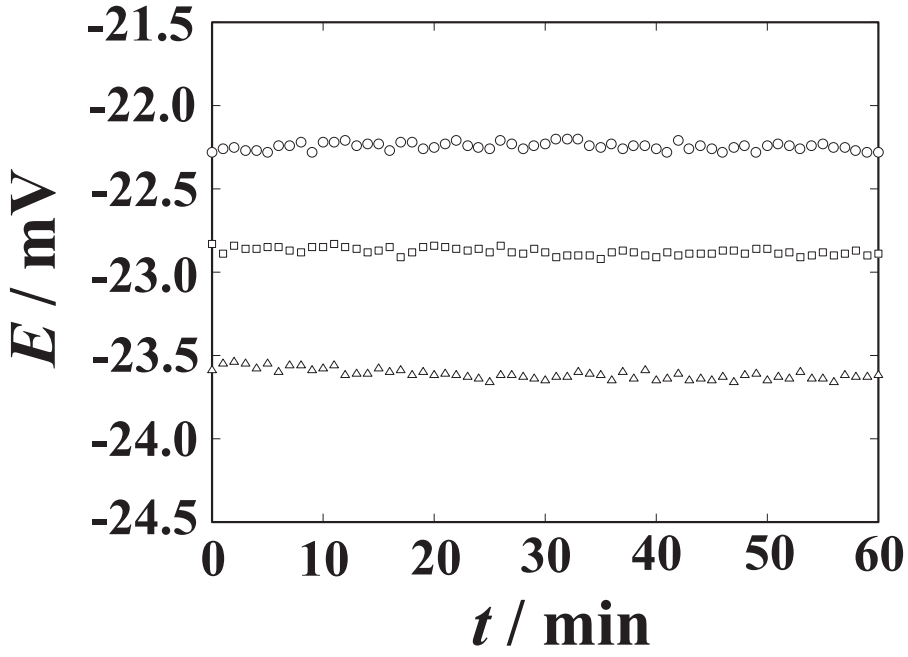

Figure 1.6: Time dependence of E for 1 h at 200 μmol dm^{-3} H_2SO_4 solution in cell (A). Open circle : first measurement, open triangle : second measurement, open square: third measurement.

Table 1.1: The experimental and calculated pH value of 20 - 200 μmol dm^{-3} H_2SO_4.

Molarity of H_2SO_4 / μmol dm^{-3}	Molality of H_2SO_4 / μmol kg^{-1}	m_{H^+} / μmol kg^{-1}	γ_{H^+}	pH_{cal}	Mean pH_{ex} ± 95 % confidence interval	pH_{ex}-pH_{cal}
20	20.06	40.04	0.9910	4.401	4.410 ± 0.021	0.009
50	50.15	99.85	0.9860	4.007	4.008 ± 0.018	0.001
100	100.30	198.87	0.9804	3.710	3.713 ± 0.026	0.003
150	150.45	297.12	0.9762	3.538	3.543 ± 0.020	0.005
200	200.59	394.67	0.9727	3.416	3.421 ± 0.029	0.005

1.3.2 Effect of the Diffusion Potential on Experimental pH Values

When the transfer of the ions in W into the IL is negligibly small, the LJP between the IL and the aqueous solution (W) is described by[35,36]

$$\Delta_{IL}^{W}\phi = \frac{1}{2F}(\Delta_{IL}^{W}G_{tr,A^-}^{IL\rightarrow W,0} - \Delta_{IL}^{W}G_{tr,C^+}^{IL\rightarrow W,0}) + \frac{RT}{2F}\ln\frac{\gamma_{C^+}^{IL}\gamma_{A^-}^{W}}{\gamma_{C^+}^{W}\gamma_{A^-}^{IL}} + \phi_{diff}^{W} \quad (1.4)$$

where $\Delta_{IL}^{W}\phi$ is the inner potential of W referred to that of the IL, $\Delta_{IL}^{W}G_{tr,C^+}^{IL\rightarrow W,0}$ and $\Delta_{IL}^{W}G_{tr,A^-}^{IL\rightarrow W,0}$ are the standard Gibbs energy of transfer of the cation (C^+) and the anion (A^-) constituting the IL from IL to W, respectively, γ_i^{IL} and γ_i^{W} are the activity coefficients of the ions (i = C^+ and A^-) in the phases IL and W, and ϕ_{diff}^{W} is the diffusion potential in W due to the different mobilities of C^+ and A^- in W. Here, ϕ_{diff}^{W} is referred to the electrostatic potential in W at the interface between the IL and W. In the right hand side of the equation (1.4), the first and second terms represent the distribution potential determined by the partition of $TBMOEPC_2C_2N$. In E_j, the sum of two LJPs at the interface between II and III and that at III and IV, the two distribution potentials are canceled out provided that the second term on the right side of the equation(1.4) is negligible. The E_j is then represented by

$$E_j = \phi_{diff}^{W2} - \phi_{diff}^{W1} = \Delta\phi_{diff}^{W} \quad (1.5)$$

where ϕ_{diff}^{W1} and ϕ_{diff}^{W2} are the diffusion potentials in 500 μmol dm^{-3} H_2SO_4 and x μmol dm^{-3} H_2SO_4, respectively.

Since the concentration of H_2SO_4 is uniform in W, the Henderson equation[37] for the diffusion potential is written by

$$\phi^{\mathrm{W}}_{\mathrm{diff}} = \left(\frac{u_{\mathrm{TBMOEP^+}} - u_{\mathrm{C_2C_2N^-}}}{u_{\mathrm{TBMOEP^+}} + u_{\mathrm{C_2C_2N^-}}}\right) \times \frac{RT}{F} \ln \frac{c^{\mathrm{W}}_{\mathrm{TBMOEPC_2C_2N}} (u_{\mathrm{TBMOEP^+}} + u_{\mathrm{C_2C_2N^-}}) + u_{\mathrm{H^+}} c_{\mathrm{H^+}} + 2u_{\mathrm{SO_4^{2-}}} c_{\mathrm{SO_4^{2-}}}}{u_{\mathrm{H^+}} c_{\mathrm{H^+}} + 2u_{\mathrm{SO_4^{2-}}} c_{\mathrm{SO_4^{2-}}}} \quad (1.6)$$

where u_i and c_i are the mobility and the molarity of ion i (i = $TBMOEP^+$, $C_2C_2N^-$, H^+, SO_4^{2-}), respectively, and $c^{\mathrm{W}}_{\mathrm{TBMOEPC_2C_2N}}$ is the solubility of $TBMOEPC_2C_2N$ and 200 μmol dm^{-3}.[28] The values of $u_{\mathrm{TBMOEP^+}}$ and $u_{\mathrm{C_2C_2N^-}}$ at 200 μmol dm^{-3} are 2.58 $\times 10^{-4}$ and 2.66 $\times 10^{-4}$ cm^2 s^{-1} V^{-1},[28] respectively, and $u_{\mathrm{H^+}}$ and $u_{\mathrm{SO_4^{2-}}}$ at 20 - 200 μmol dm^{-3} H_2SO_4 were estimated according to the procedure reported previously.[27] The values of $u_{\mathrm{H^+}}$, $u_{\mathrm{SO_4^{2-}}}$, and $\Delta\phi^{\mathrm{W}}_{\mathrm{diff}}$ are given in Table 1.2. When the effect of the diffusion potential of $TBMOEPC_2C_2N$ in W is taken into account, the experimental pH value, pH'_{ex}, is described by

$$pH'_{ex} = pH_s - \frac{F}{RT \ln 10}(E - \Delta\phi^{\mathrm{W}}_{\mathrm{diff}}) \quad (1.7)$$

The values of pH'_{ex} for 20 - 200 μmol dm^{-3} H_2SO_4 are given in Table 1.2, together with those of pH'_{ex}-pH_{cal}. The difference between the experimental and theoretical pH values becomes smaller by taking account of the possible contribution of $\Delta\phi^{\mathrm{W}}_{\mathrm{diff}}$ to E_j.

Table 1.2: The effect of the diffusion potential due to the dissolution of $TBMOEPC_2C_2N$ on experimental pH values.

Molarity of H_2SO_4 / μmol dm^{-3}	$u_{\mathrm{H^+}}$ / cm^2 s^{-1} V^{-1}	$u_{\mathrm{SO_4^{2-}}}$ / cm^2 s^{-1} V^{-1}	$\Delta\phi^{\mathrm{W}}_{\mathrm{diff}}$/mV	pH'_{ex}	pH'_{ex}-pH_{cal}
20	3.61×10^{-3}	4.13×10^{-4}	-0.199	4.407	0.006
50	3.59×10^{-3}	4.11×10^{-4}	-0.086	4.007	0.000
100	3.57×10^{-3}	4.08×10^{-4}	-0.041	3.712	0.002
150	3.55×10^{-3}	4.06×10^{-4}	-0.024	3.543	0.005
200	3.54×10^{-3}	4.04×10^{-4}	-0.016	3.421	0.005
500	3.48×10^{-3}	3.98×10^{-4}	-	-	-

1.3.3 Effect of the Change in Ionic Strength Due to the Dissolution of $TBMOEPC_2C_2N$

Second, we consider the effect of the finite solubility of the IL in the aqueous phase (W) on the activity of hydrogen ion. In the present study, we did not attempt to determine the actual concentration of $TBMOEPC_2C_2N$ in the aqueous phases. But, in the present measurement of pH using cell (A), the dissolution of $TBMOEPC_2C_2N$ in W can change the ionic strength of W, and in turn change the activity of hydrogen ions in W. When the H_2SO_4 solution is saturated with $TBMOEPC_2C_2N$, the ionic strengths of W(II) and W(IV) would increase by 200 μmol dm^{-3}. The resultant pH values in W(II) and W(IV), pH'_s and pH''_{ex}, were calculated by

$$pH''_{ex} = pH'_s - \frac{FE}{RT \ln 10}. \tag{1.8}$$

The values of pH'_{cal}, pH''_{ex}, and pH''_{ex}-pH'_{cal} are given in Table 1.3. The difference between the experimental and theoretical pH values decreased by allowing for the change in the ionic strength in W, assuming that phase IV is saturated with $TBMOEPC_2C_2N$.

Table 1.3: The effect of change in the ionic strength due to the dissolution of $TBMOEPC_2C_2N$ on experimental pH values.

Molarity of H_2SO_4 / μmol dm^{-3}	pH'_{cal}	pH''_{ex}	pH''_{ex}-pH'_{cal}
20	4.406	4.412	0.006
50	4.010	4.009	-0.001
100	3.712	3.714	0.002
150	3.540	3.544	0.004
200	3.418	3.422	0.004

Taking account of both effects, we may write pH'''_{ex} as

$$pH'''_{ex} = pH'_s - \frac{F}{RT \ln 10}(E - \Delta\phi^{W}_{diff}) \tag{1.9}$$

The values of pH'''_{ex} and pH'''_{ex}- pH'_{cal} for 20 - 200 μmol dm^{-3} H_2SO_4 are given in Table 1.4, where one can see that the difference between the experimental and theoretical pH values is 0.001 ± 0.003 in the concentration range between 20 and 200 μmol dm^{-3}.

Table 1.4: The effects of the diffusion potential and change in the ionic strength due to the dissolution of $TBMOEPC_2C_2N$ on experimental pH values.

Molarity of H_2SO_4 / μmol dm^{-3}	pH'''_{ex}	pH'''_{ex}-pH'_{cal}
20	4.408	0.002
50	4.007	-0.003
100	3.713	0.001
150	3.544	0.004
200	3.421	0.003

1.4 Conclusions

The activities of hydrogen ions in 20 - 200 μmol dm^{-3} H_2SO_4 solution have been reliably estimated using the ILSB sandwiched by two hydrogen electrodes. In other words, the assumption of the cancelling out the LJP between the two sulfuric acid solutions by use of $TBMOEPC_2C_2N$ ILSB is valid to the extent of within 0.003 pH unit or 0.2 mV. The ILSB is a better alternative to the KClSB in estimating the activity of H^+ in dilute aqueous solutions. The accurate pH determination of low ionic strength solutions would be feasible by combining an ILSB-equipped reference electrode and a glass electrode.

An immediate and practical consequence of the ILSB is perceived in pH monitoring in environmental chemistry and geochemistry. What is of more general importance envisaged from the present results is that a well designed ILSB enables us to reliably estimate single ion activities in electrolyte solutions even at higher ionic strengths.

References

(1) Sørensen, S. P. L.; Linderstrøm-Lang, K.; Lund, E. *Compt. Rend. Trav. Lab. Carlsberg* **1924**, *15*, 1–40.

(2) Buck, R. P.; Rondinini, S.; Covington, A. K.; Baucke, F. G. K.; Brett, C. M. A.; Camoes, M. F.; Milton, M. J. T.; Mussini, T.; Naumann, R.; Pratt, K. W.; Spitzer, P.; Wilson, G. S. *Pure Appl. Chem.* **2002**, *74*, 2169–2200.

(3) Galloway, J. N.; Cosby, B. J.; Likens, G. E. *Limnol. Oceanogr.* **1979**, *24*, 1161–1165.

(4) Midgley, D.; Torrance, K. *Analyst* **1979**, *104*, 63–72.

(5) Tyree, S. Y. *Atmos. Environ.* **1981**, *15*, 57–60.

(6) Covington, A. K. *Anal. Chim. Acta* **1981**, *127*, 1–21.

(7) Brezinski, D. P. *Analyst* **1983**, *108*, 425–442.

(8) McQuaker, N. R.; Kluckner, P. D.; Sandberg, D. K. *Environ. Sci. Technol.* **1983**, *17*, 431–435.

(9) Marinenko, G.; Koch, W. F. *Environ. Int.* **1984**, *10*, 315–319.

(10) Johnson, C. A.; Sigg, L. *Chimia* **1985**, *39*, 59–61.

(11) Covington, A. K.; Whalley, P. D.; Davison, W. *Anal. Chim. Acta* **1985**, *169*, 221–229.

(12) Covington, A. K.; Whalley, P. D.; Davison, W. *Pure Appl. Chem.* **1985**, *57*, 877–886.

(13) Davison, W.; Woof, C. *Anal. Chem.* **1985**, *57*, 2567–2570.

(14) Davison, W.; Gardner, M. J. *Anal. Chim. Acta* **1986**, *182*, 17–31.

(15) Koch, W. F.; Marinenko, G.; Paule, R. C. *J. Res. Natl. Bur. Stand (U.S.)* **1986**, *91*, 23–32.

(16) Metcalf, R. C. *Analyst* **1987**, *112*, 1573–1577.

(17) Midgley, D. *Atmos. Environ.* **1987**, *21*, 173–177.

(18) Harbinson, T. R.; Davison, W. *Anal. Chem.* **1987**, *59*, 2450–2456.

(19) Davison, W.; Covington, A. K.; Whalley, P. D. *Anal. Chim. Acta* **1989**, *223*, 441–447.

(20) Metcalf, R. C.; Peck, D. V.; Arent, L. J. *Analyst* **1990**, *115*, 899–905.

(21) Durst, R. A.; Davison, W.; Koch, W. F. *Pure Appl. Chem.* **1994**, *66*, 649–658.

(22) Ozeki, T.; Tsubosaka, Y.; Nakayama, S.; Ogawa, N.; Kimoto, T. *Anal. Sci.* **1998**, *14*, 749–756.

(23) Debye, P.; Hückel, E. *Physik. Z.* **1923**, *24*, 185–206.

(24) Picknett, R. G. *Trans. Faraday Soc.* **1968**, *64*, 1059–1069.

(25) Kakiuchi, T.; Tsujioka, N.; Kurita, S.; Iwami, Y. *Electrochem. Commun.* **2003**, *5*, 159–164.

(26) Kakiuchi, T.; Yoshimatsu, T. *Bull. Chem. Soc. Jpn.* **2006**, *79*, 1017–1024.

(27) Yoshimatsu, T.; Kakiuchi, T. *Anal. Sci.* **2007**, *23*, 1049–1052.

(28) Sakaida, H.; Kitazumi, Y.; Kakiuchi, T. *Talanta* **2010**, *83*, 663–666.

(29) Bradaric, C. J.; Downard, A.; Kennedy, C.; Robertson, A. J.; Zhou, Y. H. *Green Chem.* **2003**, *5*, 143–152.

(30) Earle, M. J.; Gordon, C. M.; Plechkova, N. V.; Seddon, K. R.; Welton, T. *Anal. Chem.* **2007**, *79*, 758–764.

(31) Foropoulos, J.; Desmarteau, D. D. *Inorg. Chem.* **1984**, *23*, 3720–3723.

(32) Feltham, A. M.; Spiro, M. *Chem. Rev.* **1971**, *71*, 177–193.

(33) Pitzer, K. S.; Roy, R. N.; Silvester, L. F. *J. Am. Chem. Soc.* **1977**, *99*, 4930–4936.

(34) *International Critical Tables, Vol. 3*; McGraw-Hill: New York and London, 1928.

(35) Hung, L. Q. *J. Electroanal. Chem.* **1980**, *115*, 159–174.

(36) Kakiuchi, T.; Senda, M. *Bull. Chem. Soc. Jpn.* **1987**, *60*, 3099–3107.

(37) Henderson, P. Z. *Phys. Chem.* **1908**, *63*, 325–345.

Chapter 2

Potentiometric Determination of pH Values of Dilute Sulfuric Acids with Glass Combination Electrode Equipped with Ionic Liquid Salt Bridge

2.1 Introduction

It is difficult to estimate accurately the activity of hydrogen ions in dilute aqueous solutions by potentiometry with a concentrated KCl salt bridge.[1–13] Metcalf reported that the error in the case of the measurements of 50 μmol dm^{-3} H_2SO_4 by use of a glass combination electrode equipped with a KCl salt bridge was 0.055 ± 0.05 pH (positive bias ± two standard deviations).[8] The main reasons of the difficulty are the liquid junction potential (LJP) between a KCl salt bridge (KClSB) and an aqueous solution and the increase of the ionic strength in the aqueous solution due to the dissolution of the KCl solution from the junction part. A new salt bridge composed of a moderately hydrophobic ionic liquid (IL) can solve the problems intrinsic to KClSBs.[14–16] Especially, the ionic liquid salt bridge (ILSB) that consists of the cation and anion with similar mobility in aqueous solution (W), e.g. tributyl(2-methoxyethyl)phosphonium bis(pentafluoroethanesulfonyl)amide

(TBMOEPC_2C_2N), shows a very stable LJP upon contact with a dilute aqueous solution[17,18]. In chapter 1, it was demonstrated that the activities of hydrogen ions in 20 - 200 μmol dm^{-3} H_2SO_4 solution could reliably be estimated within 0.01 pH by use of a TBMOEPC_2C_2N salt bridge sandwiched by two hydrogen electrodes.[19]

However, hydrogen electrodes have weak points in practical use, e.g., long time required for equilibration, difficulty in handling, and interference by redox active substances. A glass electrode has been widely accepted as a hydrogen-ion-responsive electrode instead of a hydrogen electrode. A pH glass electrode combined with an ILSB-type reference electrode would make pH measurements in low ionic strength solutions much more accurate, faster and easier. In the case of pH measurement with a glass electrode, the calibration with pH standard buffers is required.

In this chapter, it will be shown that the activities of the hydrogen ions in the 20 - 200 μmol dm^{-3} H_2SO_4 solution can be estimated more accurately and reliably by use of glass combination electrodes equipped with TBMOEPC_2C_2N salt bridge-type reference electrode. The glass combination electrode with the ILSB-type reference electrode allows us to obtain accurate pH values of low ionic strength solutions with the same procedure as has been used in conventional glass electrodes with KCl-type reference electrode.

2.2 Experimental

2.2.1 Reagents

The TBMOEPC_2C_2N was obtained from Kanto Chemical Co., Inc. and used without further purification. The sulfuric acids of five different concentrations, 20, 50, 100, 150 and 200 μmol dm^{-3}, were prepared according to the procedure described in chapter 1.[19] A phthalate standard solution (0.05 mol kg^{-1} $KHC_8H_4O_4$, pH = 4.008 ± 0.015 at 25°C) and a phosphate standard solution (0.025 mol kg^{-1} KH_2PO_4 + 0.025 mol kg^{-1} Na_2HPO_4, pH=6.865 ± 0.015 at 25°C) were obtained from Kanto Chemical Co., Inc. A 0.05 mol kg^{-1} citrate buffer solution (pH = 3.776 at 25°C) was prepared by dissolving 11.41 g of $KH_2C_6H_5O_7$ (Kanto Chemical Co., Inc. 99 %) in pure water and diluting it to 1.000 ± 0.0004 dm^3.[20] TBMOEPC_2C_2N was

gelled by dissolving 8 g of P(VdF-HFP) and 0.008 dm^3 TBMOEPC_2C_2N in 0.1 dm^3 acetone. The mixture was dried to remove acetone for one week at room temperature to obtain a disk-shaped membrane.[21] The ring-shaped membrane, whose outer diameter, inner diameter, and thickness were 12 mm, 5 mm, and 2.5 mm respectively, was cut out from the disk-shaped membrane.

2.2.2 Methods

Figure 2.1 illustrates the structure of a combination electrode which consists of a glass electrode and a reference electrode equipped with a gelled TBMOEPC_2C_2N salt bridge. The ring-shaped membrane of the gelled IL was mounted with a silicone O-ring to the cylindrical body of the combination electrode. In the ILSB-type reference electrode, the inner cell was composed of an Ag/AgCl electrode in a 0.1 mol dm^{-3} KCl saturated with a TBMOEPC_2C_2N and AgCl. In the glass electrode, the inner cell was composed of an Ag/AgCl electrode in a 0.1 mol dm^{-3} KCl saturated with an AgCl and 0.04 mol dm^{-3} KH_2PO_4 + 0.16 mol dm^{-3} Na_2HPO_4. The Ag/AgCl electrodes were prepared according to the procedure reported previously.[22] The pH responsive glass sticks were prepared by melting the mixture of 60SiO_2, 30Li_2O, 0.1Sc_2O_3, 0.9Y_2O_3, 3La_2O_3, 2Cs_3O, 2BaO and 2Ta_2O_5 (in mol%) and pouring the melted mixture over a Ni board. A stem glass with a pH responsive glass membrane was prepared by melting the pH responsive glass stick and sticking it, in the shape of a hemisphere whose diameter and thickness were 3.5 mm and 0.2 mm respectively, on the top of the stem glass.

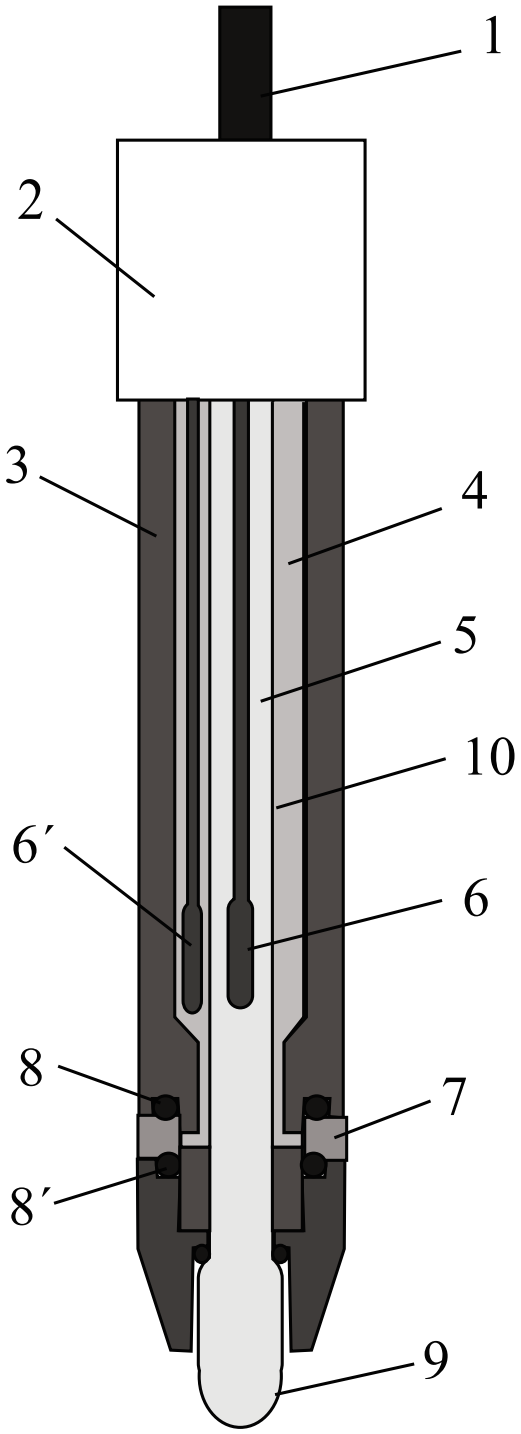

Figure 2.1: Illustration of the pH electrode combined with the glass electrode and the reference electrode equipped with the gelled TBMOEPC_2C_2N salt bridge. 1: lead wire; 2: cap; 3: cylindrical plastic body; 4: 0.1 mol dm^{-3} saturated with an AgCl and a TBMOEPC_2C_2N; 5: 0.1 mol dm^{-3} KCl saturated with an AgCl and 0.04 mol dm^{-3} KH_2PO_4 + 0.16 mol dm^{-3} Na_2HPO_4; 6 and 6′: Ag/AgCl electrode; 7: gelled TBMOEPC_2C_2N; 8 and 8′: silicon O-ring; 9: hydrogen-ion-responsive glass membrane; 10: stem glass.

The electrochemical cell with the glass electrode and the ILSB-type reference electrode employed for the pH determination is represented as

I	II	III	IV	V	VI	
Ag	AgCl	0.1 mol dm^{-3} KCl saturated with $TBMOEPC_2C_2N$ and AgCl	gelled $TBMOEPC_2C_2N$	pH standards or x μmol dm^{-3} H_2SO_4	glass electrode	(A)

The single vertical bar indicates the phase boundary, and the single dashed vertical bar indicates the liquid junction between two electrolyte solutions of different compositions.

The cell voltage, E, i.e., the potential of the right-hand-side terminal referred to that of the left in cell (A), was measured with a pH meter (Horiba, Ltd., F53) at a sampling rate of 0.3 Hz. The measurements of E for three sets of sample solutions of the same composition with three pH meters were performed in parallel. Three polypropylene containers containing 0.02 dm^3 sample solution (V in cell A) were set in a water bath kept at 25.0 ± 0.1 °C. The combination electrodes were first rinsed with MilliQ water, and then dipped into the container for potentiometric measurements. Cell A was calibrated with two pH standard buffers before the measurement of each concentration of H_2SO_4. Two sets of pH standard buffers employed for the two point calibration were (1) the phosphate buffer and the citrate buffer and (2) the phosphate buffer and the phthalate buffer. E in the phosphate buffer was first measured before the other buffer.

The E values in a sulfuric acid solution were measured for 15 min in each measurement. The measurement of E in each concentration of sulfuric acid solutions was repeated five times. The electrodes were dipped into a beaker containing 0.08 dm^3 MilliQ water and stirred gently for 10 s before pH measurements. The electrodes were washed three times with different MilliQ water. The water wetting the electrodes after the washing was wiped off with Kimwipes®. For pH measurements of H_2SO_4 solutions, after the washing with wa-

ter, the electrodes were further washed for 10 s with the same H_2SO_4 solution as the sample solution in order to remove completely the water adhered to the surface of the electrodes. Measurements of two concentrations of sulfuric acid solutions with three sets of electrodes were completed in one day, and it took 3 days to complete all measurements for 20 - 200 μmol dm^{-3} H_2SO_4 sample solutions.

2.2.3 Experimental pH Values of Dilute Sulfuric Acids

When cell (A) is calibrated with a standard buffer, pH_S, an unknown pH value of H_2SO_4 solutions, pH_x, in V in cell (A) is written by[23]

$$pH_x = pH_S - \frac{[E_{ex} - E_S - (E_{j(x)} - E_{j(S)})]F}{RT \ln 10} \tag{2.1}$$

where E_{ex} and E_S are the readings of the pH electrode for the H_2SO_4 solution and the standard buffer whose pH values are pH_x and pH_S, respectively, $E_{j(x)}$ and $E_{j(S)}$ are the LJPs at ILSB | x μmol dm^{-3} H_2SO_4 and ILSB | the standard buffer solution interfaces, F is the Faraday constant, R is the gas constant, and T is the absolute temperature. Glass electrodes may exhibit the pH response smaller than the theoretical value, $RT \ln 10/F$ volts per pH unit.[24,25] The safest procedure is to use the operative Nernst slope, k', which is obtained from the two-point calibration of the electrode.

$$k' = \frac{E_{S_1} - E_{S_2}}{pH_{S_2} - pH_{S_1}}, \tag{2.2}$$

where E_{S_1} and E_{S_2} are the pH cell voltages for the buffers pH_{S_1} and pH_{S_2}, respectively. When k' is used, eq (2.1) is represented by

$$pH_x = pH_S - \frac{E_{ex} - E_S - (E_{j(x)} - E_{j(S)})}{k'} \tag{2.3}$$

If the ILSB works ideally, $E_{j(x)}$ is equal to $E_{j(S)}$ and eq (2.3) reduces to

$$pH_x = pH_S - \frac{E_{ex} - E_S}{k'} \tag{2.4}$$

The pH_x value obtained by eq (2.4) is hereafter denoted as pH_{ex}.

2.3 Results and Discussion

2.3.1 Time Courses of *E* at Different Concentrations of Sulfuric Acids

Figure 2.2 exemplifies the time dependence of *E* in one of the combination electrodes for 15 min at phosphate (○), phthalate (△) and citrate (□) buffers. *E* reached a steady value after 1 min for the three buffers. The change in *E* from 1 min to 15 min after the start of the measurements was within 0.3 mV for all cases. The operative Nernst slope was calculated with the two values of *E* after 15 min for the phosphate and citrate standards, or the phosphate and phthalate standards from eq 2.2. Figure 2.3 exemplifies the time dependence of *E* for 15 min at 20 (○), 50 (△), 100 (□), 150 (●) and 200 (▲) μmol dm^{-3} H_2SO_4. The change in the values of *E* from 1 min to 15 min after starting the measurements was within 0.2 mV for all cases of measurements of H_2SO_4.

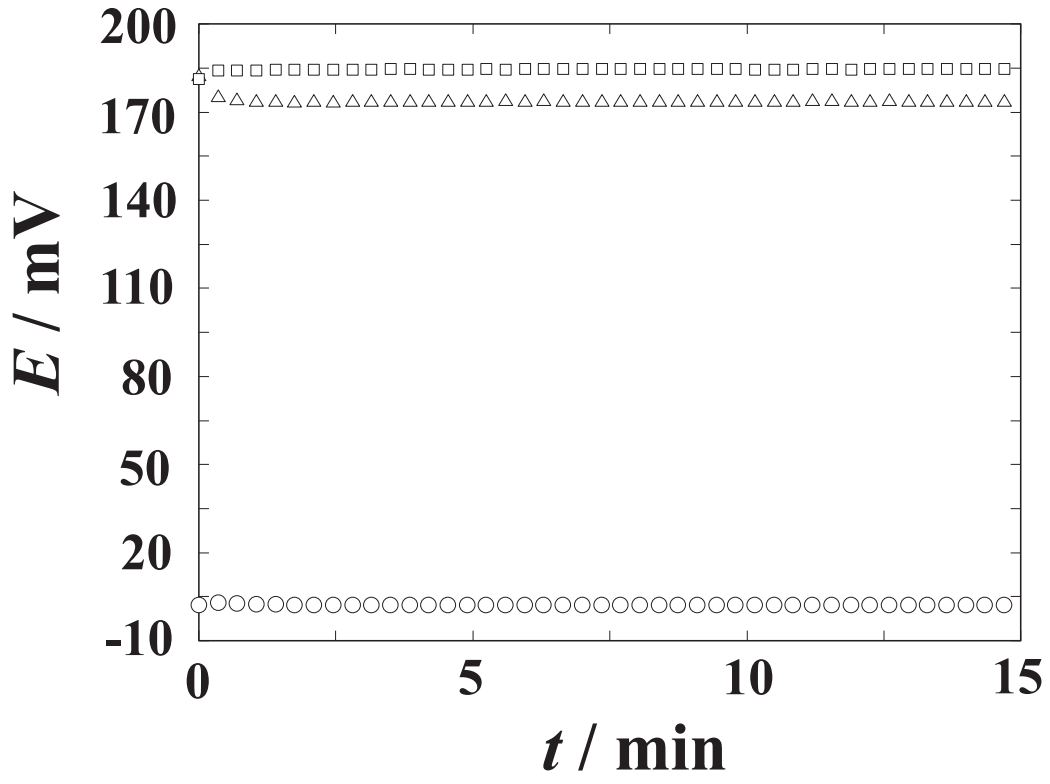

Figure 2.2: Time dependence of *E* for 15 min at pH standards in cell (A). Phosphate (○), phthalate (△) and citrate (□) standard solution.

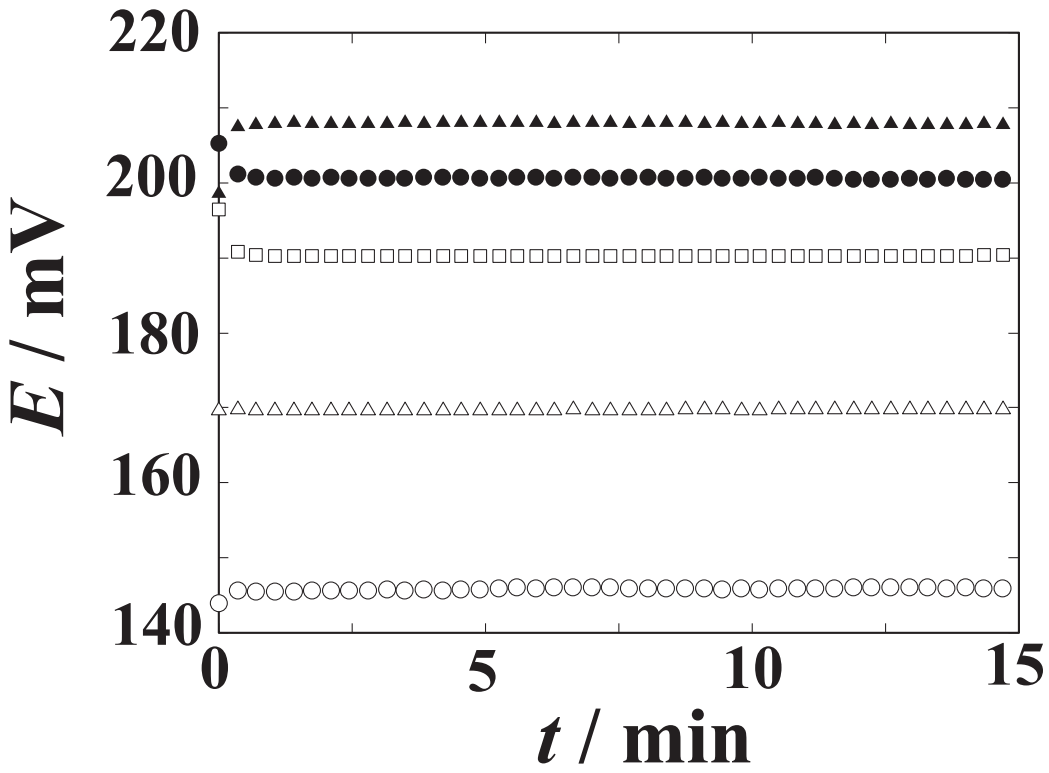

Figure 2.3: Time dependence of E for 15 min at 20 - 200 μmol dm^{-3} H_2SO_4 solutions in cell (A). 20 (○), 50 (△), 100 (□), 150 (●) and 200 (▲) μmol dm^{-3} H_2SO_4.

2.3.2 Comparison of pH Values Deduced from eq (2.4) with Theoretical Values

Table 2.1 lists the molality of H_2SO_4, the molality of H^+, m_H, the corresponding ionic activity coefficient, γ_{H^+}, the operative Nernst slope, k', the calculated pH value, pH_{cal}, and the experimental pH value, pH_{ex}, for 20, 50, 100, 150 and 200 μmol dm^{-3} H_2SO_4. The average of the values of k' obtained for each of three sets of electrodes is given in Table 2.1. The value of pH_{ex} was obtained from the E value after 15 min. The average of pH_{ex} at each concentration of H_2SO_4 was calculated from fifteen E values obtained from the measurements with three sets of electrodes. The 95 % confidence interval of pH_{ex} for fifteen measurements at each concentration is also given in the 7th column in Table 2.1. The pH_{cal} values were calculated by the Pitzer and Debye-Hückel models as described in chapter 1.[19]

Metcalf showed that the pH value of 50 μmol dm^{-3} H_2SO_4 measured by use of a glass

combination electrode equipped with a KCl salt bridge was 4.06 ± 0.05 pH (average pH value ± two standard deviations).[8] This average value is positively biased by 0.053 from the calculated value of 4.007. The present result in Table 2.1 at the 50 μmol dm^{-3} H_2SO_4 solution, 4.030 ± 0.003, is closer to the calculated value, and the 95 % confidence interval of the experimental pH values is smaller by one order of magnitude than that[8] obtained with the KClSB-type. The TBMOEPC_2C_2N salt bridge-type combination electrode thus estimates more accurately the activity of hydrogen ions based on the operational definition of the practical pH value in a dilute sulfuric acid than the KClSB-type combination electrode.

In the present study, the average pH_{ex} values (Table 2.1) showed a positive bias to the corresponding pH_{cal} values by 0.005-0.032 pH unit. Two possible factors that can give rise to this bias are the diffusion potential due to the slight difference between the mobility of TBMOEP$^+$ and $C_2C_2N^-$ in the H_2SO_4 solution and an increase in the ionic liquid strength of the H_2SO_4 solution due to the dissolution of TBMOEPC_2C_2N.

Table 2.1: Experimental pH values obtained with the two point calibration by use of the phosphate and citrate standards and calculated pH value of 20 - 200 μmol dm^{-3} H_2SO_4.

Molarity of H_2SO_4 / μmol dm^{-3}	Molality of H_2SO_4 / μmol kg^{-1}	m_H / μmol kg^{-1}	γ_H	k' / V	pH_{cal}	Mean pH_{ex} ± 95 % confidence interval	pH_{ex}-pH_{cal}
20	20.06	40.04	0.9910	0.05910	4.401	4.433 ± 0.011	0.032
50	50.15	99.85	0.9860	0.05909	4.007	4.030 ± 0.003	0.023
100	100.30	198.87	0.9804	0.05924	3.710	3.718 ± 0.003	0.008
150	150.45	297.12	0.9762	0.05905	3.538	3.544 ± 0.004	0.006
200	200.59	394.67	0.9727	0.05913	3.416	3.421 ± 0.002	0.005

2.3.3 Effect of Diffusion Potential on Experimental pH Values

If the two distribution potentials at the ILSB | H_2SO_4 and ILSB | phosphate standard solution interfaces are canceled out, the experimental pH value, pH'_{ex}, is expressed by

$$pH'_{ex} = pH_S - \frac{E_{ex} - E_S - \phi^W_{diff}}{k'} \quad (2.5)$$

where ϕ^W_{diff} is the diffusion potential due to the dissolution of IL from the ILSB in x μmol dm^{-3} H_2SO_4 solution and is referred to the electrostatic potential in the bulk sample solution phase. The diffusion potential in the phosphate and citrate standard solutions has been neglected in eq 2.5 because the ionic strength of the standard solutions is much higher than the solubility of the IL in W.[16] The values of ϕ^W_{diff} in dilute H_2SO_4 solutions[19] have been calculated from the Hendarson equation.[26] The pH'_{ex} and $pH'_{ex} - pH_{cal}$ are given in Table 2.2. When the effect of the diffusion potential of TBMOEPC_2C_2N in the H_2SO_4 due to the dissolution of TBMOEPC_2C_2N is considered, the experimental pH values are closer to the corresponding theoretical pH values by 0.001 - 0.003 than those in Table 2.1.

Table 2.2: Effect of the diffusion potential and the change in the ionic strength due to the dissolution of TBMOEPC_2C_2N on experimental pH values.

Molarity of of H_2SO_4 / μmol dm^{-3}	ϕ^W_{diff} / mV	pH'_{cal}	pH'_{ex}	pH'_{ex}-pH_{cal}	pH_{ex}-pH'_{cal}	pH'_{ex}-pH'_{cal}
20	-0.199	4.406	4.430	0.029	0.027	0.024
50	-0.086	4.010	4.028	0.021	0.020	0.018
100	-0.041	3.712	3.718	0.008	0.006	0.006
150	-0.024	3.540	3.543	0.005	0.004	0.003
200	-0.016	3.418	3.421	0.005	0.003	0.003

2.3.4 Effect of Finite Solubility of IL in W

The theoretical pH values, pH'_{cal}, are calculated taking account of the 200 μmol dm^{-3} increase of the ionic strength in the H_2SO_4 solution due to the dissolution of TBMOEPC_2C_2N.[17] pH'_{cal} and $pH_{ex} - pH'_{cal}$ are also given in Table 2.2. The difference between the experimental and theoretical pH values is thus smaller by 0.002 - 0.005 than that in Table 2.1. The values

of $pH'_{ex} - pH'_{cal}$ for 20 - 200 μmol dm^{-3} H_2SO_4 are also given in Table 2. When both effects are taken into account, the difference between the experimental and theoretical pH values is smaller than by 0.002 - 0.008 than that in Table 2.1.

2.3.5 Uncertainty of pH of Primary Standard Solutions

The values of pH_{ex} in Table 2.2 are still higher than the theoretical values by 0.003 - 0.024. A possible reason for the remaining difference between the experimental and theoretical value is the uncertainty of 0.01 in pH values assigned to the primary standards associated with the Bates-Guggenheim convention.[25,27] This uncertainty dose not arise when the pH determination for an unknown sample solution is performed based on the pH value of a sufficiently dilute aqueous solution as given in chapter 1.[19]

2.3.6 Uncertainty in Calibration of Glass Electrodes in Combination with ILSB - Equipped Reference Electrode

The deviation of about 0.01 pH unit remains even if the uncertainty of pH values assigned to pH standards is taken into account. There are two possible factors for the remaining difference. First, the operative Nernst slope, k', obtained at the two point calibration may not be the same as that obtained at the measurement of the H_2SO_4 solution. Second, the LJP between the ILSB and the standard buffer solution may shift due to the specific interaction between the hydrogen or dihydrogen phosphate ions and $TBMOEPC_2C_2N$, or the hydrogen or dihydrogen citrate ions and $TBMOEPC_2C_2N$.

2.3.7 Effect of Hydrogen Phthalate Ions on Two Point Calibration with a Phthalate Buffer

The experimental pH values, $pH_{ex(ph)}$, which were obtained in the two point calibration with the phthalate standard buffer instead of the citrate standard buffer are given in Table 2.3. The operative Nernst slopes, $k'_{(ph)}$, obtained by the two point calibration with the phosphate and phthalate standard buffers for the pH measurements of 20 - 200 μmol dm^{-3} H_2SO_4 solutions

are listed in Table 2.3. These values obtained are higher by 0.02 ~ 0.03 pH unit than those with the citrate buffer for all concentrations of H_2SO_4. The difference is ascribed to the positive shift of the LJP between the TBMOEPC_2C_2N phase and the phthalate standard due to the dissolution of hydrogen phthalate ions into the IL phase.[22] The values of $k'_{(ph)}$ listed in Table 2.3 are larger than the theoretical Nernst slope, 59.16 mV at 25 °C. When the shift of the LJP between the TBMOEPC_2C_2N phase and the phthalate standard is positive, the value of $k'_{(ph)}$ is larger than the theoretical Nernst slope. When the theoretical value, 59.16 mV, is used at the estimate of $pH_{ex(pH)}$ value in 20 μmol dm^{-3} H_2SO_4 solution instead of 59.75 mV, the value of $pH_{ex(pH)}$ is 4.439, and is nearly consistent with the value obtained in the two point calibration with the citrate buffer, 4.433. The increase of $pH_{ex(ph)}$ can thus be explained by the positive shift of the LJP due to the dissolution of hydrogen phthalate ions into the IL phase. Although the phthalate standard buffer is used more widely all over the world as a primary standard on the lower side of pH scale than a citrate, the citrate buffer is recommended in the pH determination with TBMOEPC_2C_2N - based reference electrodes.

Table 2.3: Experimental pH values obtained with the two point calibration by use of phosphate and phthalate standards.

Molarity of		Mean $pH_{ex(ph)}$	
H_2SO_4 / μmol dm^{-3}	$k'_{(ph)}$ / V	95 % confidence interval	$pH_{ex(ph)}$-pH_{cal}
20	0.05975	4.464 ± 0.005	0.063
50	0.05983	4.047 ± 0.004	0.040
100	0.05981	3.745 ± 0.003	0.035
150	0.05975	3.570 ± 0.003	0.032
200	0.05974	3.444 ± 0.007	0.028

2.4 Conclusions

By use of the combination electrode that consists of a glass electrode and a reference electrode equipped with the gelled TBMOEPC_2C_2N salt bridge, the activities of hydrogen ions in 20-200 μmol dm^{-3} H_2SO_4 solution were determined based on the two-point calibration of the electrode. The combination electrode enables us to determine more accurately pH of a dilute aqueous solution on the basis of the operative pH definition than those by use of pH electrodes in combination with KCl-type reference electrode. The ILSB-based glass combination electrode gives a solution to the problem intrinsic to pH glass combination electrodes equipped with a KCl salt bridge in determination of pH of low ionic strength samples, which are to be commonly measured in geochemistry, environmental science, and certain branches of industry and commerce.

References

(1) Galloway, J. N.; Cosby, B. J.; Likens, G. E. *Limnol. Oceanogr.* **1979**, *24*, 1161–1165.

(2) Tyree, S. Y. *Atmos. Environ.* **1981**, *15*, 57–60.

(3) Marinenko, G.; Koch, W. F. *Environ. Int.* **1984**, *10*, 315–319.

(4) Covington, A. K.; Whalley, P. D.; Davison, W. *Pure Appl. Chem.* **1985**, *57*, 877–886.

(5) Davison, W.; Woof, C. *Anal. Chem.* **1985**, *57*, 2567–2570.

(6) Davison, W.; Gardner, M. J. *Anal. Chim. Acta* **1986**, *182*, 17–31.

(7) Koch, W. F.; Marinenko, G.; Paule, R. C. *J. Res. Natl. Bur. Stand (U.S.)* **1986**, *91*, 23–32.

(8) Metcalf, R. C. *Analyst* **1987**, *112*, 1573–1577.

(9) Midgley, D. *Atmos. Environ.* **1987**, *21*, 173–177.

(10) Davison, W.; Covington, A. K.; Whalley, P. D. *Anal. Chim. Acta* **1989**, *223*, 441–447.

(11) Metcalf, R. C.; Peck, D. V.; Arent, L. J. *Analyst* **1990**, *115*, 899–905.

(12) Durst, R. A.; Davison, W.; Koch, W. F. *Pure Appl. Chem.* **1994**, *66*, 649–658.

(13) Ozeki, T.; Tsubosaka, Y.; Nakayama, S.; Ogawa, N.; Kimoto, T. *Anal. Sci.* **1998**, *14*, 749–756.

(14) Kakiuchi, T.; Tsujioka, N.; Kurita, S.; Iwami, Y. *Electrochem. Commun.* **2003**, *5*, 159–164.

(15) Kakiuchi, T.; Yoshimatsu, T. *Bull. Chem. Soc. Jpn.* **2006**, *79*, 1017–1024.

(16) Yoshimatsu, T.; Kakiuchi, T. *Anal. Sci.* **2007**, *23*, 1049–1052.

(17) Sakaida, H.; Kitazumi, Y.; Kakiuchi, T. *Talanta* **2010**, *83*, 663–666.

(18) Fujino, Y.; Kakiuchi, T. *J. Electroanal. Chem.* **2011**, *651*, 61–66.

(19) Shibata, M.; Sakaida, H.; Kakiuchi, T. *Anal. Chem.* **2011**, *83*, 164–168.

(20) Staples, B. R.; Bates, R. G. *J. Res. Nat. Bur. Stand.* **1969**, *A 73*, 37–41.

(21) Fuller, J.; Breda, A. C.; Carlin, R. T. *J. Electroanal. Chem.* **1998**, *459*, 29–34.

(22) Shibata, M.; Yamanuki, M.; Iwamoto, Y.; Nomura, S.; Sakaida, H.; Kakiuchi, T. *Anal. Sci.* **2010**, *26*, 1203–1206.

(23) Bates, R. G. *Chem. Rev.* **1948**, *42*, 1–61.

(24) Baucke, F. G. K. *Anal. Chem.* **1994**, *66*, 4519–4524.

(25) Buck, R. P.; Rondinini, S.; Covington, A. K.; Baucke, F. G. K.; Brett, C. M. A.; Camoes, M. F.; Milton, M. J. T.; Mussini, T.; Naumann, R.; Pratt, K. W.; Spitzer, P.; Wilson, G. S. *Pure Appl. Chem.* **2002**, *74*, 2169–2200.

(26) Henderson, P. Z. *Phys. Chem.* **1908**, *63*, 325–345.

(27) Bates, R. G. *Analyst* **1952**, *77*, 653–660.

Chapter 3

Reexamination of the pH Values Assigned to Aqueous Phosphate Buffers Used as a Primary Standard for pH Determination

3.1 Introduction

pH is the most widely used measure for the acidity of solutions. Accurate pH measurements are necessary in many facets of our life and environments. The notional definition[1,2] adapted internationally is

$$\mathrm{pH} = -\log a_{\mathrm{H^+}} \tag{3.1}$$

where $a_{\mathrm{H^+}}$ is the activity of hydrogen ions. However, the single ion activity can not be measured without an extrathermodynamic assumption. In practice, the pH value of unknown sample solutions is determined based on the pH value assigned to the standard buffer solutions.[3]

The pH values of primary standard buffer solutions are determined by use of the electrochemical cell, known as a Harned cell, which consists of a hydrogen electrode and a silver-silver halide electrode,[2,4] and is believed to be a cell without a liquid junction. In this method, the activity coefficient of halide ions in the buffer solution should be known to determine the activity of hydrogen ions. For the solutions of low ionic strength (I < 0.1 mol

kg^{-1}), the activity coefficient of chloride ion may be calculated from Debye-Hückel (D-H) equation[5] as a reasonably approximation:

$$\log \gamma_{Cl^-} = -\frac{A\sqrt{I}}{1 + B\text{å}\sqrt{I}} \tag{3.2}$$

where A and B are constants which vary with the temperature and dielectric constant of the solvent and å is the ion size parameter introduced to take account of the mean distance of closest approach of the ions. Bates and Guggenheim suggested that γ_{Cl^-} at ionic strengths not exceeding 0.1 mol kg^{-1} can be calculated by equation (3.2) with Bå = 1.5 $kg^{1/2}$ $mol^{-1/2}$, which is called as Bates-Guggenheim convention.[3] Bates estimated the uncertainty associated with this estimation of the activity coefficient of halide ions to be ± 0.01 pH unit on the pH determination of 0.025 mol kg^{-1} equimolal phosphate buffer solution.[6] The values of pH determined based on the pH values assigned to standard buffer solutions by use of a Harned cell in combination with Bates-Guggenheim convention thus bear the uncertainty of ± 0.01 pH unit (95 % confidence interval).[2]

This chapter describes a new method to determine the activity of hydrogen ions in phosphate standard buffer solution by use of the electrochemical cell[7] with an ionic liquid salt bridge[8–11] (ILSB). In this method, pH values of buffer solutions is determined based on the activity of hydrogen ions in a sufficient dilute sulfuric acid solution, to which the Debye-Hückel (D-H) limiting law[5] is reliable to deduce the activity coefficient of changed species assuming that the LJPs between the ILSB and the dilute H_2SO_4 solution and that between the ILSB and a buffer solution are negligible. This method of pH determination of a buffer solution is expected to be more reliable than the pH determination by use of Harned cells in combination with Bates-Guggenheim convention.

The author will show that the activity of the hydrogen ions in equimolal phosphate buffer solutions containing potassium dihydrogen phosphate and disodium hydrogen phosphate can be accurately estimated by use of an ILSB that consists of tributyl(2-methoxyethyl) phosphonium bis(pentafluoroethanesulfonyl)amide ($TBMOEPC_2C_2N$) sandwiched by two hydrogen electrodes. In other words, the $TBMOEPC_2C_2N$ salt bridge can effectively cancel out the LJP between the 50 μmol dm^{-3} H_2SO_4 solution and the equimolal phosphate buffer solution. The results suggest that the pH determination by use of an ILSB has potential to

become the more exact method than conventional pH determination by use of Harned cells in combination with the Bates-Guggenheim assumption.

3.2 Experimental

3.2.1 Reagents

The TBMOEPC_2C_2N was obtained form Kanto Chemical Co., Inc. and washed 25 times with MilliQ water to remove halide impurities. After the 15th washing, Cl^- was not detected when a few drops of a $AgNO_3$ solution were added to the supernatant solution. TBMOEPC_2C_2N was then purified by column chromatography.[12] TBMOEPC_2C_2N was saturated with MilliQ water before potentiometric pH measurements. Because the acidity of hydrogen bis(trifluoromethanesulfonyl)amide is stronger than HNO_3,[13] $C_2C_2N^-$ is presumably not protonated in contact with the aqueous dilute sulfuric acid solution and phosphate buffer solutions employed in the present study. The 50×10^{-6} mol dm^{-3} sulfuric acid solution was prepared according to the procedure described in chapter 1.[7] Equimolal phosphate buffer solutions of seven different molality, 0.01, 0.0175, 0.025, 0.0375, 0.05, 0.075, and 0.1 mol kg^{-1}, were prepared by weighing KH_2PO_4 (99.6 %), Na_2HPO_4 (99.5 %), and MilliQ water. KH_2PO_4 and Na_2HPO_4 were obtained from Kanto Chemical Co., Inc. and used without further purification. Na_2HPO_4 was dried for two hours at 110 °C before the preparation of phosphate buffer solutions. Hydrogen electrodes were prepared according to the procedure described in chapter 1.[7]

3.2.2 Methods

The electrochemical cell employed is represented as

I	II	III	IV	V	
	H_2,		H_2,		
Pt	50 μmol dm^{-3}	TBMOEPC$_2$C$_2$N	phosphate buffer	Pt	
	H_2SO_4		solution		(A)

The single dashed vertical bars indicate the interfaces between the ILSB and the aqueous solutions (II and IV). The configuration of a U-type glass cell for cell (A) was the same as what we reported previously.[7] The cell voltage, E, i.e., the potential of the right-hand-side terminal referred to that of the left in the cell (A), was measured with an electrometer (ADC Corporation, 8252) with a GPIB interface. The sampling interval was 1 min. Each of the two hydrogen electrodes was supplied with hydrogen gas (99.9995 %), which was generated by a hydrogen gas generator (Horiba Stec, OPGU-7100), at the rate of two to three bubbles per second from a jet about 1 mm in diameter. The hydrogen gas was passed through a saturator containing the same solution as the one in the hydrogen electrode compartment before it entered the cell.

E was measured at 0.01, 0.0175, 0.025, 0.0375, 0.05, 0.075, and 0.1 mol kg^{-1} phosphate buffer solutions in phase IV in cell (A). The cell was immersed in a water bath maintained at 25.0 ± 0.1 °C. The measurement at each molality of the phosphate buffer was repeated ten times. The measurement at each molality of phosphate buffer solutions was completed in three days and it took 21 days to complete all measurements. After each measurement, both 50 μmol dm^{-3} H_2SO_4 solution and phosphate buffer solution in phases II and IV in cell (A) was drained and the U-type glass cell and two platinum electrodes were washed with MilliQ water three times. The values of E were recorded for 1 h after the hydrogen gas was passed in cell (A) for 1 h. The average of E values recorded in the last ten min at each measurement was employed to estimate the pH value.

3.2.3 Experimental pH Values of Equimolal Phosphate Buffer Solutions

An unknown pH value of phosphate buffer solutions (pH_x) in IV in cell (A) is written by

$$pH_x = pH_s - \frac{F}{RT \ln 10}(E - E_j) \tag{3.3}$$

where pH_s is the pH value of the 50 μmol dm^{-3} H_2SO_4 solution in II in cell (A), and E_j is the sum of two LJPs on both sides of the ILSB in cell (A), F is the Faraday constant, R is the gas constant, and T is the absolute temperature. The value of pH_s at 25 °C was calculated by the following iterative procedure. We have the dissociation equilibrium

$$HSO_4^- = H^+ + SO_4^{2-} \tag{3.4}$$

$$K_2 = \left(\frac{m_{H^+} m_{SO_4^{2-}}}{m_{HSO_4^-}}\right)\left(\frac{\gamma_{H^+}\gamma_{SO_4^{2-}}}{\gamma_{HSO_4^-}}\right) \tag{3.5}$$

where m_{H^+}, $m_{HSO_4^-}$, and $m_{SO_4^{2-}}$ are the molalities of the hydrogen ion, hydrogen sulfate, and sulfate, respectively. In eq. (3.5), γ_{H^+}, $\gamma_{HSO_4^-}$, and $\gamma_{SO_4^{2-}}$ are the activity coefficients of the hydrogen ion, hydrogen sulfate, and sulfate, respectively. K_2 is the dissociation constant and the value at 25 °C[14] is 0.0105. First, m_{H^+} was obtained as the quadratic solution of the equation (3.5) by the substitution of $m_{HSO_4^-} = 2m - m_{H^+}$, $m_{SO_4^{2-}} = m_{H^+} - m$, where m is the molality of sulfuric acid solution, and $\gamma_{H^+}\gamma_{HSO_4^-}/\gamma_{SO_4^{2-}} = 1$ to the equation (3.5). The activity coefficients of each ionic species, γ_i (i = H^+, HSO_4^-, and SO_4^{2-}) was calculated with the ionic strength of the sulfuric acid solution in the molality scale, I, from the Debye-Hückel limiting law[5]

$$\log \gamma_i = -0.5108 z_i^2 \sqrt{I} \tag{3.6}$$

where z_i is the valence of the ion i. When the difference between K_2 and the dissociation constant recalculated from m_i and γ_i (i=H^+, HSO_4^-, and SO_4^{2-}), K_2', was greater than 10^{-9}, m_{H^+} was recalculated by substituting $K_2/\left(\frac{\gamma_{H^+}\gamma_{SO_4^{2-}}}{\gamma_{HSO_4^-}}\right)$ to $K_2'/\left(\frac{\gamma_{H^+}\gamma_{SO_4^{2-}}}{\gamma_{HSO_4^-}}\right)$ in the equation (3.5). When the iterative calculation of K_2' converged, pH_s was obtained from

$$pH_s = -\log \gamma_{H^+} m_{H^+} \tag{3.7}$$

To calculate the activity of hydrogen ions, the molarities of sulfuric acids at 20.0 °C were converted to the molalities using the densities obtained by the extrapolation of the known

densities of sulfuric acids at 20.0 °C as a function of the molarity.[15] The values of m_{H^+}, γ_{H^+}, and pH_s in 50 μmol dm^{-3} H_2SO_4 solution at 25 °C are 99.85, 0.9857, and 4.007, respectively. Assuming the ILSB works ideally, E_j is null and pH_{ex} is determined by

$$pH_x = pH_s - \frac{FE}{RT \ln 10} \tag{3.8}$$

The pH_x value obtained by the equation (3.8) is hereafter denoted as pH_{ex}.

3.3 Results and Discussion

3.3.1 Time Course of *E* at Different Molality of Phosphate Buffer Solutions at 25 °C.

Figures 3.1 - 3.7 show the time dependence of *E* for 1h at 0.01, 0.0175, 0.025, 0.0375, 0.05, 0.075, and 0.1 mol kg^{-1} phosphate buffer solutions in IV in cell (A) at 25 °C, respectively. In each run, the excursion of *E* in 1 h was within 0.6 mV (equal to about 0.01 pH), with two exceptions, 0.01 mol kg^{-1} phosphate buffer solution (1.23 and 0.75 mV). Except these two cases, the average of excursion in 1 h for all measurements was 0.26 ± 0.16 mV.

3.3.2 Comparison of Experimental pH Values Obtained by Use of ILSB with Calculated pH Values or pH Values Obtained by Use of a Harned Cell.

Figure 3.8 shows the average of experimental pH values (○), pH_{ex}, obtained from the average of *E* values for 0.01, 0.0175, 0.025, 0.0375, 0.05, 0.075, and 0.1 mol kg^{-1} phosphate buffer solutions and the error bar shows ±95 % confidence interval of the experimental pH values for ten measurements. The dashed-dotted line and solid line in Fig. 3.8 are the pH values calculated by Partanen and Minkkinen[16] from the Hückel model[17] and Pitzer equation,[18] respectively. They used the values determined by Pitzer and Mayorga[19] for the parameter values, β, in the Pitzer equation. For Θ values in Pitzer equation, the values suggested by Pitzer and Silvester[18] and Pitzer and Kim[20] were used in their calculation.

Bates previously reported pH values[4] obtained by use of the following cell

I	II	III	IV	
Pt	H_2, KH_2PO_4, Na_2HPO_4, NaX	AgX	Ag	(B)

where X = Cl (△), Br (□), or I (●), when ion size parameter, å, is 4 (*B*å = 1.3). Those pH values are also given in Fig. 3.8. The dashed lines indicate pH values[4] obtained from cell (B) where X = Cl, when å is assigned the extreme values of 3 (lower dashed line) and 8 (upper dashed line) in Fig.3.8. When the values of å are 3 and 8, the values of *B*å are 1.0 and 2.6, respectively. In the 0.01 - 0.075 mol kg^{-1} phosphate buffer solutions, the experimental values, pH_{ex}, lie in the range of the upper to lower dashed lines obtained.

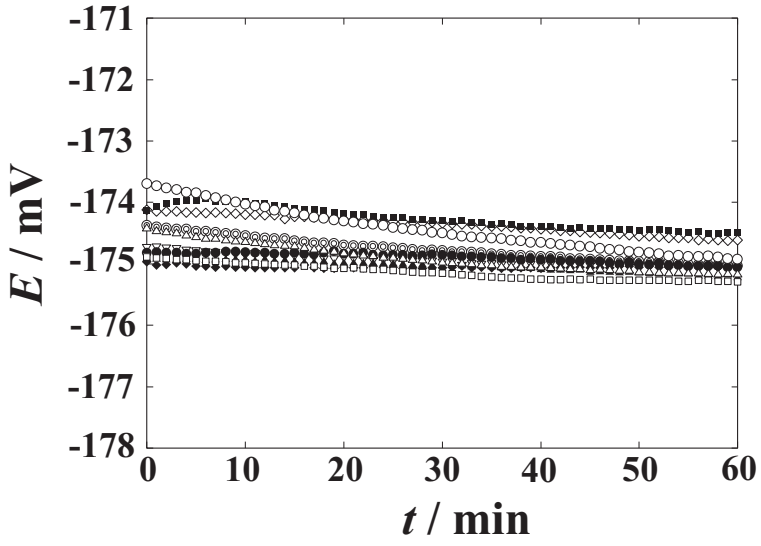

Figure 3.1: Time dependence of *E* for 1 h at 0.01 mol kg^{-1} equimolal phosphate buffer solutions in cell (A). ○ : 1st measurement, △ : 2nd measurement, □ : 3rd measurement, ● : 4th measurement, ▲ : 5th measurement, ■ : 6th measurement, ◇ : 7th measurement, ♦ : 8th measurement, ◎ : 9th measurement, ▽ : 10th measurement.

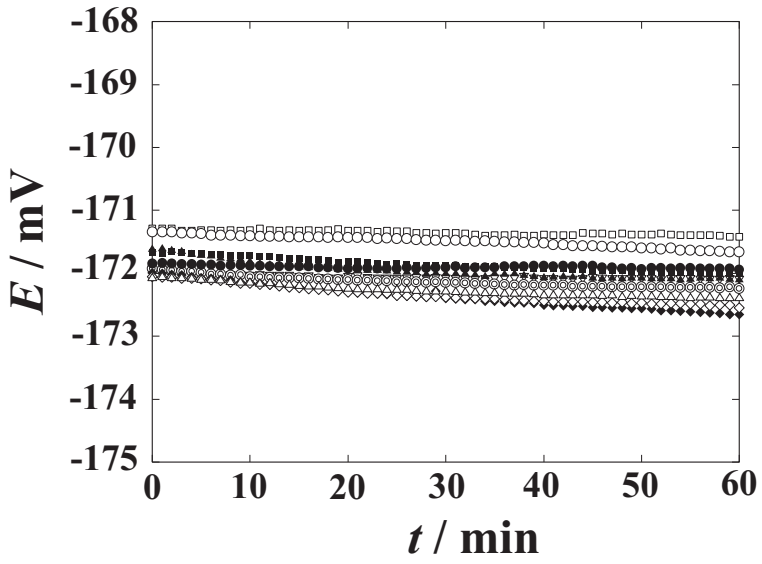

Figure 3.2: Time dependence of E for 1 h at 0.0175 mol kg^{-1} equimolal phosphate buffer solutions in cell (A). ○ : 1st measurement, △ : 2nd measurement, □ : 3rd measurement, ● : 4th measurement, ▲ : 5th measurement, ■ : 6th measurement, ◇ : 7th measurement, ♦ : 8th measurement, ◎ : 9th measurement, ▽ : 10th measurement.

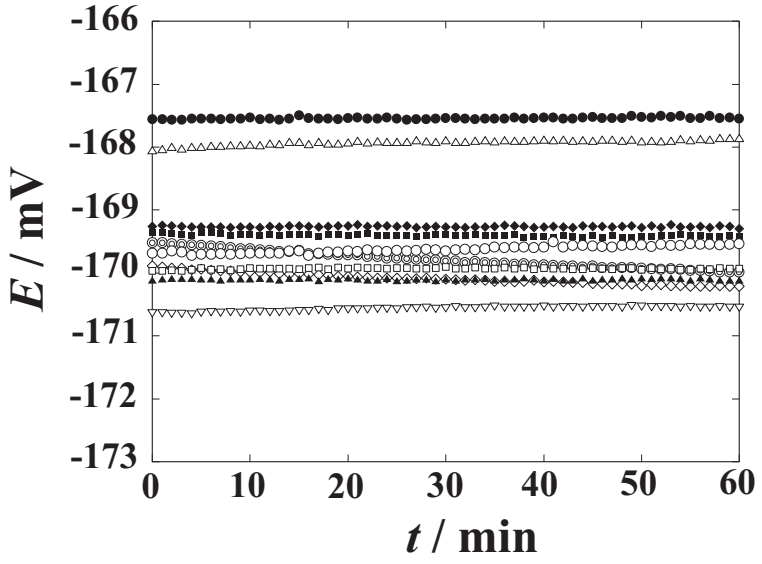

Figure 3.3: Time dependence of E for 1 h at 0.025 mol kg^{-1} equimolal phosphate buffer solutions in cell (A). ○ : 1st measurement, △ : 2nd measurement, □ : 3rd measurement, ● : 4th measurement, ▲ : 5th measurement, ■ : 6th measurement, ◇ : 7th measurement, ♦ : 8th measurement, ◎ : 9th measurement, ▽ : 10th measurement.

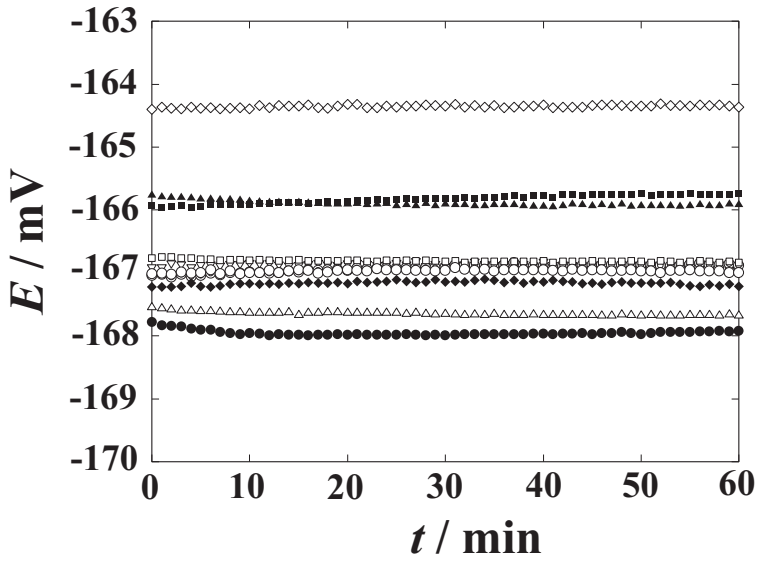

Figure 3.4: Time dependence of E for 1 h at 0.0375 mol kg^{-1} equimolal phosphate buffer solutions in cell (A). ○ : 1st measurement, △ : 2nd measurement, □ : 3rd measurement, ● : 4th measurement, ▲ : 5th measurement, ■ : 6th measurement, ◇ : 7th measurement, ♦ : 8th measurement, ◎ : 9th measurement, ▽ : 10th measurement.

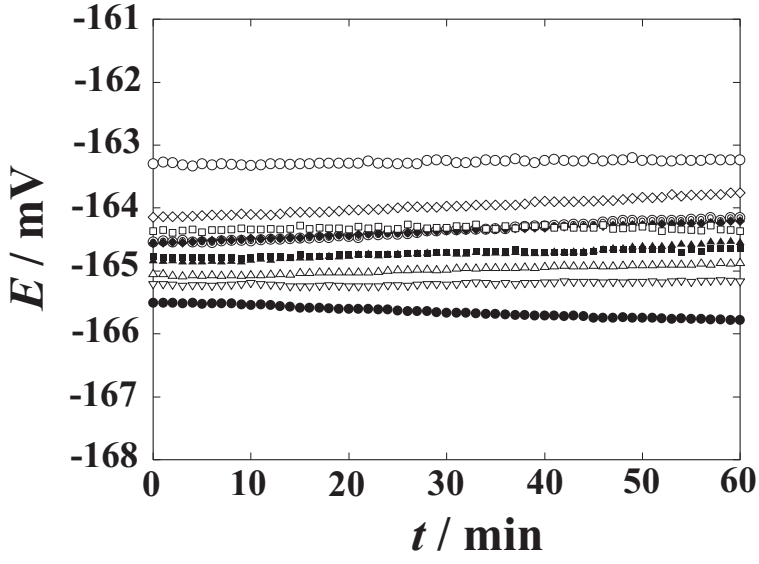

Figure 3.5: Time dependence of E for 1 h at 0.05 mol kg^{-1} equimolal phosphate buffer solutions in cell (A). ○ : 1st measurement, △ : 2nd measurement, □ : 3rd measurement, ● : 4th measurement, ▲ : 5th measurement, ■ : 6th measurement, ◇ : 7th measurement, ♦ : 8th measurement, ◎ : 9th measurement, ▽ : 10th measurement.

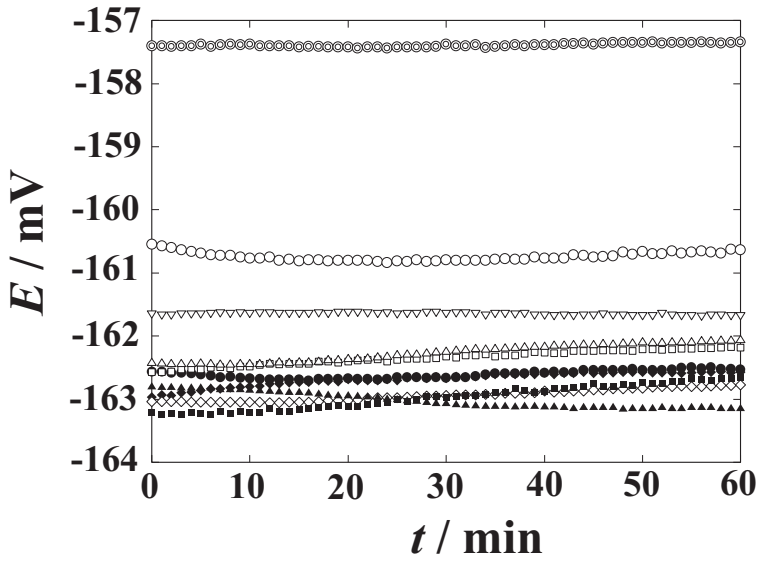

Figure 3.6: Time dependence of E for 1 h at 0.075 mol kg^{-1} equimolal phosphate buffer solutions in cell (A). ○ : 1st measurement, △ : 2nd measurement, □ : 3rd measurement, ● : 4th measurement, ▲ : 5th measurement, ■ : 6th measurement, ◇ : 7th measurement, ♦ : 8th measurement, ◎ : 9th measurement, ▽ : 10th measurement.

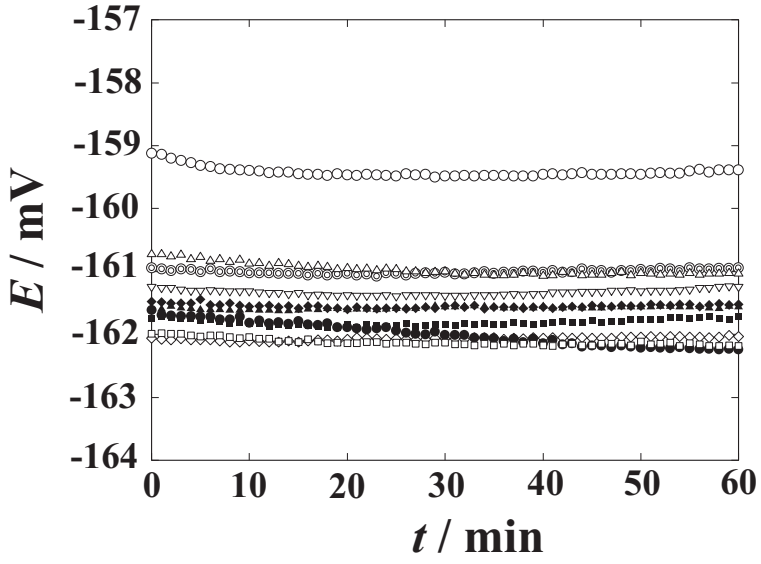

Figure 3.7: Time dependence of E for 1 h at 0.1 mol kg^{-1} equimolal phosphate buffer solutions in cell (A). ○ : 1st measurement, △ : 2nd measurement, □ : 3rd measurement, ● : 4th measurement, ▲ : 5th measurement, ■ : 6th measurement, ◇ : 7th measurement, ♦ : 8th measurement, ◎ : 9th measurement, ▽ : 10th measurement.

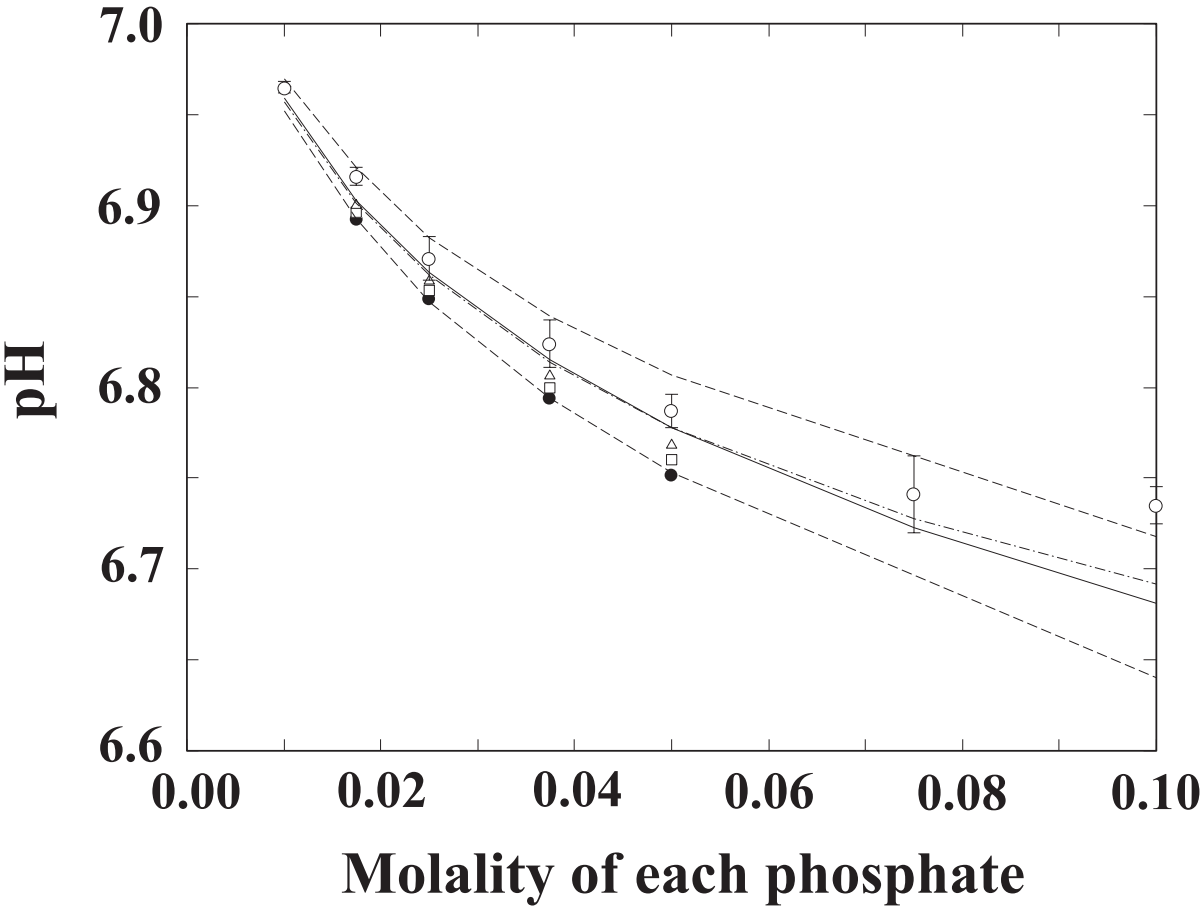

Figure 3.8: Experimental pH values (○) obtained by use of the ILSB, pH values obtained by Harned cells with silver chloride (△), silver bromide (□), and sliver iodide (●) electrodes, and calculated pH values obtained from the Hückel equation (dashed-dotted line) and Pitzer equation (solid line) at 0.01 ~ 0.1 mol kg^{-1} equimolal phosphate buffer solutions. The dashed lines indicate the course of the curve of pH values for å values of 8 (upper line) and 3 (lower line).

Figure 3.9 shows the difference between pH_{ex} values (○) obtained by use of the ILSB and the calculated values with Pitzer equation. The differences between the pH values obtained by Harned cells with silver chloride (△), silver bromide (□), or sliver iodide (●) electrodes and the calculated values with Pitzer equation are also given in Fig.3.9. The average values of pH_{ex} obtained by use of the ILSB at 0.01 - 0.075 mol kg^{-1} phosphate buffer solutions are closer to calculated values with the Hückel and Pitzer equation by about 0.01 than the values obtained by use of Harned cell at the values of å of 3 and 8. The pH determination by use of a Harned cell has the uncertainty ascribed to the estimation of the value of the ion size parameter and the kind of halide ion at the reference electrode in the Harned cell. On the other hand, the pH determination by use of an ILSB does not have such uncertainty because a pH value is estimated based on the activity of hydrogen ions which is sufficient dilute to apply the D-H limiting law. The experimental values obtained by use of the ILSB has the dispersion of 0.003 ~ 0.021 pH unit (95 % confidence interval). In Fig. 3.8, the experimental pH values including the error bar which shows 95 % confidence interval lie in the range of the upper to lower dashed lines obtained by use of a Harned cell at 0.01 ~ 0.075 mol kg^{-1} phosphate buffer solutions. The method by use of an ILSB can more accurately determine the activity of hydrogen ions in the phosphate buffer solution than by use of Hanred cell.

However, the values of pH_{ex} are higher by 0.01 pH than the calculated values obtained from the Pitzer equation at 0.01 ~ 0.075 mol kg^{-1} phosphate buffer solutions. Taking account of the diffusion potential of $TBMOEPC_2C_2N$ and the increase of ionic strength in 50 μmol dm^{-3} H_2SO_4 solution due to the dissolution of the $TBMOEPC_2C_2N$,[7] the difference between the experimental and calculated values is larger than that without taking into account. The effects of the diffusion potential of $TBMOEPC_2C_2N$ and the increase of ionic strength in 50 μmol dm^{-3} H_2SO_4 solution can not explain the difference between the experimental and calculated values.

A possible reason for the difference between the experimental and calculated values is the difference of two distribution potential at the interface between II and III and that at III and IV in cell (A). When the transfer of the ions in W to the IL is negligibly small, the distribution potential determined by the partition of the IL between the IL and the aqueous

solution (W) is described by[21,22]

$$\Delta_{\mathrm{IL}}^{\mathrm{W}}\phi = \frac{1}{2F}(\Delta_{\mathrm{IL}}^{\mathrm{W}}G_{\mathrm{tr,A^-}}^{\mathrm{IL}\rightarrow\mathrm{W},0} - \Delta_{\mathrm{IL}}^{\mathrm{W}}G_{\mathrm{tr,C^+}}^{\mathrm{IL}\rightarrow\mathrm{W},0}) + \frac{RT}{2F}\ln\frac{\gamma_{\mathrm{C^+}}^{\mathrm{IL}}\gamma_{\mathrm{A^-}}^{\mathrm{W}}}{\gamma_{\mathrm{C^+}}^{\mathrm{W}}\gamma_{\mathrm{A^-}}^{\mathrm{IL}}} \tag{3.9}$$

where $\Delta_{\mathrm{IL}}^{\mathrm{W}}\phi$ is the inner potential of W referred to that of the IL, $\Delta_{\mathrm{IL}}^{\mathrm{W}}G_{\mathrm{tr,C^+}}^{\mathrm{IL}\rightarrow\mathrm{W},0}$ and $\Delta_{\mathrm{IL}}^{\mathrm{W}}G_{\mathrm{tr,A^-}}^{\mathrm{IL}\rightarrow\mathrm{W},0}$ are the standard Gibbs energy of transfer of the cation (C^+) and the anion (A^-) constituting the IL from IL to W, respectively, $\gamma_{\mathrm{i}}^{\mathrm{IL}}$ and $\gamma_{\mathrm{i}}^{\mathrm{W}}$ are the activity coefficients of the ions (i = C^+ and A^-) in the phases IL and W. The two distribution potentials at the interface between II and III and that at III and IV are not canceled out because the second term on the right side of the equation(3.9) is not negligible when the difference of the ionic strength between the aqueous solutions in II and IV phase is great. $\Delta_{\mathrm{IL}}^{\mathrm{W}}\phi$ is expected to decrease as the ionic strength of the phosphate buffer solution is high because the ion size of $TBMOEP^+$ is larger than that of $C_2C_2N^-$, and hence pH_{ex} will shift to the positive direction. The expected increase of pH_{ex} is consistent with the results given in Fig. 3.9. Assuming that the values of ion size parameter, å, for $TBMOEP^+$ and $C_2C_2N^-$ are 0.5 nm and 0.4 nm, respectively, the values of $\gamma_{\mathrm{TBMOEP^+}}^{\mathrm{W}}$ and $\gamma_{\mathrm{C_2C_2N^-}}^{\mathrm{W}}$ were calculated from the D-H equation for the ionic strengths of 0.01 ~ 0.1 mol kg^{-1}. The values of $RT/2F\ln(\gamma_{\mathrm{C_2C_2N^-}}^{\mathrm{W}}/\gamma_{\mathrm{TBMOEP^+}}^{\mathrm{W}})$ calculated with $\gamma_{\mathrm{TBMOEP^+}}^{\mathrm{W}}$ and $\gamma_{\mathrm{C_2C_2N^-}}^{\mathrm{W}}$ for the ionic strengths of 0.01 ~ 0.1 mol kg^{-1} are given in Fig.3.10. The value of $RT/2F\ln(\gamma_{\mathrm{C_2C_2N^-}}^{\mathrm{W}}/\gamma_{\mathrm{TBMOEP^+}}^{\mathrm{W}})$ at 0.1 mol kg^{-1} is -0.23 × 10^{-3} V (0.004 pH), therefore, the measured pH_{ex} is expected to increase by 0.004 pH. This shift of pH_{ex} can explain somewhat the difference between measured and calculated pH values at the 0.025 mol kg^{-1} (I = 0.1 mol kg^{-1}) phosphate buffer, however the difference still remains.

Another two possibilities are considered. First is the change in $\Delta_{\mathrm{IL}}^{\mathrm{W}}\phi$. However, this is unlikely because the upper deviation of experimental pH values from calculated values (dashed-dotted line and solid line) is seen even at lowered ionic strength examined and the magnitude of the difference dose not depend on the buffer concentration.

Second is the uncertainty of the calculated pH values with the Pitzer equation. Although the date of the uncertainty in Pitzer equation for the phosphate buffer is not available, Spitzer et al. reported the uncertainty of pH values calculated with the Pitzer equation for 0.05 molal solution of acetic acid in KNO_3 medium.[23] From their report, we can estimate the uncertainty of a pH value calculated with the Pitzer equation for that solution as ± 0.01 pH unit (95 %

confidence interval) at 0.1 mol kg^{-1} ionic strength. We need to consider the uncertainty of Pitzer equation at ionic strength exceeding 0.1 mol kg^{-1} which is corresponding to the ionic strength of 0.025 mol kg^{-1} phosphate buffer solution.

The pH_{ex} value at 0.1 mol kg^{-1} is higher by 0.05 pH than the calculated pH value. According to the concept of mixed potential for the phase boundary potential across two immiscible electrolyte solutions,[24,25] the deviation in this direction may be caused by the interference by cations in the phosphate buffer solution or by anions in IL phase.

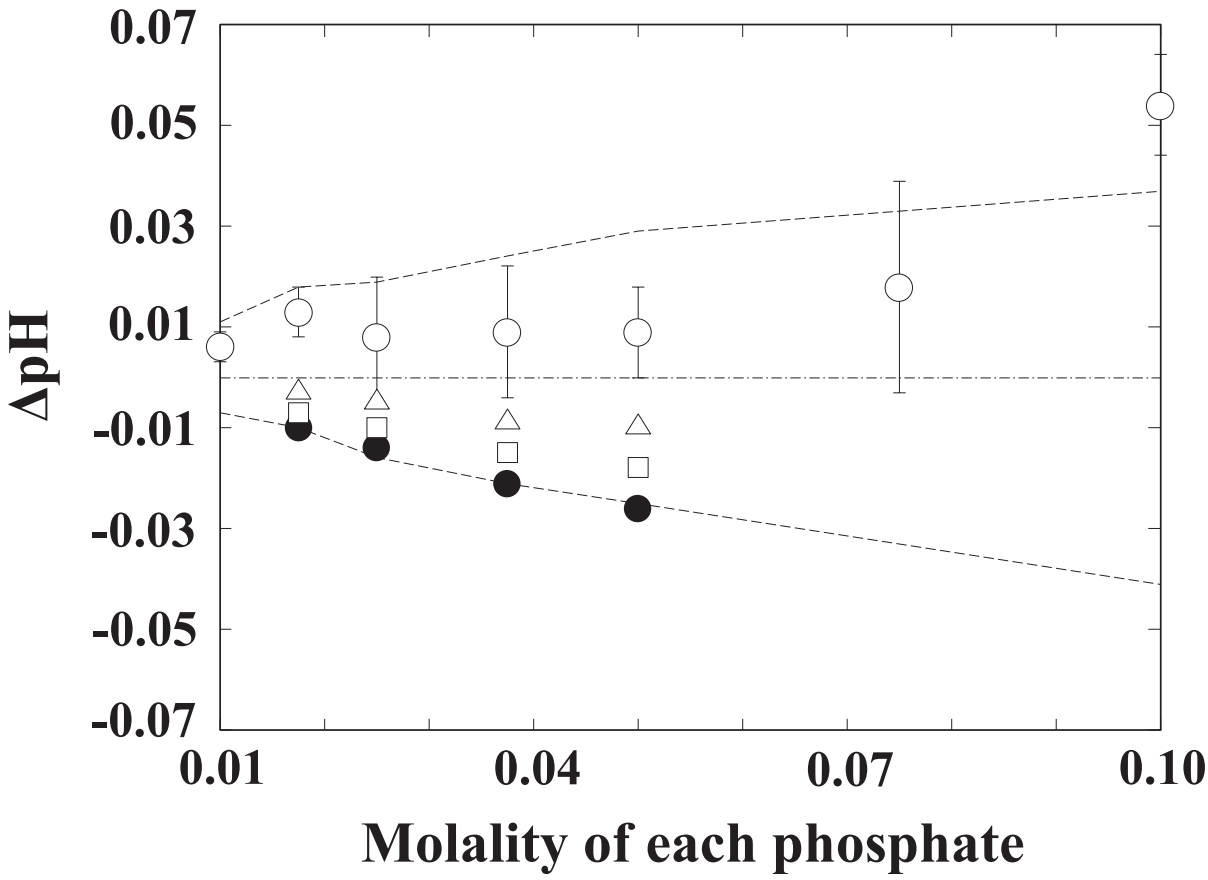

Figure 3.9: Difference between experimental pH values (○) obtained by use of the ILSB and the calculated pH values with the Pitzer equation at 0.01 ~ 0.1 mol kg^{-1} equimolal phosphate buffer solutions. Difference between pH values obtained by Harned cells with silver chloride (△), silver bromide (□), or sliver iodide (●) electrodes and the calculated pH values with the Pitzer equation. The dashed lines indicate the curve of the difference between pH values for å values of 8 (upper line) or 3 (lower line) and the calculated pH values with the Pitzer equation.

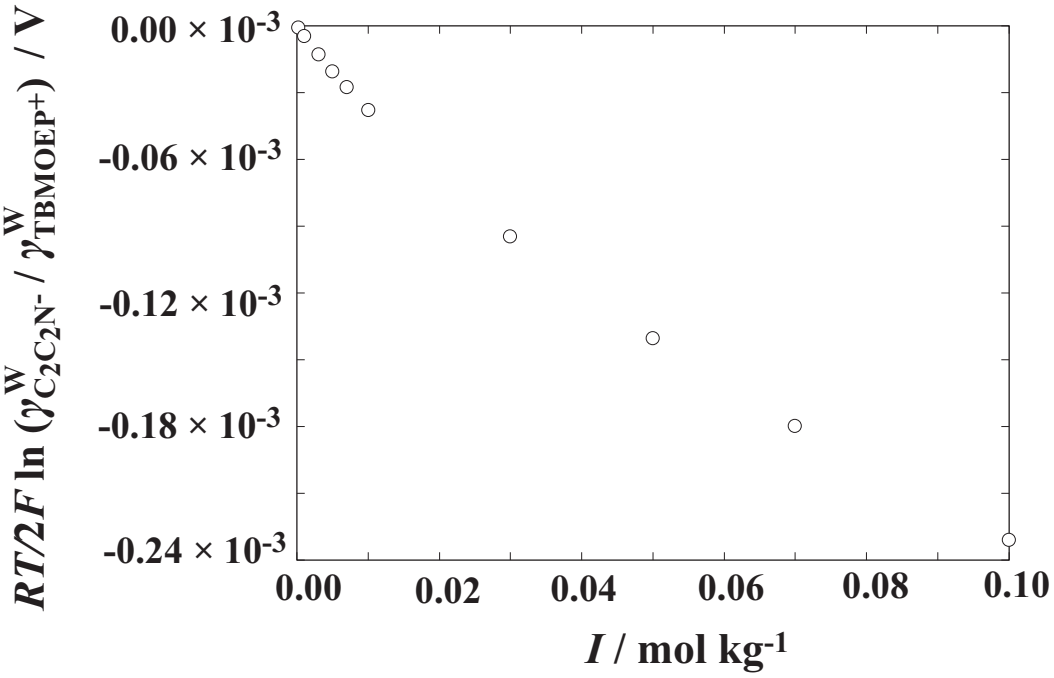

Figure 3.10: The values of $RT/2F \ln(\gamma^{W}_{C_2C_2N^-}/\gamma^{W}_{TBMOEP^+})$ calculated for the ionic strengths of 0.01 ~ 0.1 mol kg^{-1}.

3.4 Conclusions

The activities of hydrogen ions in 0.01 - 0.05 mol kg^{-1} equimolal phosphate buffer solution have been reliably estimated using the ILSB sandwiched by two hydrogen electrodes. In other words, the assumption of the cancelling out the LJP between the dilute sulfuric acid solution and phosphate buffer solution by use of TBMOEPC_2C_2N salt bridge is valid to the extent of within 0.01pH unit or 0.6 mV. The pH determination by use of an ILSB is exact and can be a better alternative to that by use of Harned cell in estimating the activity of hydrogen ions in phosphate buffer solutions.

References

(1) Sørensen, S. P. L.; Linderstrøm-Lang, K.; Lund, E. *Compt. Rend. Trav. Lab. Carlsberg* **1924**, *15*, 1–40.

(2) Buck, R. P.; Rondinini, S.; Covington, A. K.; Baucke, F. G. K.; Brett, C. M. A.; Camoes, M. F.; Milton, M. J. T.; Mussini, T.; Naumann, R.; Pratt, K. W.; Spitzer, P.; Wilson, G. S. *Pure Appl. Chem.* **2002**, *74*, 2169–2200.

(3) Bates, R. G.; Guggenheim, E. A. *Pure Appl. Chem.* **1960**, *1*, 163–168.

(4) Bates, R. G. *Chem. Rev.* **1948**, *42*, 1–61.

(5) Debye, P.; Hückel, E. *Physik. Z.* **1923**, *24*, 185–206.

(6) Bates, R. G. *Analyst* **1952**, *77*, 653–660.

(7) Shibata, M.; Sakaida, H.; Kakiuchi, T. *Anal. Chem.* **2011**, *83*, 164–168.

(8) Kakiuchi, T.; Tsujioka, N.; Kurita, S.; Iwami, Y. *Electrochem. Commun.* **2003**, *5*, 159–164.

(9) Kakiuchi, T.; Yoshimatsu, T. *Bull. Chem. Soc. Jpn.* **2006**, *79*, 1017–1024.

(10) Sakaida, H.; Kitazumi, Y.; Kakiuchi, T. *Talanta* **2010**, *83*, 663–666.

(11) Fujino, Y.; Kakiuchi, T. *J. Electroanal. Chem.* **2011**, *651*, 61–66.

(12) Earle, M. J.; Gordon, C. M.; Plechkova, N. V.; Seddon, K. R.; Welton, T. *Anal. Chem.* **2007**, *79*, 758–764.

(13) Foropoulos, J.; Desmarteau, D. D. *Inorg. Chem.* **1984**, *23*, 3720–3723.

(14) Pitzer, K. S.; Roy, R. N.; Silvester, L. F. *J. Am. Chem. Soc.* **1977**, *99*, 4930–4936.

(15) *International Critical Tables, Vol. 3*; McGraw-Hill: New York and London, 1928.

(16) Partanen, J. I.; Minkkinen, P. O. *J. Solution Chem.* **1997**, *26*, 709–727.

(17) Partanen, J. I.; Juusola, P. M.; Minkkinen, P. O. *Acta Polytech. Scand., Chem. Technol. Ser.* **1995**, *231*, 1.

(18) Pitzer, K. S.; Silvester, L. F. *J. Solution Chem* **1976**, *5*, 269–278.

(19) Pitzer, K. S.; Mayorga, G. *J. Phys. Chem.* **1973**, *77*, 2300–2308.

(20) Pitzer, K. S.; Kim, J. J. *J. Am. Chem. Soc.* **1974**, *96*, 5701–5707.

(21) Hung, L. Q. *J. Electroanal. Chem.* **1980**, *115*, 159–174.

(22) Kakiuchi, T.; Senda, M. *Bull. Chem. Soc. Jpn.* **1987**, *60*, 3099–3107.

(23) Spitzer, P.; Fisicaro, P.; Meinrath, G.; Stoica, D. *Accred. Qual. Assur.* **2011**, *16*, 191–198.

(24) Kakiuchi, T.; Senda, M. *Bull. Chem. Soc. Jpn.* **1984**, *57*, 1801–1808.

(25) Kakiuchi, T.; Obi, I.; Senda, M. *Bull. Chem. Soc. Jpn.* **1985**, *58*, 1636–1641.

Chapter 4

Determination of the Activity of Hydrogen Ions in Phosphate Buffer by Use of Ionic Liquid Salt Bridge at 5-60 °C

4.1 Introduction

A new type of salt bridge made of a moderately hydrophobic ionic liquid (ILSB) recently proposed[1–5] is superior to KCl salt bridges (KClSBs), in that the solubility of the ionic liquid (IL) employed for ILSBs is less than 1 mmol dm^{-3} and the principle of cancelling out the liquid junction potential (LJP) between a sample solution and the inner solution of the reference electrode is based on the partition of the IL into the sample side.[2]

In chapter 3, it was demonstrated that the assumption of the cancelling out the LJP between the dilute sulfuric acid solution and phosphate buffer solution by use of TBMOEPC_2C_2N salt bridge was valid in the pH determination phosphate buffer solution at 25 °C. In previous studies conducted to show the performance of ILSBs, temperature was always 25 °C.[2–7] What is required for application of an ILSB to potentiometric pH measurement is an ILSB that maintains the LJP constant over a wide range of temperature.

This chapter describes that the activity of the hydrogen ions in phosphate buffer containing 0.025 mol kg^{-1} potassium dihydrogen phosphate and 0.025 mol kg^{-1} disodium hydrogen

phosphate can be accurately estimated by use of a $TBMOEPC_2C_2N$ salt bridge sandwiched by two hydrogen electrodes at 5 - 60 °C and that the $TBMOEPC_2C_2N$ salt bridge can effectively cancel out the LJP between the 50 μmol dm^{-3} H_2SO_4 solution and equimolal phosphate buffer solution at 5 - 60 °C. The results suggest that a pH combination electrode equipped with the $TBMOEPC_2C_2N$ salt bridge is applicable to pH determination at 5 - 60 °C.

4.2 Experimental

4.2.1 Reagents

The $TBMOEPC_2C_2N$ was obtained form Kanto Chemical Co., Inc. and purified according to the procedure described in chapter 3. The 50×10^{-6} mol dm^{-3} sulfuric acid solution and the hydrogen electrodes were prepared as described in chapter 1.[6] 0.025 mol kg^{-1} equimolal phosphate buffer solution was prepared according to the procedure described in chapter 3.

4.2.2 Methods

The electrochemical cell employed is represented by

I	II	III	IV	V	
	H_2,		H_2,		
Pt	50 μmol dm^{-3} H_2SO_4	$TBMOEPC_2C_2N$	phosphate buffer solution	Pt	(A)

The single dashed vertical bars indicate the interfaces between the ILSB and the aqueous solutions (II and IV). The configuration of a U-type glass cell for cell (A) was the same as what we reported previously.[6] The cell voltage, E, i.e., the potential of the right-hand-side terminal referred to that of the left in the cell (A), was measured with an electrometer (ADC

Corporation, 8252) with a GPIB interface. The sampling interval was 1 min. Each of the two hydrogen electrodes was supplied with hydrogen gas (99.9995 %), which was generated by a hydrogen gas generator (Horiba Stec, OPGU-7100), at the rate of two to three bubbles per second from a jet about 1 mm in diameter during measurements. The gas was passed through a saturator containing the same solution as the one in the hydrogen electrode compartment before it entered the cell.

The cell was immersed in a water bath maintained at 5.0 ± 0.1 °C, 15.0 ± 0.1 °C, 25.0 ± 0.1 °C, 35.0 ± 0.1 °C, 45.0 ± 0.1 °C, and 60.0 ± 0.1 °C. The value of E was measured at 0.025 mol kg^{-1} phosphate buffer solutions in phase IV in cell (A) at each temperature. The measurement at each temperature was repeated five times. The measurement for each temperature was completed in two days and it took 12 days to complete all measurements. After each measurement, both 50 μmol dm^{-3} H_2SO_4 solution and phosphate buffer solution in phases II and IV in cell (A) was drained and the U-type glass cell and two platinum electrodes were washed with MilliQ water three times. The E was recorded for 1 h after the hydrogen gas was passed in cell (A) for 1 h. The average of E values recorded in the last ten min at each measurement was employed to estimate the pH value.

4.2.3 Experimental pH Values of Equimolal Phosphate Buffer Solution

An unknown pH value of phosphate buffer solutions (pH_x) in IV in cell (A) is written by

$$pH_x = pH_s - \frac{F}{RT \ln 10}(E - E_j) \tag{4.1}$$

where pH_s is the pH value of the 50 μmol dm^{-3} H_2SO_4 solution in II in cell (A), and E_j is the sum of two LJPs on both sides of the ILSB in cell (A), F is the Faraday constant, R is the gas constant, and T is the absolute temperature. The value of pH_s at 5 - 60 °C are obtained from molality of hydrogen ions and the corresponding activity coefficient calculated from the Debye-Hückel (D-H) limiting law[8] as the procedure described in chapter 3. In the calculation of pHs at 5 - 60 °C, the dissociation constant of sulfuric acid solution at 5 - 60 °C is calculated from the following equation[9]

$$\ln K_2 = -14.0321 + 2825.2/T \tag{4.2}$$

To calculate the activity of hydrogen ions, the molarities of sulfuric acids at 20.0 °C were converted to the molalities using the densities obtained by the extrapolation of the known densities of sulfuric acids at 20.0 °C as a function of the molarity.[10] The constants[11] of D-H theory, A, and values of m_H, γ_H, ionic strength in the molality scale, I, and pH_s in 50 μmol dm^{-3} H_2SO_4 solution at 5 - 60 °C are listed in Table 4.1. If the ILSB works ideally, E_j is null and the equation (4.1) reduces to

$$pH_x = pH_s - \frac{FE}{RT \ln 10} \tag{4.3}$$

The pH_x value obtained by the equation (4.3) is hereafter denoted as pH_{ex}.

Table 4.1: Constants of the Debye-Hückel theory and the values of γ_H, m_H, I, and pH_s in 50 μmol dm^{-3} H_2SO_4 solution at 5-60 °C.

Temperature, °C	A[11]	γ_H	m_H / μmol kg^{-1}	I / μmol kg^{-1}	pH_s
5	0.4952	0.9861	100.07	149.99	4.006
15	0.5026	0.9859	99.97	149.80	4.006
25	0.5108	0.9857	99.85	149.55	4.007
35	0.5196	0.9855	99.69	149.24	4.008
45	0.5291	0.9852	99.50	148.85	4.009
60	0.5448	0.9849	99.12	148.09	4.010

4.3 Results and Discussion

4.3.1 Time Course of *E* at Equimolal Phosphate Buffer Solution at 5 - 60 °C.

Figures 4.1 - 4.5 show the time dependence of E for 1 h at 0.025 mol kg^{-1} phosphate buffer solutions in IV in cell (A) at 5.0, 15.0, 25.0, 35.0, 45.0, and 60.0 °C, respectively. In each run, the excursion of E in 1 h was within 0.8 mV (equal to about 0.013 pH), with three

exceptions, 5 °C (1.53 and 1.62 mV) and 15 °C (1.27 mV). Except these three cases, the average of excursion in 1 h for all measurements was 0.34 ± 0.22 mV.

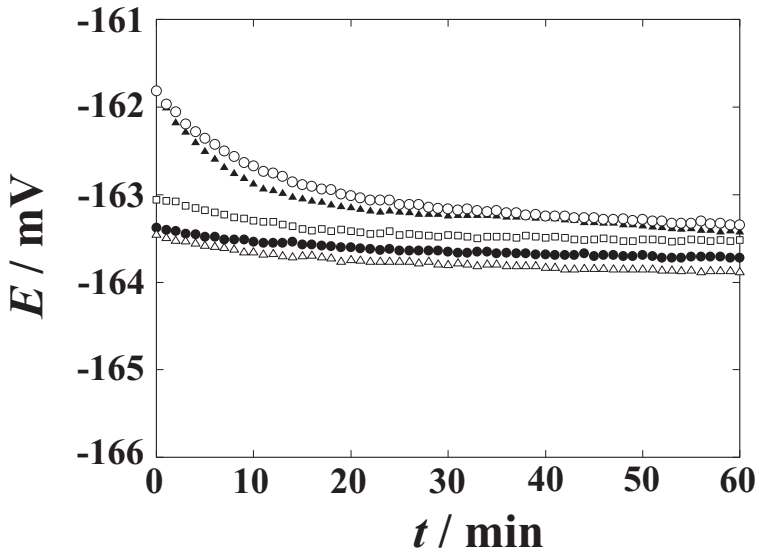

Figure 4.1: Time dependence of E for 1 h at 0.025 mol kg^{-1} equimolal phosphate buffer solutions in cell (A) at 5 °C. ○ : 1st measurement, △ : 2nd measurement, □ : 3rd measurement, ● : 4th measurement, ▲ : 5th measurement.

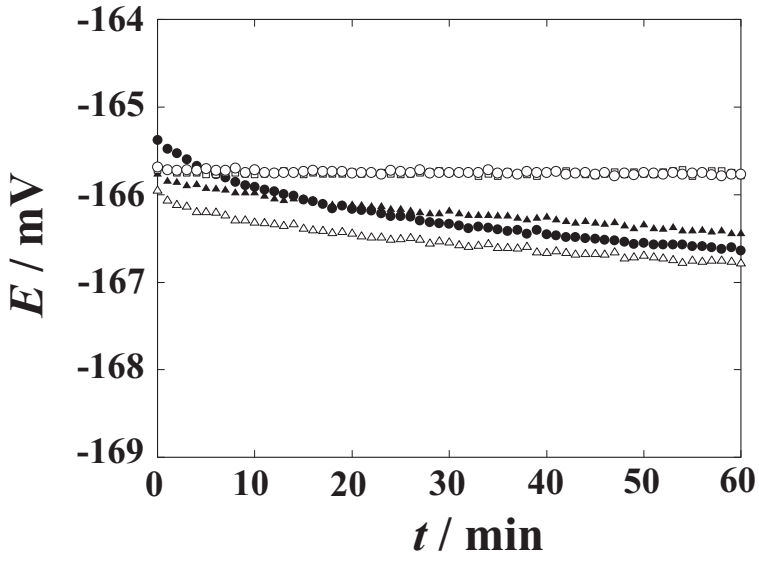

Figure 4.2: Time dependence of E for 1 h at 0.025 mol kg^{-1} equimolal phosphate buffer solutions in cell (A) at 15 °C. ○ : 1st measurement, △ : 2nd measurement, □ : 3rd measurement, ● : 4th measurement, ▲ : 5th measurement.

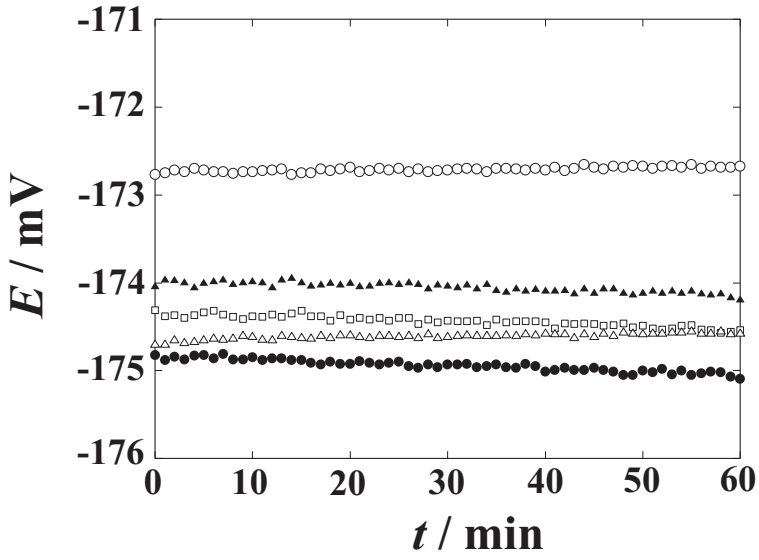

Figure 4.3: Time dependence of E for 1 h at 0.025 mol kg^{-1} equimolal phosphate buffer solutions in cell (A) at 35 °C. ○ : 1st measurement, △ : 2nd measurement, □ : 3rd measurement, ● : 4th measurement, ▲ : 5th measurement.

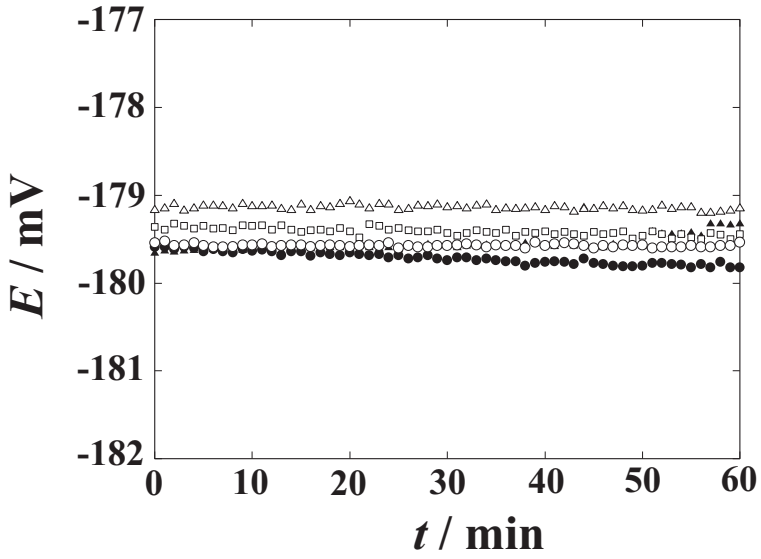

Figure 4.4: Time dependence of E for 1 h at 0.025 mol kg^{-1} equimolal phosphate buffer solutions in cell (A) at 45 °C. ○ : 1st measurement, △ : 2nd measurement, □ : 3rd measurement, ● : 4th measurement, ▲ : 5th measurement.

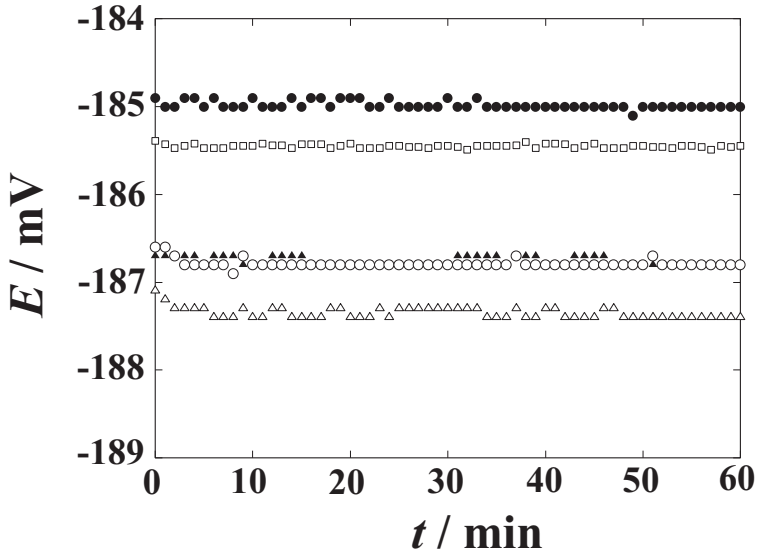

Figure 4.5: Time dependence of E for 1 h at 0.025 mol kg^{-1} equimolal phosphate buffer solutions in cell (A) at 60 °C. ○ : 1st measurement, △ : 2nd measurement, □ : 3rd measurement, ● : 4th measurement, ▲ : 5th measurement.

4.3.2 Comparison of Experimental pH Values Obtained by Use of ILSB with Those Values Obtained by Use of Harned Cells.

Figure 4.6 shows the experimental pH values (○), pH_{ex}, obtained from the average of *E* values for 0.025 mol kg^{-1} phosphate buffer solutions at 5 - 60 °C and the error bar shows 95 % confidence interval of pH_{ex} for the five measurements. Bates previously reported pH values obtained by use of the following Harned cell.[12]

I	II	III	IV	
Pt	H_2, KH_2PO_4, Na_2HPO_4, NaCl	AgCl	Ag	(B)

The pH values (□) determined by the Harned cell are also given in Fig. 4.6.

Figure 4.7 shows the difference between pH_{ex} values (○) and those values by use of the Harned cell at 0.025 mol kg^{-1} phosphate buffer solutions at 5 - 60 °C. The average values of pH_{ex} obtained by use of the ILSB are agreement within 0.02 pH unit with pH values determined by use of the Harned cell. Except for 60 °C, the difference between the pH_{ex} values and pH values determined by use of a Harned cell, pH_{Harned}, was nearly constant. This suggests that TBMOEPC_2C_2N salt bridge works satisfactorily over a wide range of temperature.

It is reported that the calculated pH values with Pitzer model, pH_{cal}, are higher by 0.004 ~ 0.01 pH unit than that obtained by use of the Harned cell at 0 ~ 50 °C.[13] Therefore, the pH_{ex} values are higher by 0.003 ~ 0.01 pH unit than the pH_{cal}. The effects of the diffusion potential of TBMOEPC_2C_2N and the increase of ionic strength in 50 μmol dm^{-3} H_2SO_4 solution can not explain the difference between the pH_{ex} values and pH_{cal} values as discussed in the chapter 3.

A possible reason for the difference between the experimental and calculated values is the difference of two distribution potential at the interface between II and III and that at III

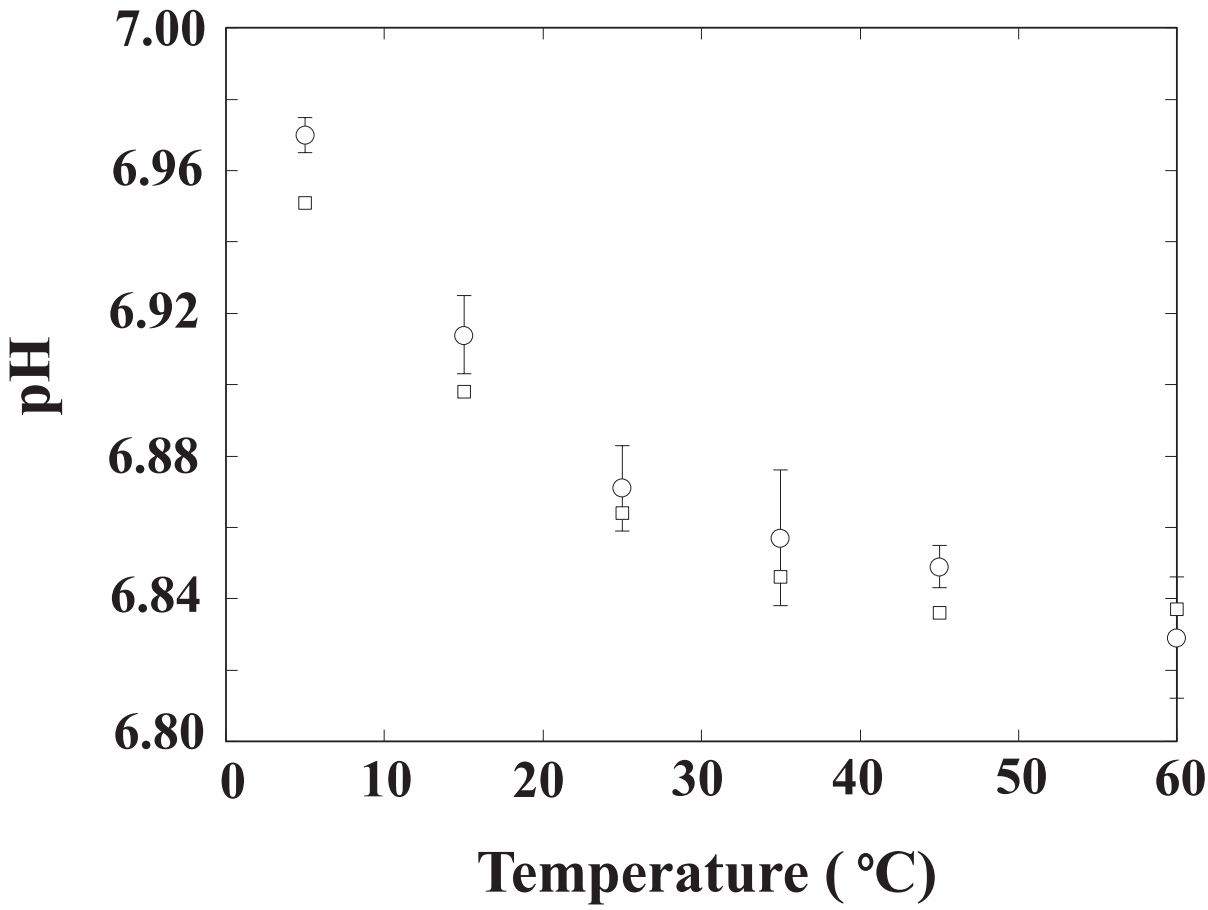

Figure 4.6: Experimental pH values (○) obtained by use of the ILSB and pH values obtained by a Harned cell (□) at 0.025 mol kg^{-1} equimolal phosphate buffer solutions at 5 - 60 °C.

and IV in cell (A). $\Delta^{W}_{IL}\phi$ decreases when the ionic strength of the phosphate buffer solution is high because the ion size of $TBMOEP^{+}$ is larger than that of $C_2C_2N^{-}$, and hence pH_{ex} shifts to the positive direction. The expected increase of pH_{ex} is consistent with the results given in Fig. 4.7 except for the pH value at 60 °C.

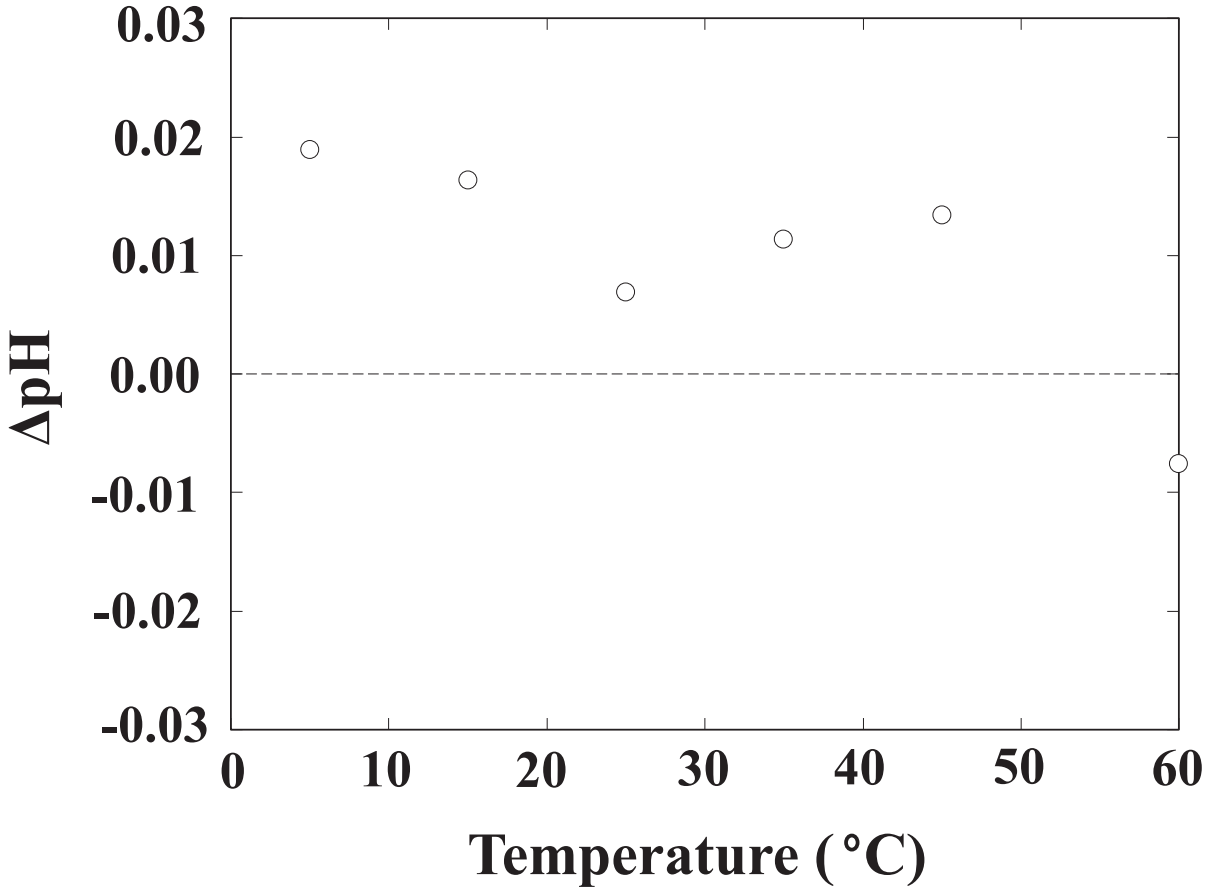

Figure 4.7: Difference between experimental pH values obtained by use of the ILSB and pH values obtained by a Harned cell at 0.025 mol kg^{-1} equimolal phosphate buffer solutions at 5 - 60 °C. $\Delta pH = pH_{ex} - pH_{Harned}$.

4.4 Conclusions

The activities of hydrogen ions in 0.025 mol kg^{-1} equimolal phosphate buffer solution at 5 - 60 °C have been reliably estimated using the ILSB sandwiched by two hydrogen electrodes. In other words, the assumption of the cancelling out the LJP between the dilute sulfuric acid solution and phosphate buffer solution by use of TBMOEPC_2C_2N salt bridge is valid to the extent of within 0.02 pH unit or 1.2 mV at 5 - 60 °C. Combination electrodes equipped with an ILSB is applicable to pH determination at 5 - 60 °C.

References

(1) Kakiuchi, T.; Tsujioka, N.; Kurita, S.; Iwami, Y. *Electrochem. Commun.* **2003**, *5*, 159–164.

(2) Kakiuchi, T.; Yoshimatsu, T. *Bull. Chem. Soc. Jpn.* **2006**, *79*, 1017–1024.

(3) Yoshimatsu, T.; Kakiuchi, T. *Anal. Sci.* **2007**, *23*, 1049–1052.

(4) Sakaida, H.; Kitazumi, Y.; Kakiuchi, T. *Talanta* **2010**, *83*, 663–666.

(5) Fujino, Y.; Kakiuchi, T. *J. Electroanal. Chem.* **2011**, *651*, 61–66.

(6) Shibata, M.; Sakaida, H.; Kakiuchi, T. *Anal. Chem.* **2011**, *83*, 164–168.

(7) Shibata, M.; Yamanuki, M.; Iwamoto, Y.; Nomura, S.; Sakaida, H.; Kakiuchi, T. *Anal. Sci.* **2010**, *26*, 1203–1206.

(8) Debye, P.; Hückel, E. *Physik. Z.* **1923**, *24*, 185–206.

(9) Pitzer, K. S.; Roy, R. N.; Silvester, L. F. *J. Am. Chem. Soc.* **1977**, *99*, 4930–4936.

(10) *International Critical Tables, Vol. 3*; McGraw-Hill: New York and London, 1928.

(11) Bates, R. G. In *Determination of pH*; Wiley: New York, 1973.

(12) Bates, R. G. *J. Res. Natl. Bur. Stand* **1962**, *66A*, 179–184.

(13) Camoes, M. F.; Lito, M. J. G.; Ferra, M. I. A.; Covington, A. K.; Lito, M. J. G.; Ferra, M. I. A.; Covington, A. K. *Pure Appl. Chem.* **1997**, *69*, 1325–1333.

Chapter 5

Stability of a Ag/AgCl Reference Electrode Equipped with an Ionic Liquid Salt Bridge Composed of 1-Methyl-3-Octylimidazolium Bis(trifluoromethanesulfonyl) amide in Potentiometry of pH Standard Buffers

5.1 Introduction

Recently, a new salt bridge using a hydrophobic ionic liquid has been proposed[1–3] as an alternative to the conventional KCl salt bridge (KClSB). The ionic liquid salt bridge (ILSB) is promising for solving most problems inherent to conventional KClSB, such as the contamination of samples, the requirement of frequently renewing the KCl solution, clogging of the junction, and the dependence of the liquid junction potential (LJP) on the type of

junction.[2] The ILSB has distinct advantages over the KClSB in potemtiometric measurements of the pH, for which it has been known that problems associated with the conventional KClSB hamper accurate pH determinations.[4–7] In potentiometric pH measurements using a glass electrode and a reference electrode, a pH cell should be calibrated using pH standards, such as phosphate, phthalate, and borate buffers before a measurement.[8,9] A salt bridge that shows a stable liquid junction potential between a salt bridge and a pH standard over time is desirable when one standard is replaced by another.

In this chapter, we gelled an ionic liquid, 1-methyl-3-octylimidazolium bis(trifluoromethanesulfonyl)amide ($C_8mimC_1C_1N$), to form a disk and mounted it on a cylindrical plastic tube membrane holder for examining the stability of the potential with respect to a double junction-type reference electrode equipped with a KClSB. We will demonstrate that the ILSB shows a stable potential in pH standard buffers, and meets the requirements for a reference electrode, except for the case of the phthalate buffer, where hydrogen phthalate ions interfere with the phase boundary potential (PBP) across the ILSB | phthalate buffer interface. We will show that an ILSB made of 1-methyl-3-hexylimidazolium bis(pentafluoroethanesulfonyl)amide ($C_6mimC_2C_2N$) can reduce the shift of the PBP across the ILSB | phthalate buffer interface by the partition of the hydrogen phthalate ions.

5.2 Experimental

5.2.1 Reagents

1-Methyl-3-octylimidazolium bis(trifluoromethanesulfonyl)amide ($C_8mimC_1C_1N$) was obtained from Nippon Synthetic Chemical Industry Co., Ltd. Poly (vinylidene fluoride-co-hexafluoropropylene) (PVdF-HFP, average MW 40,000) was obtained from Aldrich.

1-methylimidazole (> 98 %) and 1-Chlorohexane were obtained from Wako Pure Chemical Industries, Ltd., and Sigma Aldrich Co., respectively. An aqueous solution (0.7 mass fraction) of the acid form of bis(pentafluoroethanesulfonyl)amide (HC_2C_2N > 99 %) was obtained from Central Glass Co., Ltd. 1-Methyl-3-hexylimidazolium chloride (C_6mimCl) was synthesized according to the method of Gordon et al.[10] by mixing 1-methylimidazole

and 1-Chlorohexane at 110 °C for 19 h. The crude C_6mimCl, a yellowish and viscous liquid, was washed with ethyl acetate under reflux five times, after which volatile trace impurities were removed with a vacuum pump. To prepare $C_6mimC_2C_2N$, equimolar amounts of C_6mimCl and an aqueous solution of HC_2C_2N were mixed in methanol. Methanol was then removed with an evaporator, and HCl was extracted in water from remaining liquid (a mixture of $C_6mimC_2C_2N$ and HCl) by use of a dichloromethane-water two-phase system. The washing was repeated 15 times, until Cl^- was not detected when a few drops of a $AgNO_3$ solution were added to the supernatant solution. The $C_6mimC_2C_2N$ obtained was dried under vacuum.

A phthalate standard solution (0.05 mol kg^{-1} $KHC_8H_4O_4$, pH = 4.01 ± 0.05 at 25 °C), a phosphate standard solution (0.025 mol kg^{-1} KH_2PO_4 + 0.025 mol kg^{-1} Na_2HPO_4, pH = 6.86 ± 0.05 at 25 °C), and a borate standard solution (0.01 mol kg^{-1} $Na_2B_4O_7 \cdot 10H_2O$, pH = 9.18 ± 0.05 at 25 °C) were obtained from Horiba, Ltd (150-4, 150-7, and 150-9). The 0.05 mol kg^{-1} citrate buffer solution (pH 3.78 at 25 °C)[11] was prepared by dissolving 11.41 g of $KH_2C_6H_5O_7$ (Kanto Chemical Co.,Inc. 98 %) in pure water and diluting it to 1.000 ± 0.0004 dm^3. A 3.33 mol dm^{-3} potassium chloride solution (Horiba, 300) was used. Other Chemicals were of reagent grade.

$C_8mimC_1C_1N$ was gelled by dissolving 8 g of P(VdF-HFP) and 0.008 dm^3 $C_8mimC_1C_1N$ in 0.1 dm^3 acetone and evaporating acetone in the mixture for two weeks at room temperature to obtain a disk-shaped membrane.[12]

5.2.2 Methods

Evaluate the IL-Type Reference Electrode Equipped with $C_8mimC_1C_1N$ Salt Bridge

Figure 5.1 illustrates the structure of an ionic liquid-type reference electrode equipped with gelled $C_8mimC_1C_1N$. In the IL-type reference electrode, a disk-shaped membrane of the gelled ionic liquid, whose diameter and thickness were 12 mm and 1 mm, respectively, was mounted with a silicone O-ring to the cylindrical body of a reference electrode. The inner cell was composed of an Ag/AgCl electrode in a 3.3 mol dm^{-3} KCl aqueous solution. The Ag/AgCl electrode was prepared by immersing a 0.8 mm diameter silver wire

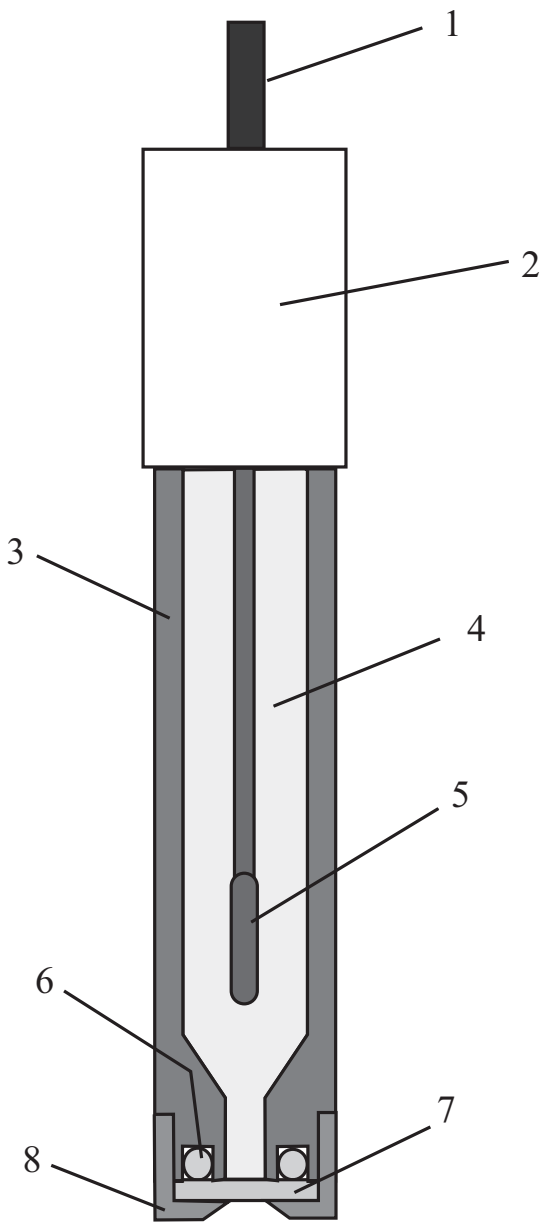

Figure 5.1: Schematic view of the ionic liquid-type reference electrode. 1, lead wire; 2, cap; 3, plastic tube; 4, 3.3 mol dm^{-3} KCl aqueous solution; 5, Ag/AgCl electrode; 6, O-ring; 7, gelled ionic liquid; 8, cylindrical cap

in molten AgCl at 480 °C, and drying it at room temperature. The resistance of the gelled $C_8mimC_1C_1N$ membrane obtained by measuring the resistance between the ionic liquid-type reference electrode and the Ag/AgCl electrode in a 3.3 mol dm^{-3} KCl aqueous solution with a resistance meter (ADC Corporation 8340A) was about 5×10^3 ohm.

Schemes 1 and 2 show the electrochemical cells that we employed to evaluate the IL-type

and KCl-type references, respectively.

I	II	III	IV	V	VI	VII	
	3.3	3.3	pH		3.3		
Ag/AgCl	mol dm^{-3}	mol dm^{-3}	standard	gelled	mol dm^{-3}	AgCl/Ag	(A)
	KCl	KCl	solutions	IL	KCl		

Scheme 1.

I	II	III	IV	V	VI	
	3.3	3.3	pH	3.3		
Ag/AgCl	mol dm^{-3}	mol dm^{-3}	standard	mol dm^{-3}	AgCl/Ag	(B)
	KCl	KCl	solutions	KCl		

Scheme 2.

The left-half cells (phase I and II) in the entire cells (A) and (B) were composed of double junction-type reference electrodes (Horiba, Ltd. 2565A); the right-half cells in cells (A) and (B) were composed of an IL-type (Fig. 5.1) and a ceramic junction-type (Horiba, Ltd. 2060A) reference electrode, respectively. The double-dashed vertical bar indicates a liquid-liquid junction between two electrolyte solutions of the same composition, and the single dashed vertical bar indicates a liquid-liquid junction between two electrolyte solutions of different compositions.

The cell voltage, E, i.e., the potential of the right-hand-side terminal referred to that of the left in cell (A) or (B), was measured with a pH meter (Horiba, Ltd. F55) at a sampling rate of 0.1 Hz. A beaker containing a sample solution was set in a water bath kept at 25.0 ± 0.1 °C for the potentiometry with cell (A) or (B). The electrodes were first rinsed with MilliQ

water, and then dipped into a beaker for a potentiometric measurement. The *E* of cell (A) or (B) was measured for 3 min in each measurement. Phase IV in cells (A) and (B) was changed in the following order: phosphate, phthalate, citrate, and borate. A series of measurements was repeated three times. The electrodes used for the measurements were washed for ten seconds with MilliQ water after a measurement in each solution.

Examine of the Influence of the Interference by Ions in W

Scheme 3 shows the electrochemical cell that we employed to examine the influence of the interference by the partition of the hydrogen phthalate (HPh^-) in IL phases.

I	II	III	IV	V	
	0.01 mol dm^{-3}				
Ag/AgCl	C_6mimCl	C_6mimC_2C_2N	0.01 mol dm^{-3} KCl	AgCl/Ag	(C)
	or C_8mimCl	or C_8mimC_1C_1N	+ *x* mol dm^{-3} KHPh		
	(W_{ref})	(IL)	(W)		

Scheme 3.

The thermal-electrolytic type of silver-silver chloride electrode was employed in Scheme 3. The base for the silver-silver chloride electrode was a helix of platinum wire about 7 mm in length and about 2 mm in diameter, sealed in a tube of Pyrex glass. The bases were cleaned in warm 6 mol dm^{-3} nitric acid and a thick paste of silver oxide (>99.99 % Sigma-Aldrich Co.) and water was applied to each helix. The electrodes were suspended in an electric furnace heated to about 500 °C and allowed to remain there for 10 min or until they are completely white. A second layer of silver was formed in a similar manner with a slightly thinner paste to make the surface smooth. Each silver electrode was mounted in a cell of modified U-tube design and electrolyzed in a 1 mol dm^{-3} hydrochloric acid for 45 min at a current 10 mA. C_6mim^+ and C_8mim^+ in W_{ref} are the potential-determining ions that assure the stable PBP between the IL and the W_{ref} phases. The cell voltage, i.e., the potential of the right-hand-side terminal referred to that of the left in the cell (C), *E*, was measured with an electrometer

(ADC Corporation R8240) with a GPIB interface. The structure of the U-type glass cell for potentiometric measurements is shown in Fig. 5.2.

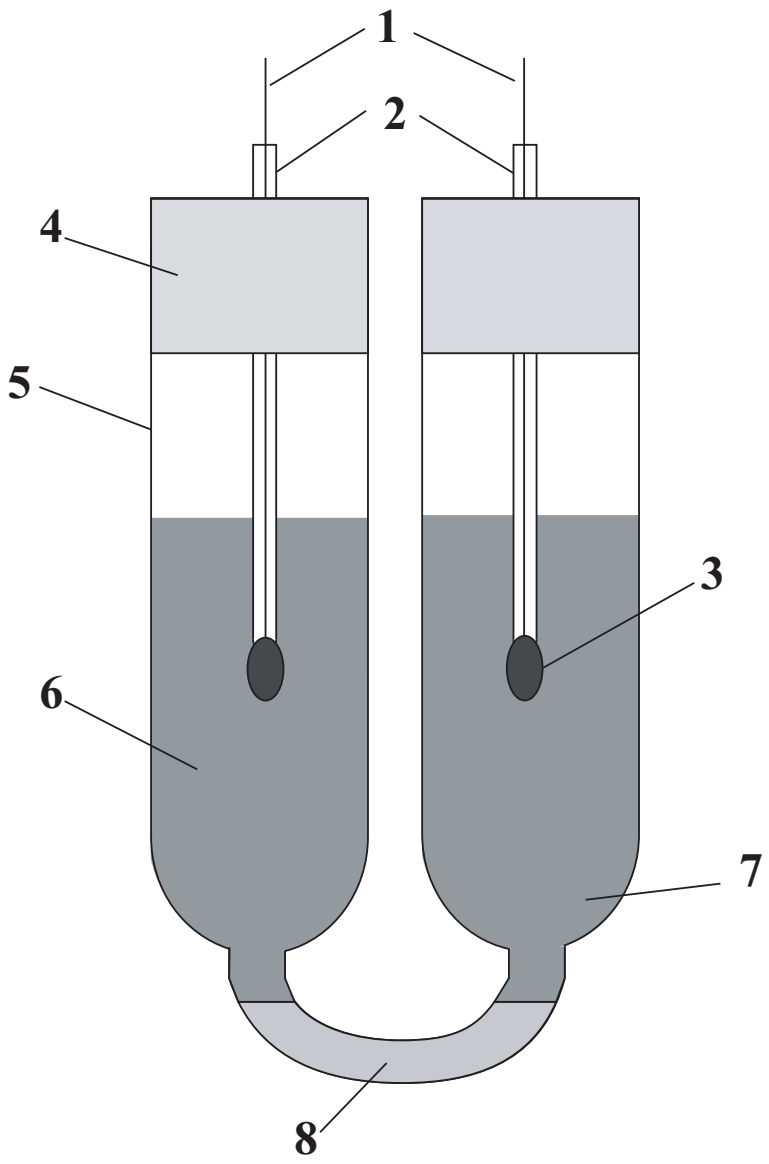

Figure 5.2: Illustration of the electrochemical cell using a ILSB sandwiched by two silver-silver chloride electrodes. 1: Pt wire; 2: Pyrex glass tube; 3: silver-silver chloride; 4: silicon rubber stopper; 5: U-type glass cell; 6: 0.01 mol dm^{-3} C_6mimCl or C_8mimCl; 7: 0.01 mol dm^{-3} KCl + x mol dm^{-3} KHPh; 8: $C_6mimC_2C_2N$ or $C_8mimC_1C_1N$.

The U-type glass cell was set in a water bath kept in 25.0 ± 0.1 °C. The value of E was measured at 0, 0.001, 0.005, 0.01, 0.05, 0.1, and 0.2 mol dm^{-3} potassium hydrogen

phthalate (KHPh) in phase IV in cell (C). The measurement at each concentration of KHPh was repeated three times. After each measurement, both solutions in phase II and IV in cell (C) were drained, and U-type glass cell and two Ag/AgCl electrodes were washed with Milli-Q water three times.

5.3 Results and Discussion

5.3.1 Time Course of *E* at pH Standard Buffers

Figure 5.3 shows the time dependence of *E* for 3 min in four buffers. *E* reached a steady value after 3 min for all cases. The change in the values of *E* was within 0.3 mV in a few minutes after starting the measurements for the four buffers.

The values of *E* after 3 min in a series of measurements are given in Fig. 5.4. The results of the same measurements using a ceramic junction-type reference electrode are also shown in Fig. 5.4.

The variation of *E* in Fig. 5.4 is ascribed to the variation of the LJP between the KCl solution (phase Ⅲ) and each buffer (phase Ⅳ), and that of the PBP between the IL (phase V) and the buffer (phase Ⅳ). The variation of the LJP between the KCl solution and each buffer is known to be within 0.01 pH or 0.6 mV at 25 °C.[13] The PBP between the IL (phase V) and the buffer (phase Ⅳ) is determined dominantly by the distribution potential by the partition of the cation and anion constituting the IL between the IL and an aqueous solution, when the ionic strength of the aqueous solution contacting with the IL is higher than 1 mmol dm^{-3}.[3] We therefore presume that the variation of *E* in cell (A) was caused by the distribution potential of the IL between the IL and a buffer solution. In Fig. 5.4, *E* in the phthalate buffer is lower than that in other buffer solutions by 4 mV. In contrast, the change in *E* was less than 1 mV in the citrate standard, whose pH was close to that of the phthalate standard. The small change in *E* in the citrate standard indicates that the specific change of *E* observed only in the phthalate buffer depends not on the pH, but on the composition of the solution.

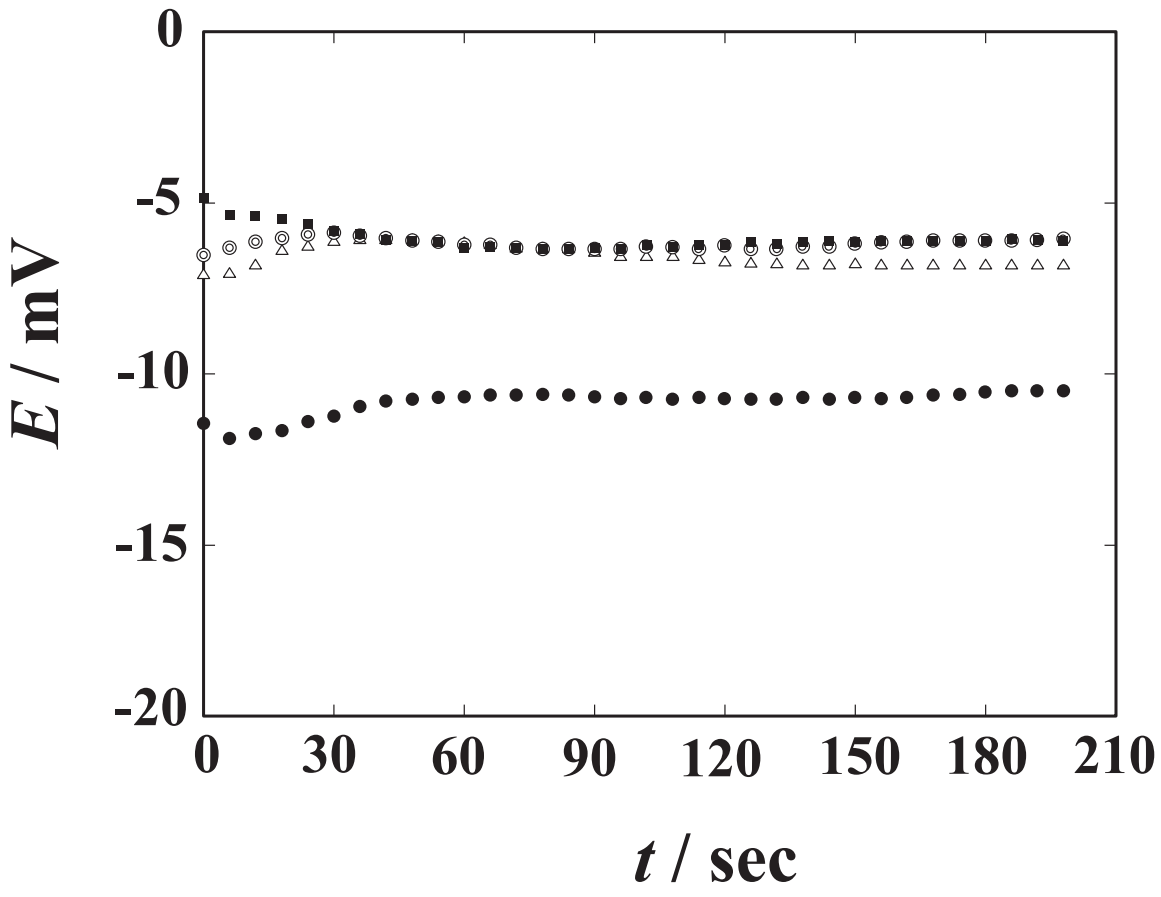

Figure 5.3: Time dependence of *E* in cell (A) for 3 min in a phosphate standard, a phthalate standard, a borate standard, and a citrate standard. Double circle, a phosphate standard; filled circle, a phthalate standard; filled square, a borate standard; open triangle, a citrate standard.

5.3.2 Interference by the Partition of HPh^- in $C_8mimC_1C_1N$

The reproducible drop of *E* in the phthalate buffer suggests that the partition of the hydrogen phthalate (HPh^-) in $C_8mimC_1C_1N$ is non-negligible, and influences the PBP across the interface between $C_8mimC_1C_1N$ and the phthalate standard. The PBP between an IL and water is constant, provided that the dissolution of the ions in W to the IL is negligible. The standard ion-transfer potential of the HPh^- in the nitrobenzene-water two phase system, $\Delta^{W}_{NB}\phi^{0}_{HPh^-}$, is -195 mV,[14] which is close to that of C_8mim^+ ion, $\Delta^{W}_{NB}\phi^{0}_{C_8mim^+}$ = -220 mV;[15] that is, the hydrophobicity of the HPh^- is similar to that of C_8mim^+. The dissolution of HPh^- into the ILSB in exchange for the transfer of $C_1C_1N^-$, whose $\Delta^{W}_{NB}\phi^{0}_{C_1C_1N^-}$ = 114 mV,[16] from the ILSB to the phthalate buffer is therefore likely to take place, causing a change in the PBP. From a

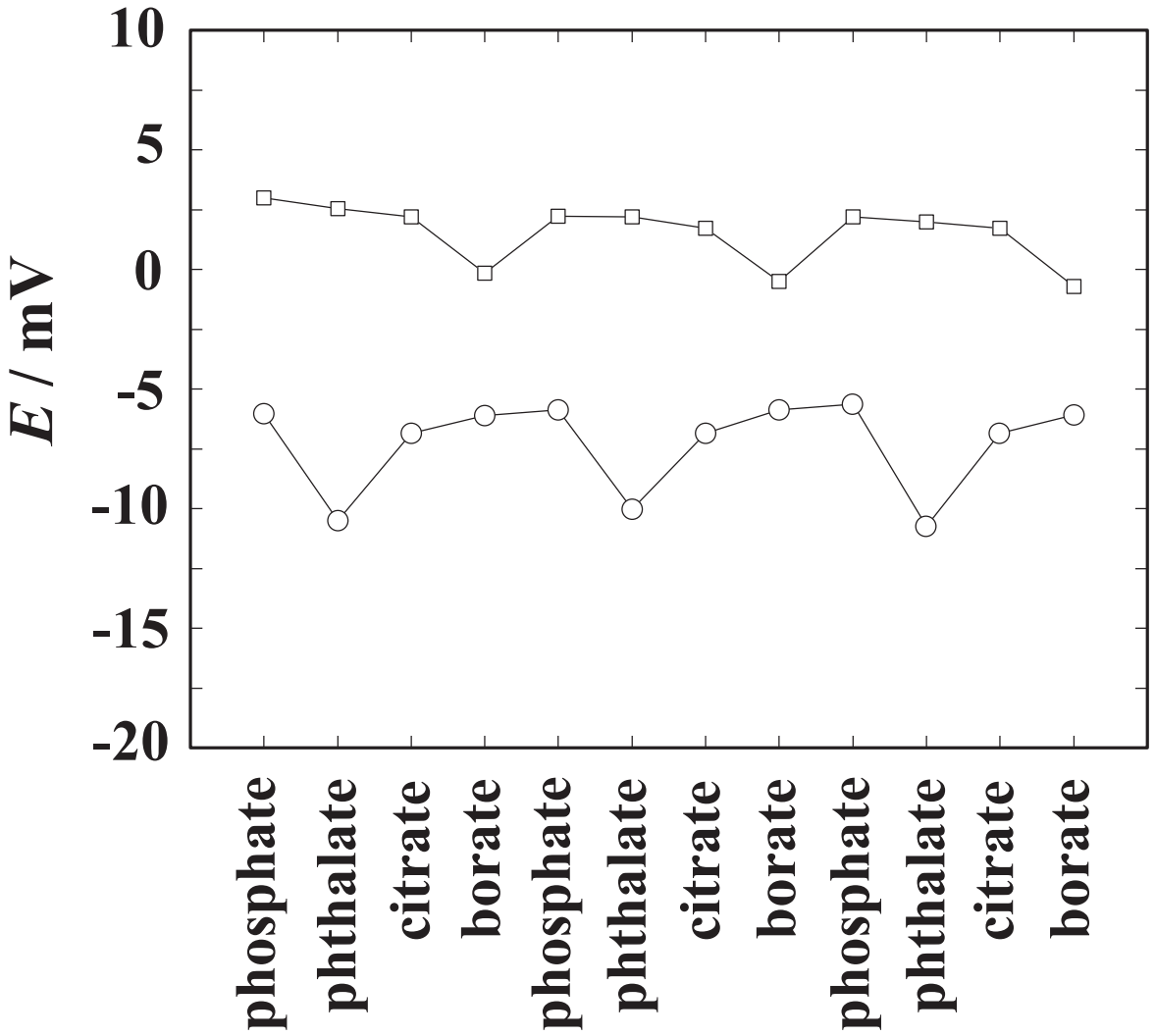

Figure 5.4: E of IL-type and KCl-type electrodes after 3 min for measurements of pH standard solutions. open circle, IL-type; open square, KCl-type.

model[17,18] of the mixed potential for the PBP across the two immiscible electrolyte solutions, it is expected that the PBP between the IL and the phthalate buffer, $\Delta_{\mathrm{IL}}^{\mathrm{phtha}}\phi = \phi_{\mathrm{phtha}} - \phi_{\mathrm{IL}}$, where ϕ_{phtha} and ϕ_{IL} are the inner potentials in the phthalate buffer and the IL, respectively, shifts to the positive direction, and hence E in cell (A) shifts to the negative. The expected direction of the shift of E is consistent with the results given in Fig. 5.4.

The variation in E of an IL-type reference electrode when one standard buffer solution was replaced by another was within 1 mV for the phosphate, borate, and citrate standards. The standard deviation of E for triplicate measurements of the same solution was 0.4 mV. Figure 5.4 shows that the variation in the liquid junction potential of the ILSB is comparable

to that of the KClSB, except for the case of the phthalate standard.

When a two-point calibration of a pH cell composed of a glass electrode and a reference electrode with buffers having pH values of pH_{S_1} and pH_{S_2} is made, the operative Nernst slope, k', is represented by

$$k' = \frac{E_{S_2} - E_{S_1}}{pH_{S_2} - pH_{S_1}} \tag{5.1}$$

where E_{S_2} and E_{S_1} are the pH cell voltage for buffers pH_{S_2} and pH_{S_1}, respectively, referred to the reference electrode. Practically, it may seem that the reproducible deviation of the PBP by 4 mV in the case of the phthalate buffer can be taken into account by the calibration procedure of the electrochemical cell. When the calibration is made at 25 °C with the phthalate buffer (pH = 4.005) and the phosphate buffer (pH = 6.865), the theoretical difference in E is 169.20 mV. Assuming 4 mV deviation of the PBP at the IL | buffer interface, we would read 173.2 mV for ΔE, and the calibration slope would be -60.56 mV / pH. If a sample solution whose pH value is 4.005, but with no partitioning of ions in the IL is measured with this cell, the reading of a pH meter using this cell would give a value of 4.069. Whether the error of 0.064 pH unit is permissible depends on the purpose of the pH measurements.

One serious problem concerning HPh^- interference in an ILSB made of $C_8mimC_1C_1N$ is that HPh^- replaces $C_1C_1N^-$ in the IL, and remains in the IL after contact of the ILSB with a HPh^- buffer. In this respect, the use of a citrate buffer, whose dissolution into the ILSB is negligible, is highly recommended when the two-point calibration of the pH cell is made before measuring an acid solution. It is expected that the HPh^- interference in the ILSB is reduced by positively shifting the standard transfer potentials of ions constituting the IL.

In Fig. 5.4, the ceramic plug-type KClSB showed an offset voltage of about 2 mV and a slight drift with the repetition of the measurements. Moreover, this KClSB showed a systematically lower value of E in the borate buffer. The reason for this behavior is not clear at this moment, but is likely to be ascribed to the ceramic plug.[19]

5.3.3 Reduction of the Shift of the PBP Due to the Interference by Ions in W

Figure 5.5 exemplifies the time dependence of E for 15 min at 0 ~ 0.2 mol dm^{-3} KHPh in IV and C_8mimCl in II and C_8mimC_1C_1N in III in cell (C). Figure 5.6 exemplifies the

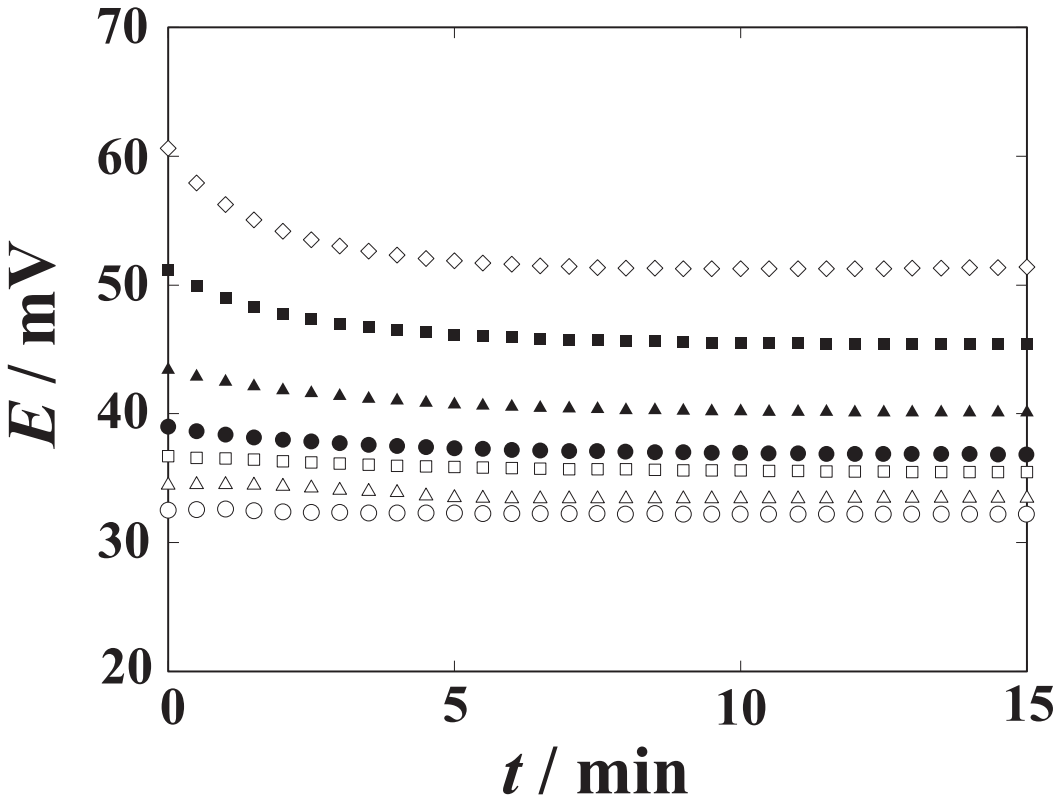

Figure 5.5: Time dependence of E for 15 min at 0 ~ 0.2 mol dm^{-3} KHPh in IV and C_8mimCl in II and C_8mimC_1C_1N in III in cell (C). ○ : 0 mol dm^{-3}, △ : 0.001 mol dm^{-3}, □ : 0.005 mol dm^{-3}, ● : 0.01 mol dm^{-3}, ▲ : 0.05 mol dm^{-3}, ■ : 0.1 mol dm^{-3}, ◇ : 0.2 mol dm^{-3}.

time dependence of E for 15 min at 0 ~ 0.2 mol dm^{-3} KHPh in IV and C_6mimCl in II and C_6mimC_2C_2N in III in cell (C). The excursion of E for 5 ~ 15 min was within 0.8 mV in each run. As the concentration of KHPh was greater, the variation of E for 0 ~ 5 min was greater. The difference between the values of E at each concentration of KHPh and the value of E at zero concentration of KHPh in IV in cell (C) for 0.001 ~ 0.2 mol dm^{-3} KHPh is shown in Fig. 5.7.

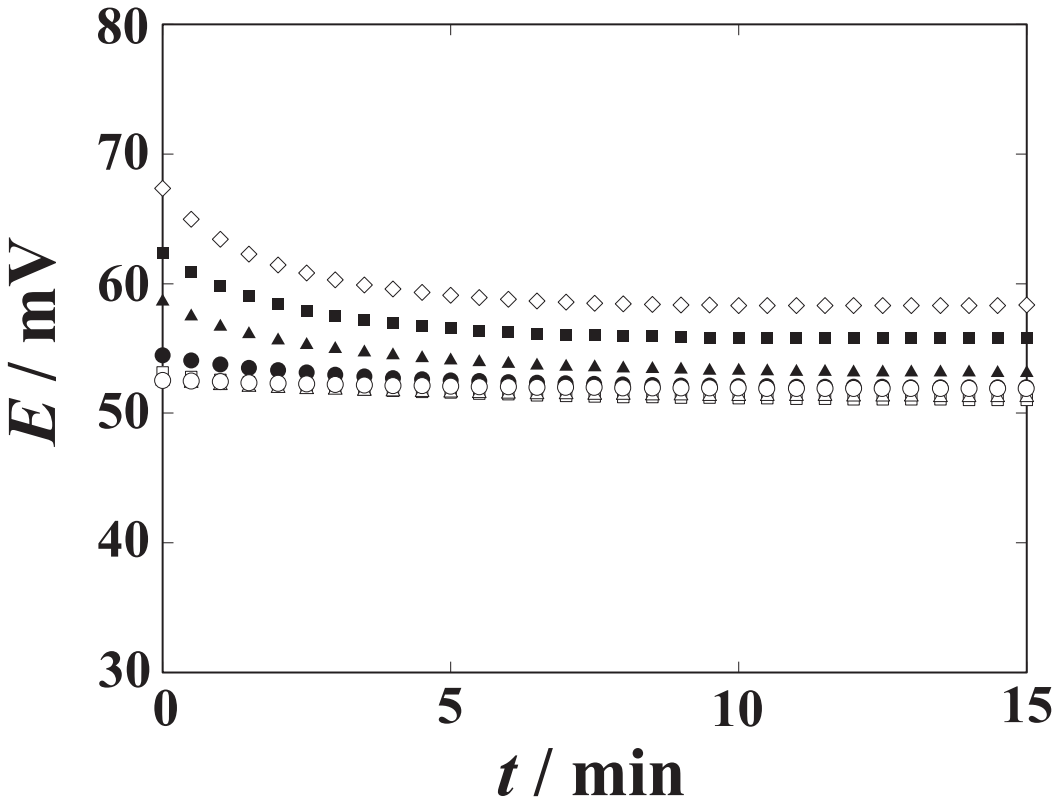

Figure 5.6: Time dependence of E for 15 min at 0 ~ 0.2 mol dm^{-3} KHPh in IV and C_6mimCl in II and C_6mimC_2C_2N in III in cell (C). ○ : 0 mol dm^{-3}, △ : 0.001 mol dm^{-3}, □ : 0.005 mol dm^{-3}, ● : 0.01 mol dm^{-3}, ▲ : 0.05 mol dm^{-3}, ■ : 0.1 mol dm^{-3}, ◇ : 0.2 mol dm^{-3}.

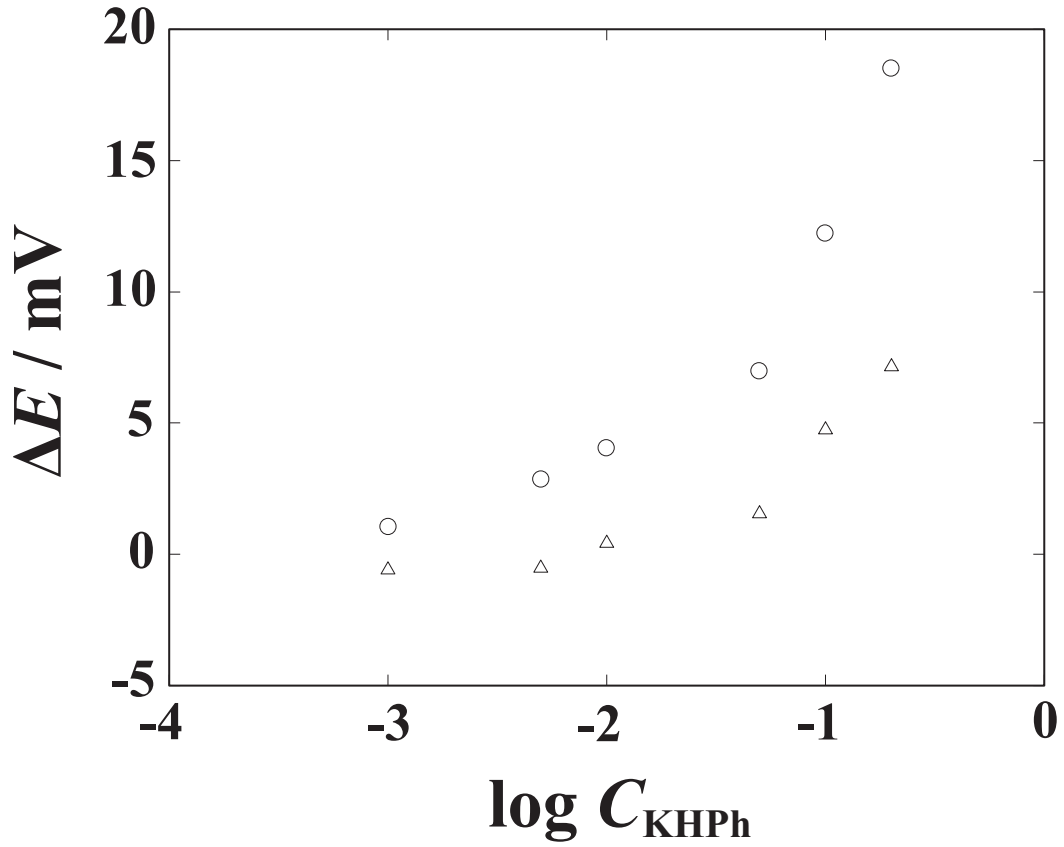

Figure 5.7: Difference between the values of E at each concentration of KHPh and the value of E at zero concentration of KHPh in IV in cell (C) for 0.001 ~ 0.2 mol dm^{-3} KHPh.
○ : $C_8mimC_1C_1N$, △ : $C_6mimC_2C_2N$.

Each point represents the average value of triplicate measurements over 15 min. The values of ΔE at $C_6mimC_2C_2N$ were smaller than those at $C_8mimC_1C_1N$ in Fig. 5.7. Fig. 5.8 shows the standard ion-transfer potential of several ions in the nitrobenzene-water two phase system. The standard ion-transfer potential between IL and W of C_6mim^+, $\Delta^{W}_{NB}\phi^{0}_{C_6mim^+}$, is greater than that of C_8mim^+, $\Delta^{W}_{NB}\phi^{0}_{C_8mim^+}$, and is away from that of HPh^-. Therefore, from a model of the mixed potential for the PBP across the two immiscible electrolyte solutions, it is expected that the interference by the partition of HPh^- in $C_6mimC_2C_2N$ is reduced compared with $C_8mimC_1C_1N$. The expected decrease of ΔE at $C_6mimC_2C_2N$ is consistent with the results given in Fig. 5.7. Thus, we can reduce the shift of PBP due to the interference by HPh^- in W by tuning the $\Delta^{W}_{IL}\phi^{0}$ of ions constituting the IL.

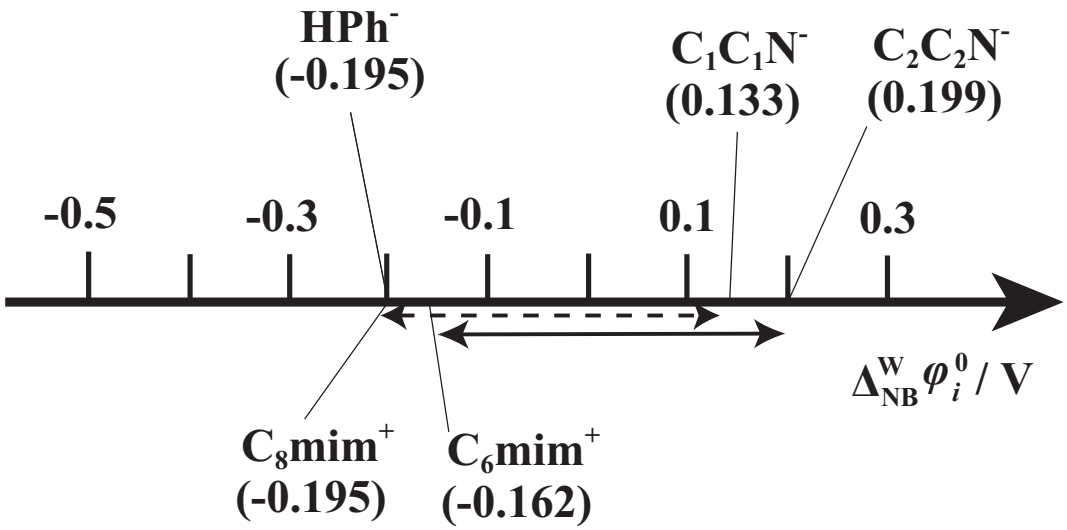

Figure 5.8: Standard ion-transfer potential of several ions in the nitrobenzene-water two phase system.

5.4 Conclusions

The variation of the liquid junction potential of the ILSB when one standard buffer solution was replaced by another is within 1mV for phosphate, borate, and citrate standards and comparable to that of the KClSB, except for the case of the phthalate standard. The time course of the potential of the IL-type is stable with a standard deviation of 0.4 mV in the buffer solutions. The specific deviation of the PBP between $C_8mimC_1C_1N$ and the phthalate standard was observed. The partition of the hydrogen phthalate in $C_8mimC_1C_1N$ shifts the PBP across the interface between $C_8mimC_1C_1N$ and the phthalate standard. If a citrate standard is used instead of the phthalate, the ILSB works more satisfactorily as a salt bridge suitable to potentiometoric pH measurements in an acidic pH range. The present test of the stability of the ILSB equipped reference electrodes is based on the assumption that the double junction-type KClSB reference electrode is stable within an error of ± 0.1 mV in pH standard buffers, the assumption of which may be questioned for a more critical evaluation of the stability of ILSBs. The shift of PBP due to the interference by ions in W was reduced by tuning the $\Delta_{IL}^{W}\phi^0$ of ions constituting the IL.

References

(1) T. Kakiuchi, N. Tsujioka, S. Kurita, and Y. Iwami, *Electrochem. Commun.*, **2003**, *5*, 159–164.

(2) T. Kakiuchi and T. Yoshimatsu, *Bull. Chem. Soc. Jpn.*, **2006**, *79*, 1017–1024.

(3) T. Yoshimatsu and T. Kakiuchi, *Anal. Sci.*, **2007**, *23*, 1049–1052.

(4) R. A. Durst, W. Davison, and W. F. Koch, *Pure Appl. Chem.*, **1994**, *66*, 649–658.

(5) R. C. Metcalf, *Analyst*, **1987**, *112*, 1573–1577.

(6) D. Midgley and K. Torrance, *Analyst*, **1979**, *104*, 63–72.

(7) T. Ozeki, Y. Tsubosaka, S. Nakayama, N. Ogawa, and T. Kimoto, *Anal. Sci.*, **1998**, *14*, 749–756.

(8) R. G. Bates and E. A. Guggenheim, *Pure Appl. Chem.*, **1960**, *1*, 163–168.

(9) R. P. Buck, S. Rondinini, A. K. Covington, F. G. K. Baucke, C. M. A. Brett, M. F. Camoes, M. J. T. Milton, T. Mussini, R. Naumann, K. W. Pratt, P. Spitzer, and G. S. Wilson, *Pure Appl. Chem.*, **2002**, *74*, 2169–2200.

(10) C. M. Gordon, J. D. Holbrey, A. R. Kennedy, and K. R. Seddon, *J. Mater. Chem.*, **1998**, *8*, 2627–2636.

(11) B. R. Staples and R. G. Bates, *J. Res. Nat. Bur. Stand.*, **1969**, *A73*, 37–41.

(12) J. Fuller, A. C. Breda, and R. T. Carlin, *J. Electroanal. Chem.*, **1998**, *459*, 29–34.

(13) A. K. Covington and M. J. F. Rebelo, *Anal. Chim. Acta*, **1987**, *200*, 245–260.

(14) S. Kanemura, T. Yoshimatsu, N. Nishi, and T. Kakiuchi, paper presented at the annual meeting of the Polarography Society of Japan (November 22-23, 2008, Kumamoto), Abstract: *Rev. Polarogr.*, **2008**, *54*, 199.

(15) T. Kakiuchi and N. Nishi, *Electrochemistry*, **2006**, *74*, 942–948.

(16) N. Nishi, S. Imakura, and T. Kakiuchi, *Anal. Chem.*, **2006**, *78*, 2726–2731.

(17) T. Kakiuchi and M. Senda, *Bull. Chem. Soc. Jpn.*, **1984**, *57*, 1801–1808.

(18) T. Kakiuchi, I. Obi, and M. Senda, *Bull. Chem. Soc. Jpn.*, **1985**, *58*, 1636–1641.

(19) G. A. Perley, *Trans. Electrochem. Soc.*, **1947**, *92*, 497–504.

Chapter 6

Determination of the Activity of Hydrogen Ions in Buffers Used for pH Measurement of Physiological Solutions by Use of Ionic Liquid Salt Bridge

6.1 Introduction

The accurate pH measurements of blood and plasma are an important indispensable part of clinical diagnosis. In the potentiometric pH measurement of an isotonic saline media of ionic strength, $I = 0.16$ mol kg^{-1}, such as blood plasma, with a glass combination electrode equipped with a KCl salt bridge (KClSB), the liquid junction potential (LJP) between a KClSB and the isotonic saline media causes errors amounting to 0.03 -0.05 pH unit.[1] Bates reported that the residual liquid junction potential, that is the difference of two LJPs at the interface between primary standard buffers and KClSB and that at the isotonic saline media and KClSB, can be nearly eliminated by matching the ionic strength of the standard buffer solution to that of the clinical sample.[1] Clinical chemists and biological researchers have used the reference standard solution[1–11] at the ionic strength, $I = 0.16$, which has compatibility with biological fluids, for the potentiometric pH measurement of blood and biological

fluids.

A new type of salt bridge made of a moderately hydrophobic ionic liquid (ILSB) recently proposed[12–16] is superior to KClSBs, in that the solubility of the ionic liquid (IL) employed for ILSBs is less than 1 mmol dm^{-3} and the principle of cancelling out the LJP between a sample solution and the inner solution of the reference electrode is based on the partition of the IL into the sample side.[13] An ILSB is expected to be useful on the pH measurement of blood and biological fluids.

In this chapter, the author estimates pH of reference buffer solutions for pH measurement of physiological solutions by use of ILSB made of tributyl(2-methoxyethyl)phosphonium bis(pentafluoroethanesulfonyl)amide ($TBMOEPC_2C_2N$), sandwiched by two hydrogen electrodes at 25 and 37 °C. The author investigates the source of the difference between the experimental pH values obtained by the ILSB and pH values obtained by an Harned cell.

6.2 Experimental

6.2.1 Reagents

The $TBMOEPC_2C_2N$ was obtained form Kanto Chemical Co., Inc. and purified according to the procedure described in chapter 3. The TBMOEPCl was prepared according to the procedure described in chapter 1. The 50×10^{-6} mol dm^{-3} sulfuric acid solution and the hydrogen electrodes were prepared as described in chapter 1.[17] 0.025 mol kg^{-1} equimolal phosphate buffer solution was prepared according to the procedure described in chapter 3. Tris(hydroxymethyl)aminomethane (Tris; 99 %), Tris-HCl (99 %), *N*-tris(hydroxymethyl) methyl-2-aminomethanesulfonic acid (TES; 99 %), *N*-2-hydroxyethylpiperazine-*N′*-2-ethanesulfonic acid (HEPES; 99 %), and NaHEPES (99 %) were obtained from Nacalai Tesque, Inc. NaTES (99 %) was obtained from Sigma-Aldrich Co. All of these reagents were used without further purification. The structures of Tris, TES, and HEPES are given in Fig. 6.1. Na_2HPO_4 and NaCl were dried for two hours at 110 °C before the preparation of phosphate buffer solutions. The buffer solutions were prepared by weighing the buffer substances, NaCl, MilliQ water. The buffer solutions studied had the following compositions, where the figures

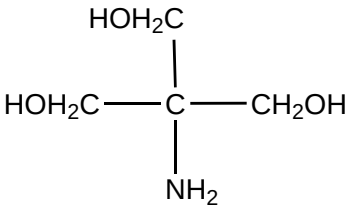

Tris(hydroxymetyl)aminomethane (Tris)

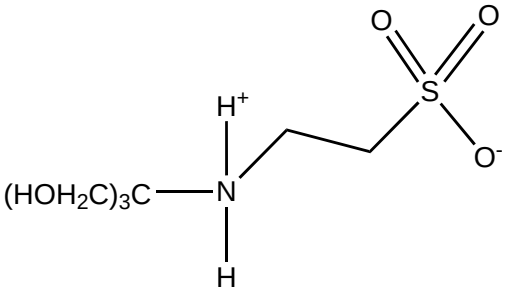

N-tris(hydroxymethyl)metyl-2-aminoethanesulfonic acid (TES)

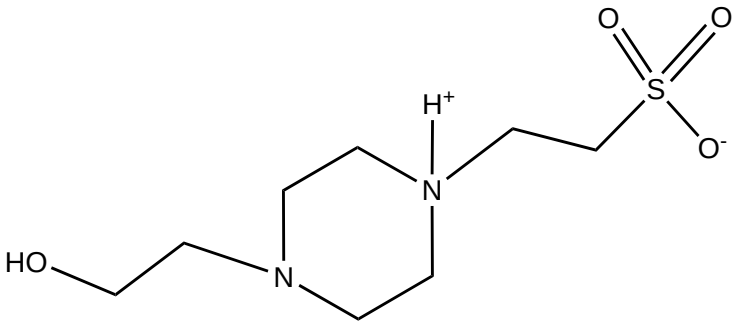

N-2-hydroxyethylpiperazine-*N*'-2-ethanesulfonic acid (HEPES)

Figure 6.1: Structures of Tris, TES, and HEPES

in parentheses are molalities:

1: 3.5 phosphate: KH_2PO_4 (0.005217), Na_2HPO_4 (0.018258), NaCl (0.1)

1:3 Tris: Tris-HCl (0.05), Tris (0.01667), NaCl (0.11)

1:2 HEPES: HEPES (0.02), NaHEPES (0.04), NaCl (0.12)

1:2 TES: TES (0.02), NaTES (0.04), NaCl (0.12)

The Tetraoctylammonium tetraphenylborate (TOcATPB) was synthesized as described else-

where.[18] Sodium tetraphenylborete (NaTPB) was obtained from DOJINDO LABORATORIES. Li_2SO_4, $MgCl_2$, and LiOH were used without further purification. The hydrogen electrodes were prepared according to the procedure described in chapter 1.[17]

6.2.2 Methods

Potentiometric Determination of pH

The electrochemical cell employed is represented by

I	II	III	IV	V	
	H_2,		H_2,		
Pt	50 μmol dm^{-3}	TBMOEPC$_2$C$_2$N	standard buffer	Pt	(A)
	H_2SO_4		solution		

The single dashed vertical bars indicate the interfaces between the ILSB and the aqueous solutions (II and IV). The configuration of a U-type glass cell for cell (A) was the same as what we reported previously.[17] The cell voltage, E, i.e., the potential of the right-hand-side terminal referred to that of the left in the cell (A), was measured with an electrometer (ADC Corporation, 8252) with a GPIB interface. The sampling interval was 1 min. Each of the two hydrogen electrodes was supplied with hydrogen gas (99.9995 %), which was generated by a hydrogen gas generator (Horiba Stec, OPGU-7100), at the rate of two to three bubbles per second from a jet about 1 mm in diameter during measurements. The gas was passed through a saturator containing the same solution as the one in the hydrogen electrode compartment before it entered the cell.

The value of E was measured at standard buffer solutions studied in phase IV in cell (A) at 25 and 37 °C. The cell was immersed in a water bath maintained at 25.0 ± 0.1 or 37.0 ± 0.1 °C. The measurement at each standard buffer solutions was repeated five times. The measurement for each standard buffer solutions was completed in two days and it took 8 days

to complete all measurements. After each measurement, both 50 μmol dm^{-3} H_2SO_4 solution and standard buffer solution in phases II and IV in cell (A) was drained and the U-type glass cell and two platinum electrodes were washed with MilliQ water three times. The *E* was recorded for 1 h after the hydrogen gas was passed in cell (A) for 1 h. The average of *E* values recorded in the last ten min at each measurement was employed to estimate the pH value.

Cyclic Voltammetry for the Transfer of Ions across the NB | W Interface

The electrochemical cell employed for ion transfer voltammetry is represented as:

Ag	AgCl	5 mM NaTPB 10 mM $MgCl_2$ (W2)	50 mM TOcATB (NB)	10 mM Li_2SO_4 50 mM Tris-HCl or 60 mM HEPES + LiOH or 60 mM TES + LiOH (W1)	AgCl	Ag	(B)

The potential of right-hand-side terminal with respect to the left is hereafter denoted as *E*. The current, *I*, corresponding to the flow of the positive charge from W1 to IL is taken to be positive. The Ag/Ag_2SO_4 electrode was prepared by electrolysis in a 2 wt% Na_2SO_4 aqueous solution by use of a Ag wire as the anode. The configuration of the cell is illustrated in Fig. 6.2. A flat interface was made in a four electrode cell for voltammetry of ion transfer. The area of the interface was 0.16 cm^2. The temperature of the cell was maintained at 25.0 °C by circulating water through the outer jacket of the cell. The potential drop across the polarized liquid | liquid interface was controlled with a potentiostat (Hokuto Denko, HA1010mA1A). A positive feedback method was applied for the iR-drop compensation.

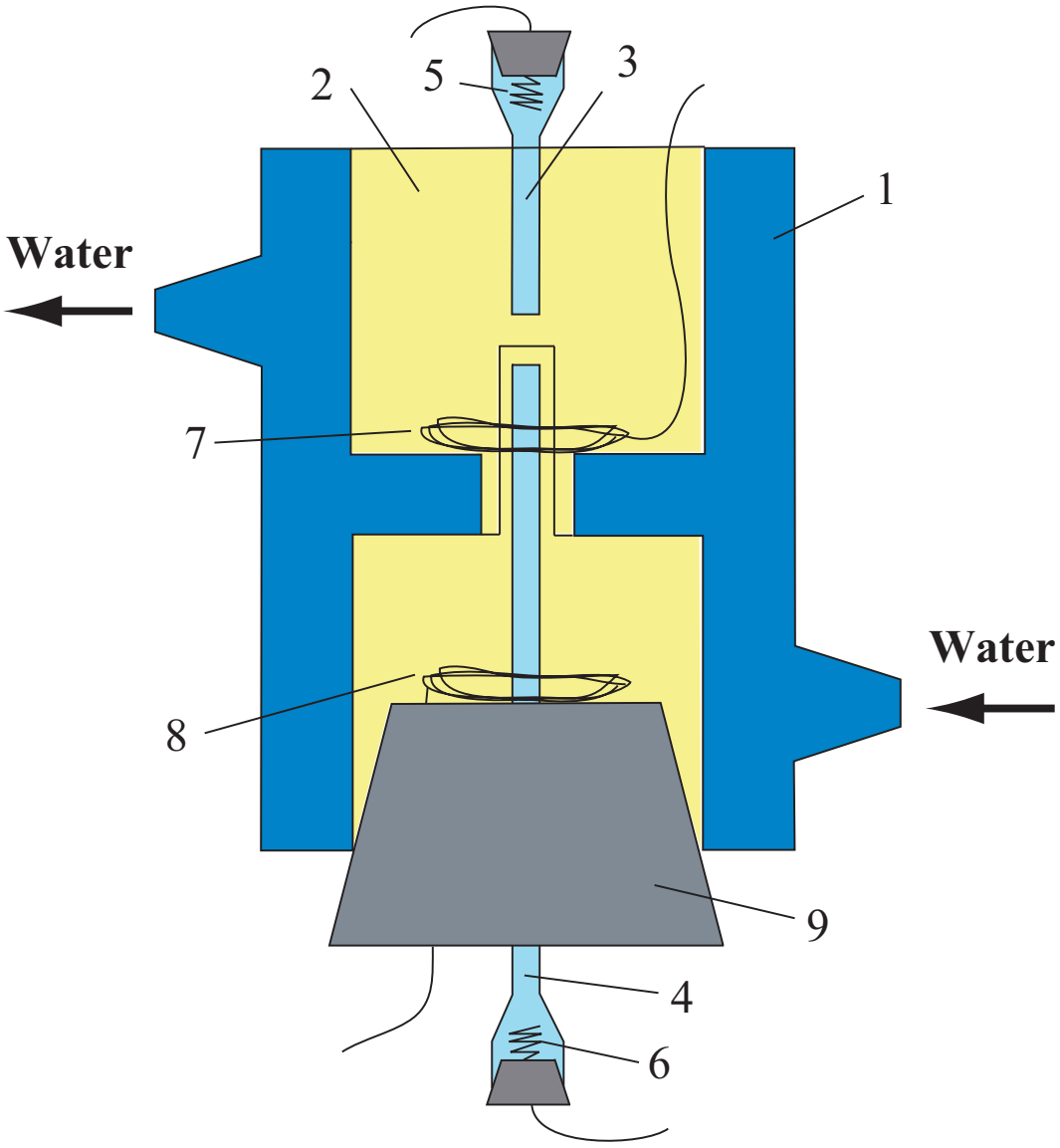

Figure 6.2: Illustration of the electrochemical cell for cyclic voltammetry for the transfer of ions across the NB |W Interface. 1: glass jacket, 2: 50 mM NB TOcATB in NB, 3: W1 (10 mM Li_2SO_4, 10 mM Li_2SO_4 + 50 mM Tris-HCl, 10 mM Li_2SO_4 + 60 mM HEPES + LiOH, or 10 mM Li_2SO_4 + 60 mM TES + LiOH), 4: W2 (5 mM NaTPB + 10 mM $MgCl_2$), 5: Ag/Ag_2SO_4 electrode, 6: Ag/AgCl electrode, 7 and 8: Pt wires, 9: silicon rubber stopper.

Cyclic Voltammetry for the Transfer of Ions across the IL | W Interface

The electrochemical cell employed for recording current-potential curves is represented as:

Ag | AgCl	10 mmol dm^{-3} TBMOEPCl (W2)	TBMOEPC_2C_2N (IL)	0.12 mol kg^{-1} NaCl or the buffer + 0.12 mol kg^{-1} NaCl (W1)	AgCl	Ag	(C)

The cell configuration is given Fig. 6.3. The potential of right-hand-side terminal with respect to the left is hereafter denoted as E. The current, I, corresponding to the flow of the positive charge from W1 to IL is taken to be positive. Micropipettes were made from borosilicate glass capillaries (G-1, Narishige, o.d. / i.d. = 1.0 mm / 0.6 mm) by use of a pipette puller (PC-10, Narishige). An optical microscope (BX-60, x200-x1000, Olympus) was used to observe the tip of a pipette for determining the inner diameter of the tip, d, prior to an electrochemical measurement. A micropipette filled with the W phase was immersed in the IL phase to form a micro liquid|liquid interface. Electrochemical measurements were made by use of a microelectrode potentiostat (HECS-972C, Fusou Electro Chemical System) without Ohmic drop compensation. Cyclic voltammograms were recorded with a homemade computer-controlled system.

6.2.3 Experimental pH Values of Standard Buffer Solutions

An unknown pH value of standard buffer solutions (pH_x) in IV in cell (A) is written by

$$pH_x = pH_s - \frac{F}{RT \ln 10}(E - E_j) \tag{6.1}$$

where pH_s is the pH value of the 50 μmol dm^{-3} H_2SO_4 solution in II in cell (A), and E_j is the sum of two LJPs on both sides of the ILSB in cell (A), F is the Faraday constant, R is

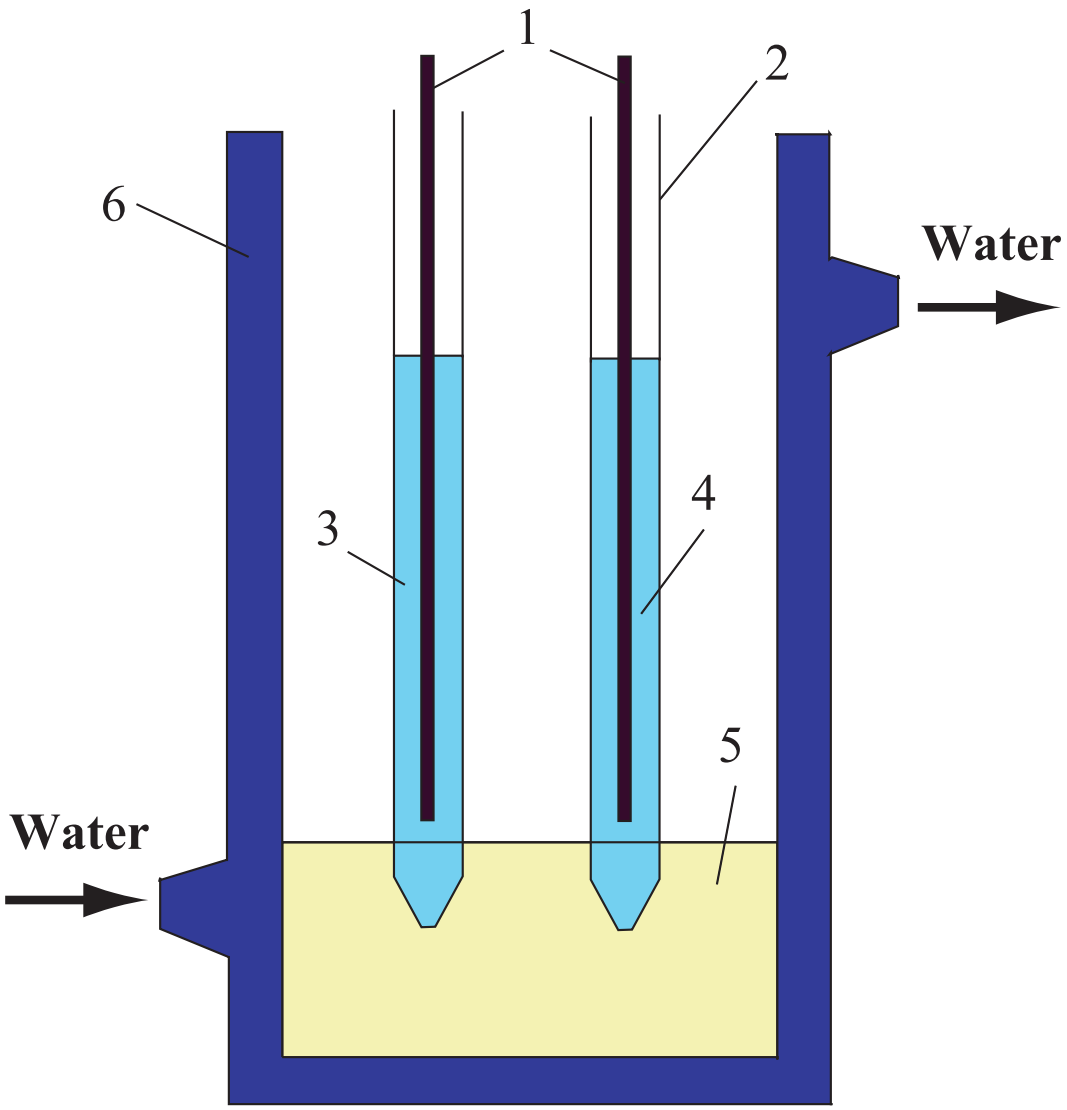

Figure 6.3: Illustration of the electrochemical cell for cyclic voltammetry. 1: Ag/AgCl electrode, 2: micropipette, 3: 10 mmol dm^{-3} TBMOEPCl, 4: buffer solution or 0.12 mol kg^{-1} NaCl, 5: $TBMOEPC_2C_2N$, 6: glass jacket.

the gas constant, and T is the absolute temperature. The value of pH_s at 25 and 37 °C are obtained from molality of hydrogen ions and the corresponding activity coefficient calculated from the Debye-Hückel (D-H) limiting law[19] as the procedure described in chapter 3. In the calculation of pHs at 37 °C, the dissociation constant of sulfuric acid solution at 37 °C is calculated from the following equation[20]

$$\ln K_2 = -14.0321 + 2825.2/T \tag{6.2}$$

The constant of D-H theory in the D-H limiting law at 37 °C is obtained by the interpolation of the known constants of D-H theory at 20, 25, 30, 35, 38, 40, and 45 °C.[21] To calculate the activity of hydrogen ions, the molarities of sulfuric acids at 20.0 °C were converted to the molalities using the densities obtained by the extrapolation of the known densities of sulfuric acids at 20.0 °C as a function of the molarity.[22] The constants of D-H theory, A, and values of m_{H^+}, γ_{H^+}, ionic strength in the molality scale, I, and pH_s in 50 μmol dm^{-3} H_2SO_4 solution at 25 and 37 °C are listed in Table 6.1. If the ILSB works ideally, E_j is null and the equation (6.1) reduces to

$$pH_x = pH_s - \frac{FE}{RT \ln 10} \tag{6.3}$$

The pH_x value obtained by the equation (6.3) is hereafter denoted as pH_{ex}.

Table 6.1: Constants of the Debye-Hückel theory, A, and the values of γ_{H^+}, m_{H^+}, I, and pH_s in 50 μmol dm^{-3} H_2SO_4 solution at 25 and 37 °C.

t / °C	A	γ_{H^+}	m_{H^+} / μmol kg^{-1}	I / μmol kg^{-1}	pH_s
25	0.5108	0.9857	99.85	149.55	4.007
37	0.5216	0.9854	99.66	149.17	4.008

6.3 Results and Discussion

6.3.1 Time Course of *E* at Standard Buffer Solutions at 25 and 37 °C.

Figures 6.4 - 6.7 show the time dependence of E for 1 h at 1:3.5 phosphate, 1:3 Tris, 1:2 HEPES, 1:2 TES buffer solutions in cell (A) at 25 °C, respectively and Fig. 6.8 - 6.11 show the time dependence of E for 1 h at 1:3.5 phosphate, 1:3 Tris, 1:2 HEPES, 1:2 TES buffer solutions in IV in cell (A) at 37 °C, respectively. In each run, the excursion of E in 1 h was within 0.7 mV (equal to about 0.012 pH). The average of excursion in 1 h for all measurements was 0.33 ± 0.18 mV.

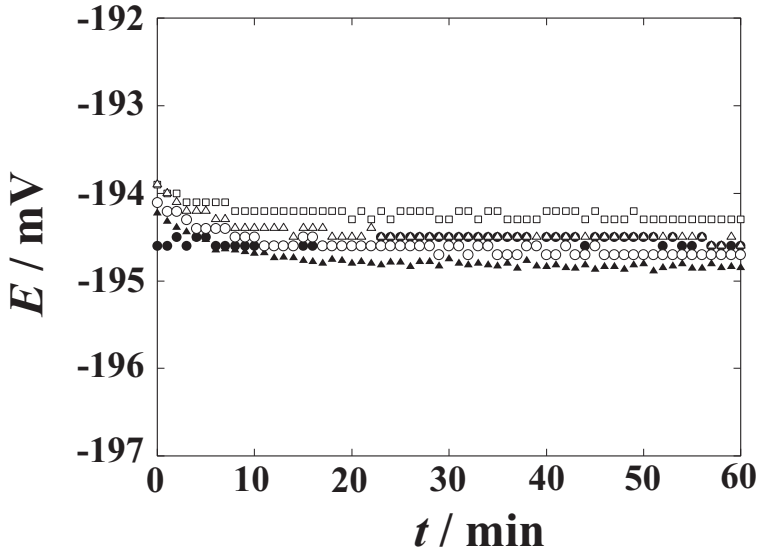

Figure 6.4: Time dependence of *E* for 1 h at 1:3.5 phosphate buffer solution in cell (A) at 25 °C. ○ : 1st measurement, △ : 2nd measurement, □ : 3rd measurement, ● : 4th measurement, ▲ : 5th measurement.

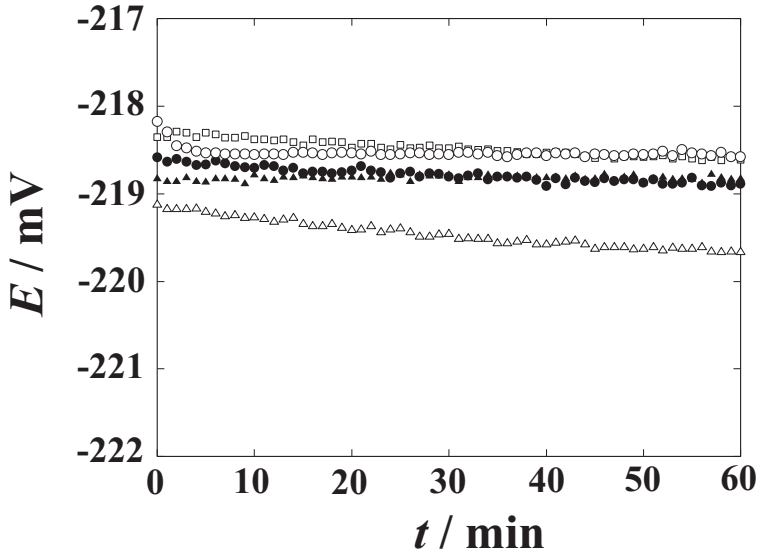

Figure 6.5: Time dependence of *E* for 1 h at 1:3 Tris buffer solution in cell (A) at 25 °C. ○ : 1st measurement, △ : 2nd measurement, □ : 3rd measurement, ● : 4th measurement, ▲ : 5th measurement.

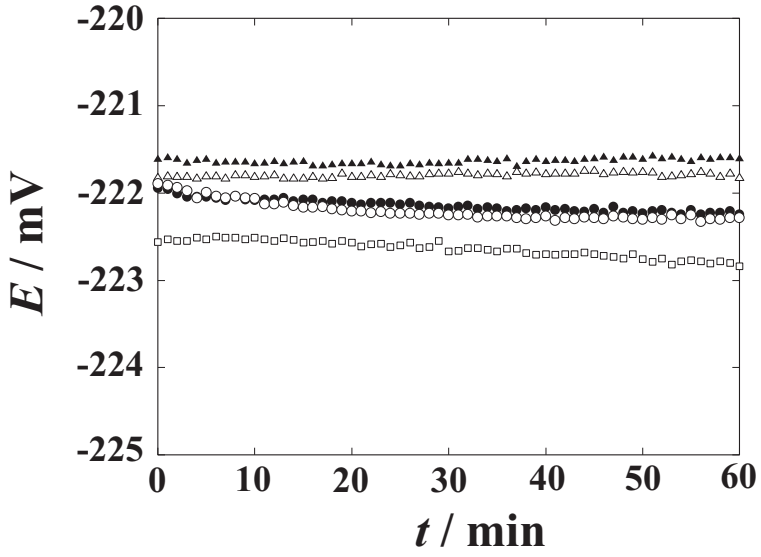

Figure 6.6: Time dependence of *E* for 1 h at 1:2 HEPES buffer solution in cell (A) at 25 °C. ○ : 1st measurement, △ : 2nd measurement, □ : 3rd measurement, ● : 4th measurement, ▲ : 5th measurement.

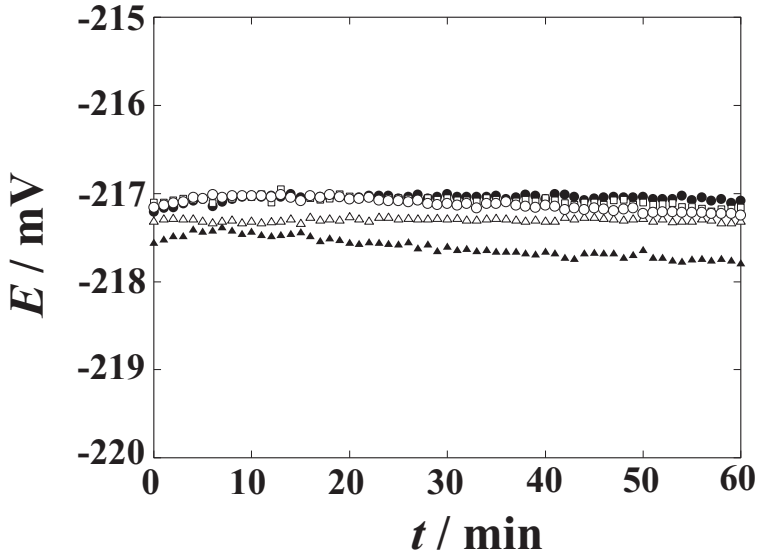

Figure 6.7: Time dependence of *E* for 1 h at 1:2 TES buffer solution in cell (A) at 25 °C. ○ : 1st measurement, △ : 2nd measurement, □ : 3rd measurement, ● : 4th measurement, ▲ : 5th measurement.

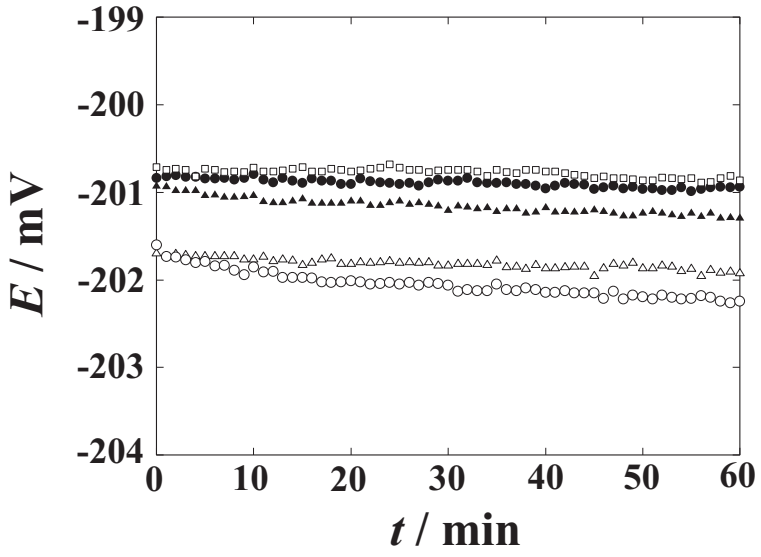

Figure 6.8: Time dependence of *E* for 1 h at 1:3.5 phosphate buffer solution in cell (A) at 37 °C. ○ : 1st measurement, △ : 2nd measurement, □ : 3rd measurement, ● : 4th measurement, ▲ : 5th measurement.

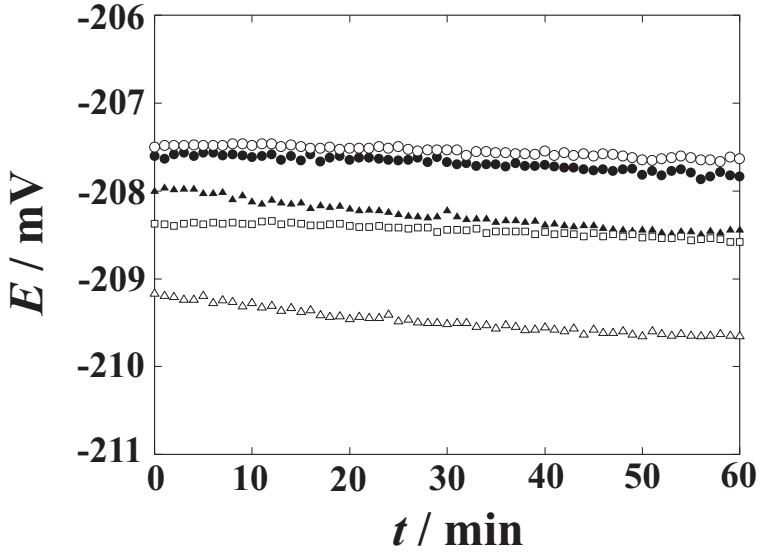

Figure 6.9: Time dependence of *E* for 1 h at 1:3 Tris buffer solution in cell (A) at 37 °C. ○ : 1st measurement, △ : 2nd measurement, □ : 3rd measurement, ● : 4th measurement, ▲ : 5th measurement.

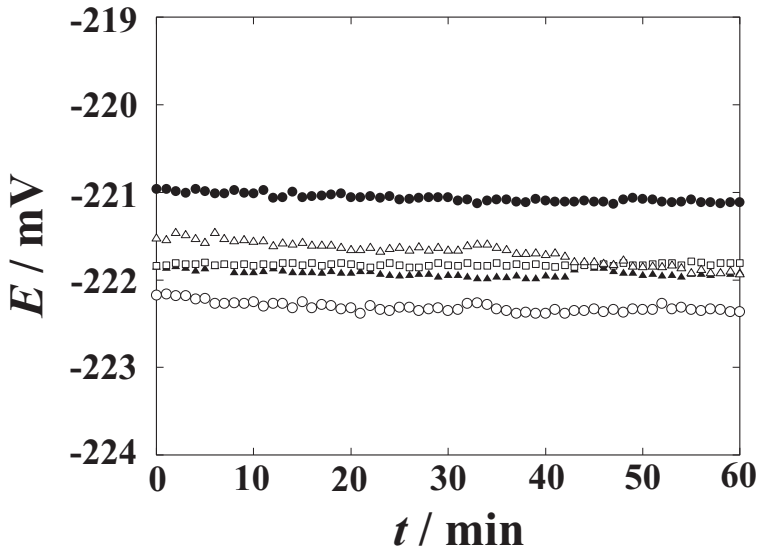

Figure 6.10: Time dependence of *E* for 1 h at 1:2 HEPES buffer solution in cell (A) at 37 °C. ○ : 1st measurement, △ : 2nd measurement, □ : 3rd measurement, ● : 4th measurement, ▲ : 5th measurement.

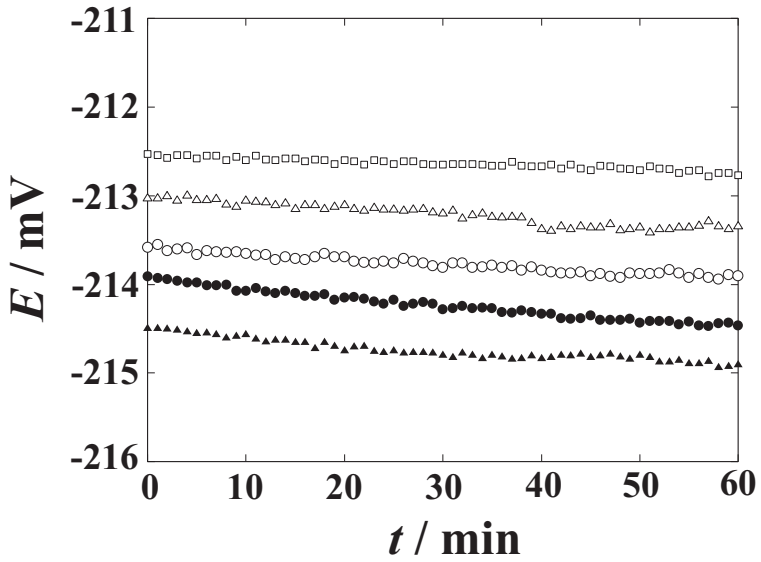

Figure 6.11: Time dependence of *E* for 1 h at 1:2 TES buffer solution in cell (A) at 37 °C. ○ : 1st measurement, △ : 2nd measurement, □ : 3rd measurement, ● : 4th measurement, ▲ : 5th measurement.

6.3.2 Comparison of Experimental pH Values Obtained by Use of ILSB with pH Values Obtained by Use of Harned Cell or KClSB at 25 and 37 °C.

Table 6.2 and 6.3 list the experimental pH values, pH_{ex}, for each buffer solution at 25 and 37 °C, respectively. Bates et al.[1] reported the pH values obtained by use of the following two types of cells for each buffer solution at 25 and 37 °C.

I	II	III	IV	
Pt	H_2, buffer solutions, NaCl	AgCl	Ag	(D)

I	II	III	IV	V	
Hg	Hg_2Cl_2	3.5 mol kg^{-1} KCl	buffer solutions, H_2	Pt	(E)

The pH values obtained by use of cell (D) and (E) at 25 and 37 °C, where the former is denoted as pH_{Harned} and the later is denoted as pH_{KClSB}, are also given in Table 6.2 and 6.3, respectively. The value of pH_{ex} was obtained from the average *E* value for each measurement. The ±95 % confidence interval of pH_{ex} for the five measurements at each buffer solution is also given in Table 6.1. Although the pH_{ex} values for 1:3.5 phosphate and 1:3 Tris at 25 and 37 °C are closer to the pH_{Harned} values than the pH_{KClSB} values, the pH_{ex} values for 1:3.5 phosphate and 1:3 Tris are lower by 0.015 - 0.037 pH than the pH_{Harned} values. The difference between pH_{ex} values and pH_{Harned} for 1:2 HEPES and TES is greater than that between pH_{KClSB} and pH_{Harned}.

Table 6.2: Experimental pH values obtained by use of ILSB and pH values by use of a Harned cell or KClSB at reference buffer solutions studied at 25 °C.

buffer solution	pH_{Harned}	pH_{KClSB}	Mean pH_{ex} ±95 % confidence interval	$pH_{KClSB} - pH_{Harned}$	$pH_{ex} - pH_{Harned}$
1:3.5 phosphate	7.323	7.281	7.297 ± 0.004	-0.042	-0.026
1:3 Tris	7.746	7.685	7.709 ± 0.008	-0.061	-0.037
1:2 HEPES	7.805	7.764	7.763 ± 0.011	-0.041	-0.042
1:2 TES	7.758	7.714	7.680 ± 0.006	-0.044	-0.078

Table 6.3: Experimental pH values obtained by use of ILSB and pH values by use of a Harned cell or KClSB at reference buffer solutions studied at 37 °C.

buffer solution	pH_{Harned}	pH_{KClSB}	Mean pH_{ex} ±95 % confidence interval	$pH_{KClSB} - pH_{Harned}$	$pH_{ex} - pH_{Harned}$
1:3.5 phosphate	7.297	7.267	7.282 ± 0.012	-0.030	-0.015
1:3 Tris	7.427	7.381	7.395 ± 0.015	-0.046	-0.032
1:2 HEPES	7.661	7.631	7.613 ± 0.008	-0.030	-0.048
1:2 TES	7.535	7.503	7.484 ± 0.017	-0.032	-0.051

6.3.3 Effect of the Diffusion Potential and Finite Solubility of IL in W on Experimental pH Values

If the two distribution potentials at the ILSB | H_2SO_4 and ILSB | standard buffer solution interfaces are canceled out, the experimental pH value, pH'_{ex}, is expressed by

$$pH'_{ex} = pH_s - \frac{F}{RT \ln 10}(E + \phi^{W}_{diff}) \tag{6.4}$$

where ϕ^{W}_{diff} is the diffusion potential due to the dissolution of IL from the ILSB in 50 μmol dm^{-3} H_2SO_4 solution and is referred to the electrostatic potential in the bulk sample solution

phase. The diffusion potential in standard buffer solutions has been neglected in eq 6.4 because the ionic strength of the standard solutions is much higher than the solubility of the IL in W.[14] The value of ϕ^{W}_{diff} in 50 μmol dm^{-3} H_2SO_4 solutions[17] have been calculated from the Hendarson equation[23] and is -0.097 mV at 25 °C. The pH'_{ex} and $pH'_{ex}-pH_{Harned}$ at 25 °C are given in Table 6.4.

The value of pHs is calculated to be 4.011 at 25 °C taking account of the increase of ionic strength of 50 μmol dm^{-3} H_2SO_4 in II phase in cell (A) due to the dissolution $TBMOEPC_2C_2N$ into the H_2SO_4 solution. The pH_{ex} obtained from pH_s recalculated taking account of the increase of ionic strength, pH''_{ex}, and $pH''_{ex}- pH_{Harned}$ are also given in Table 6.4. The pH_{ex} obtained taking account of both effects of the diffusion potential and increase of ionic strength, pH'''_{ex}, and $pH'''_{ex}- pH_{Harned}$ are also given in Table 6.4. The pH'''_{ex} values are still smaller by 0.022 - 0.073 than the pH_{Harned} values. The effects of the diffusion potential of $TBMOEPC_2C_2N$ and the increase of ionic strength in 50 μmol dm^{-3} H_2SO_4 solution due to the dissolution of the $TBMOEPC_2C_2N$ is expected to be also small at 37 °C.

Table 6.4: Effects of the diffusion potential and the change in the ionic strength due to the dissolution of $TBMOEPC_2C_2N$ on experimental pH values at 25 °C.

buffer solution	pH'_{ex}	pH''_{ex}	pH'''_{ex}	$pH'_{ex}-pH_{Harned}$	$pH''_{ex}-pH_{Harned}$	$pH'''_{ex}-pH_{Harned}$
1:3.5 phosphate	7.298	7.300	7.301	-0.025	-0.023	-0.022
1:3 Tris	7.710	7.712	7.713	-0.036	-0.034	-0.033
1:2 HEPES	7.764	7.766	7.767	-0.041	-0.039	-0.038
1:2 TES	7.682	7.683	7.685	-0.076	-0.075	-0.073

6.3.4 Interference by Ions in W

Cyclic Voltammetry for the Transfer of Ions across the NB|W Interface

A possibility reason of the difference between pH_{ex} and pH_{Harned} at 1:3 Tris, 1:2 HEPES, and 1:2 TES buffer solutions is the shift of the LJP between the ILSB and the buffer solutions

due to the partition of ions in buffer solutions in the ILSB. We evaluated the hydrophobicity of protonated Tris (Tris·H^+), $HEPES^-$, and TES^-. Figures 6.12 ~ 6.15 show voltammograms for the transfer of ions across the NB | W interface at the scan rate of applied voltage, *v*, are 10, 20, 50, and 100 mV s^{-1}, respectively. Curves 1 ~ 4 in Fig. 6.12 ~ 6.15 indicate voltammograms at 10 mM Li_2SO_4, 10 mM Li_2SO_4 + 50 mM Tris-HCl, 10 mM Li_2SO_4 + 60 mM HEPES + 60 mM LiOH, and 10 mM Li_2SO_4 + 60 mM TES + 60 mM LiOH in W1 in cell (B), respectively. In Fig. 6.12 ~ 6.15, the curves 3 and 4 did not change compared with the curve 1 except the shift of the location of polarized potential window (ppw), and no ion-transfer current due to the transfer of ions in W1 across the NB | W interface appeared. The width of ppw in the curve 2 was narrower than that of curve 1. Therefore, the shift of the LJP between the IL and the 1:3 Tris buffer, $\Delta_{IL}^{buff}\phi = \phi_{buff} - \phi_{IL}$, where ϕ_{buff} and ϕ_{IL} are the inner potentials in the Tris buffer and the IL, respectively, due to the partition of Tris·H^+ in IL may occur.

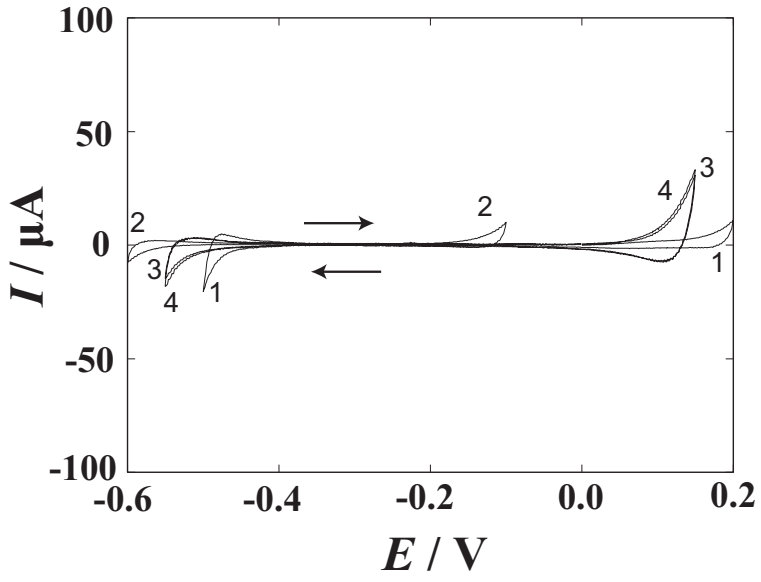

Figure 6.12: Cyclic voltammograms for the 10 mM Li_2SO_4 (Curve 1), 10 mM Li_2SO_4 + 50 mM Tris-HCl (Curve 2), 10 mM Li_2SO_4 + 60 mM HEPES + 60 mM LiOH (Curve 3), and 10 mM Li_2SO_4 + 60 mM TES + 60 mM LiOH (Curve 4) in W1 in cell (B). The scan rate: 10 mV s^{-1}. Arrows by the line indicate the direction of the scanning.

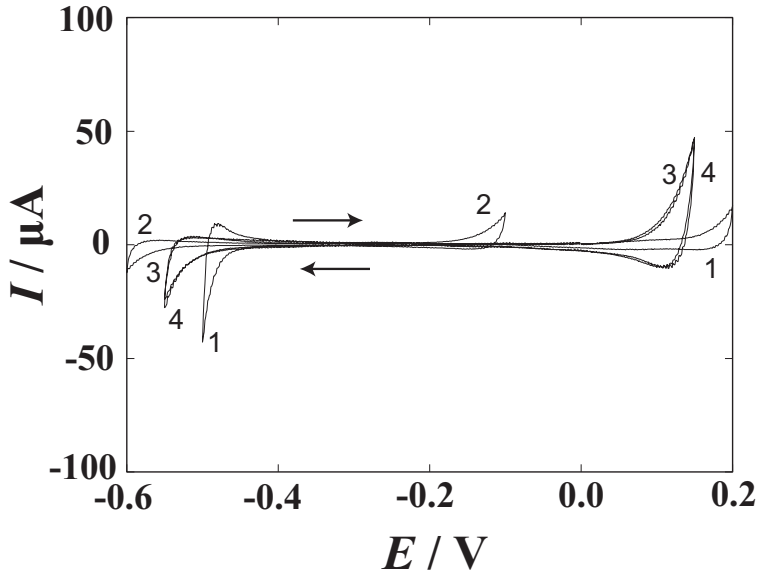

Figure 6.13: Cyclic voltammograms for the 10 mM Li_2SO_4 (Curve 1), 10 mM Li_2SO_4 + 50 mM Tris-HCl (Curve 2), 10 mM Li_2SO_4 + 60 mM HEPES + 60 mM LiOH (Curve 3), and 10 mM Li_2SO_4 + 60 mM TES + 60 mM LiOH (Curve 4) in W1 in cell (B). The scan rate: 20 mV s^{-1}. Arrows by the line indicate the direction of the scanning.

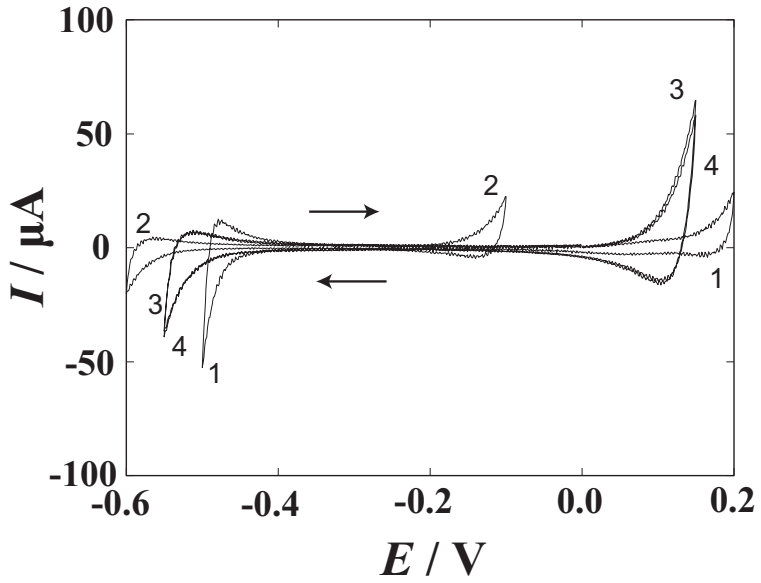

Figure 6.14: Cyclic voltammograms for the 10 mM Li_2SO_4 (Curve 1), 10 mM Li_2SO_4 + 50 mM Tris-HCl (Curve 2), 10 mM Li_2SO_4 + 60 mM HEPES + 60 mM LiOH (Curve 3), and 10 mM Li_2SO_4 + 60 mM TES + 60 mM LiOH (Curve 4) in W1 in cell (B). The scan rate: 50 mV s^{-1}. Arrows by the line indicate the direction of the scanning.

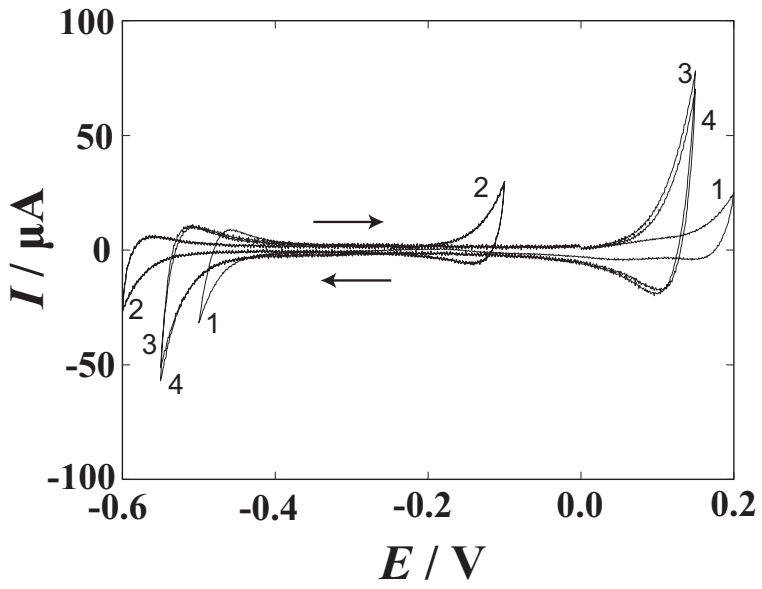

Figure 6.15: Cyclic voltammograms for the 10 mM Li_2SO_4 (Curve 1), 10 mM Li_2SO_4 + 50 mM Tris-HCl (Curve 2), 10 mM Li_2SO_4 + 60 mM HEPES + 60 mM LiOH (Curve 3), and 10 mM Li_2SO_4 + 60 mM TES + 60 mM LiOH (Curve 4) in W1 in cell (B). The scan rate: 100 mV s^{-1}. Arrows by the line indicate the direction of the scanning.

However, it is expected that the LJP due to the partition of $Tris{\cdot}H^+$ in IL shifts to negative direction, and then the measured pH value increases. The expected shift of pH value in 1:3 Tris is not consistent with the results given in Table 6.2 and 6.3. The difference between pH_{ex} and pH_{Harned} at 1:3 Tris can not be explained by the shift of the LJP due to the partition of $Tris{\cdot}H^+$ in IL. The shift of the location of ppw in curve 2 ~ 4 in Fig. 6.12 ~ 6.15 may be ascribed to the change of potential of Ag/Ag_2SO_4 electrode.

Cyclic Voltammetry for the Transfer of Ions across the IL |W Interface

Figures 6.16 ~ 6.18 show voltammograms for the transfer of ions across the micro liquid | liquid interface supported at the tip of the micropipette when d = 4 μm, the scan rates of applied voltage, v, are 20, 50, and 100 mV s^{-1}, respectively. Curves 1 ~ 3 in Fig. 6.16 ~ 6.18 indicate voltammograms at 0.012 mol kg^{-1} NaCl, 1:2 HEPES, and 1:2 TES in W1 in cell (B), respectively.

The currents at 1:2 HEPES and 1:2 TES in W1 in cell (B) are larger than the NaCl solution at all studied scan rates. Two possible reasons for the increase of current is the transfer

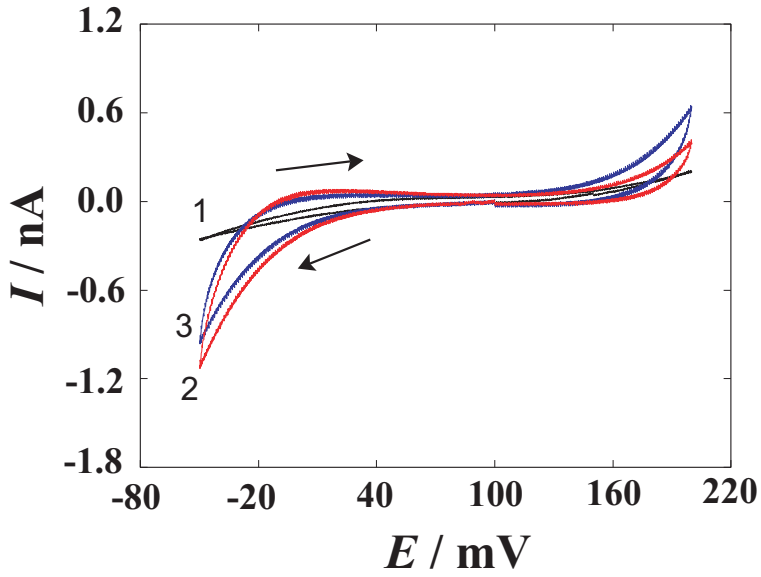

Figure 6.16: Cyclic voltammograms for the 0.12 mol kg^{-1} NaCl (Curve 1), 1:2 HEPES (Curve 2), 1:2 TES (Curve 3) in W1 in cell (B). The scan rate: 20 mV s^{-1}. Arrows by the line indicate the direction of the scanning.

of ions constituting the IL to W1 and the transfer of ions in W1 at 1:2 HEPES and 1:2 TES. The negative end of ppw in curves 2 and 3 shifted to more positive potentials than that of ppw in curve 1. Therefore, from a model of the mixed potential[24,25] as mentioned in chapter 5, the LJP between the IL and the 1:2 HEPES or 1:2 TES buffer, $\Delta_{IL}^{buff}\phi$, is expected to shift positively. When the LJP between the IL and 1:2 HEPES or TES buffer shifts positively, the direction of shift in the cell voltage in cell (A) is positive, and then the pH values determined with cell (A) decrease. The expected direction of shift of pH values at 1:2 HEPES and 1:2 TES buffers is consistent with the results obtained from potentiometry with cell (A). The sources of negative currents may be HEPES$^-$ or TES$^-$ ions as well as the hydrogen phthalate discussed in chapter 5.

The negative end at 1:2 TES shifted to more positive potential than that at 1:2 HEPES except for the 20 mV s^{-1} scan rate. This suggests the PBP between the IL and 1:2 TES shifts more positively than that of 1:2 HEPES, that is, the measured pH values decrease. The expected direction of shift in measured pH value is consistent with the experimental results.

From the voltammogram at 0.012 mol kg^{-1} NaCl in cell (B), the interface at the TBMOE-

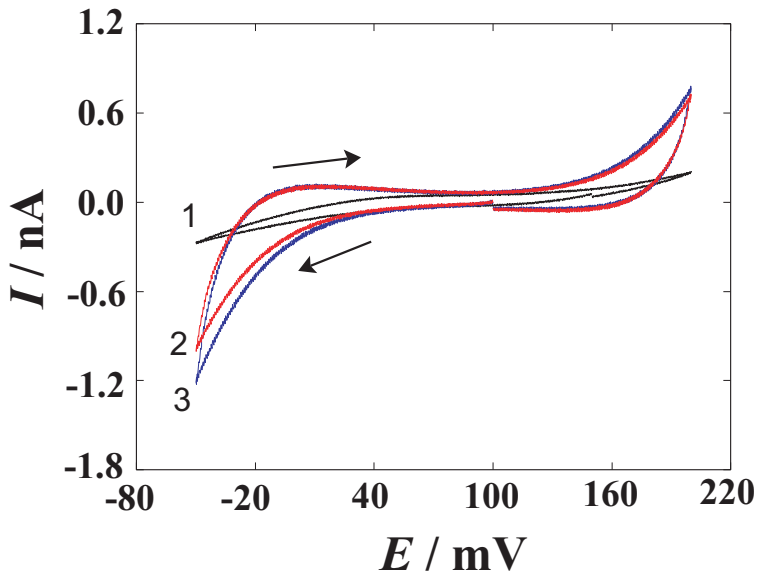

Figure 6.17: Cyclic voltammograms for the 0.12 mol kg^{-1} NaCl (Curve 1), 1:2 HEPES (Curve 2), 1:2 TES (Curve 3) in W1 in cell (B). The scan rate: 50 mV s^{-1}. Arrows by the line indicate the direction of the scanning.

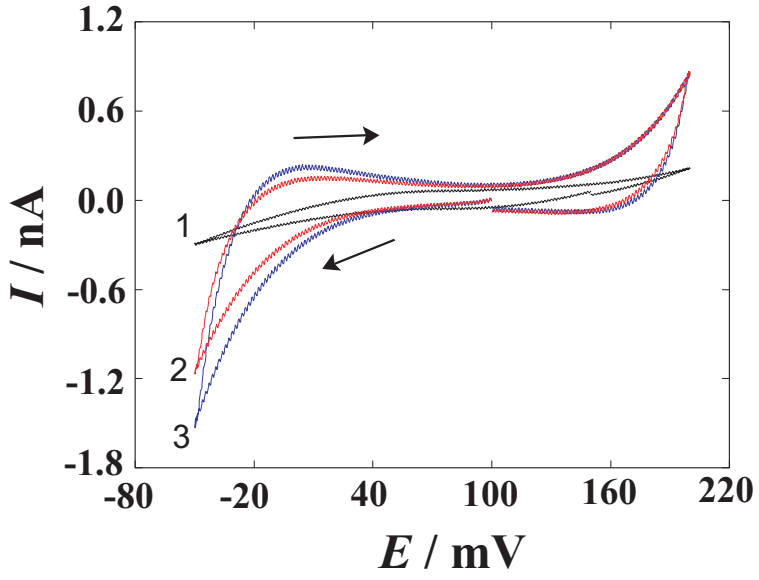

Figure 6.18: Cyclic voltammograms for the 0.12 mol kg^{-1} NaCl (Curve 1), 1:2 HEPES (Curve 2), 1:2 TES (Curve 3) in W1 in cell (B). The scan rate: 100 mV s^{-1}. Arrows by the line indicate the direction of the scanning.

PC_2C_2N and W is polarized due to the low solubility of TBMOEPC_2C_2N to W.[26] Therefore, the PBP between TBMOEPC_2C_2N and W is susceptible to the interference by the ions in W. On the other hand, in practice, the low solubility of IL to W has advantage in terms of life time of ILSB. We need to tune $\Delta_{IL}^{W}\phi^0$ of ions constituting an IL and the solubility of the IL for the pH measurement of physiological solutions.

6.4 Conclusions

The activities of hydrogen ions in 1:3.5 phosphate and 1:3 Tris buffer solutions have been more accurately estimated by use of the TBMOEPC_2C_2N salt bridge than by use of a KClSB. However, experimental pH values of 1:3 Tris, 1:2 HEPES and TES are smaller than those obtained by use of the Harned cell. In the case of 1:2 HEPES and TES, the difference between pH values obtained by use of the ILSB and Harned cell may be because the distribution potential between ILSB and buffer solutions shifts by the interference of the $HEPES^-$ or TES^- in buffer solutions. We need to optimize $\Delta_{IL}^{W}\phi^0$ of ions constituting an IL and the solubility of the IL for the pH measurement of physiological solutions.

References

(1) Bates, R. G.; Vega, C. A.; D. R. White, J. *Anal. Chem.* **1978**, *50*, 1295–1300.

(2) Durst, R. A.; Staples, B. R. *Clin. Chem.* **1972**, *18*, 206–208.

(3) Bower, V. E.; Paabo, M.; Bates, R. G. *J. Res. Natl. Bur. Stand* **1961**, *65A*, 267–270.

(4) Roy, R. N.; Roy, L. N.; Denton, C. E.; LeNoue, S. R.; Fuge, M. S.; Dunseth, C. D.; Durden, J. L.; Roy, C. N.; Bwashi, A.; Wollen, J. T.; DeArmon, S. J. *J. Chem. Eng. Data* **2009**, *54*, 428–435.

(5) Wu, Y. C.; Berezansky, P. A.; Feng, D.; Koch, W. F. *Anal. Chem.* **1993**, *65*, 1084–1087.

(6) Roy, R. N.; Mrad, D. R.; Lord, P. A.; Carlsten, J. A.; Good, W.; Allsup, P.; Roy, L. N.; Kuhler, K. M.; Koch, W. F.; Wu, Y. C. *J. Solution Chem.* **1998**, *27*, 73–87.

(7) Roy, R. N.; Roy, L. N.; Tabor, B. J.; Richards, C. A.; Simon, A. N.; Moore, A. C.; Seing, L. A.; Craig, H. D.; Robinson, K. T. *J. Solution Chem.* **2004**, *33*, 1199–1211.

(8) Roy, R. N.; Roy, L. N.; Denton, C. E.; LeNoue, S. R.; Roy, C. N.; Ashkenazi, S.; Williams, T. R.; Church, D. R.; Fuge, M. S.; Sreepada, K. N. *J. Solution Chem.* **2006**, *35*, 605–624.

(9) Bates, R. G.; Roy, R. N.; Robinson, R. A. *Anal. Chem.* **1973**, *45*, 1663–1666.

(10) Roy, R. N.; Roy, L. N.; Stegner, J. M.; A.Sechler, S.; Jenkins, A. L.; Krishchenko, R.; Henson, I. B. *J. Electroanal. Chem.* **2011**, *663*, 8–13.

(11) Roy, R. N.; Roy, L. N.; Ashkenazi, S.; Wollen, J. T.; Dunseth, C. D.; Fuge, M. S.; Durden, J. L.; Roy, C. N.; ; Hughes, H. M.; Morris, B. T.; Cline, K. L. *J. Solution Chem.* **2009**, *38*, 449–458.

(12) Kakiuchi, T.; Tsujioka, N.; Kurita, S.; Iwami, Y. *Electrochem. Commun.* **2003**, *5*, 159–164.

(13) Kakiuchi, T.; Yoshimatsu, T. *Bull. Chem. Soc. Jpn.* **2006**, *79*, 1017–1024.

(14) Yoshimatsu, T.; Kakiuchi, T. *Anal. Sci.* **2007**, *23*, 1049–1052.

(15) Sakaida, H.; Kitazumi, Y.; Kakiuchi, T. *Talanta* **2010**, *83*, 663–666.

(16) Fujino, Y.; Kakiuchi, T. *J. Electroanal. Chem.* **2011**, *651*, 61–66.

(17) Shibata, M.; Sakaida, H.; Kakiuchi, T. *Anal. Chem.* **2011**, *83*, 164–168.

(18) Nishi, N.; Izawa, K.; Yamamoto, M.; Kakiuchi, T. *J. Phys. Chem. B* **2001**, *105*, 8162–8169.

(19) Debye, P.; Hückel, E. *Physik. Z.* **1923**, *24*, 185–206.

(20) Pitzer, K. S.; Roy, R. N.; Silvester, L. F. *J. Am. Chem. Soc.* **1977**, *99*, 4930–4936.

(21) Bates, R. G. In *Determination of pH*; Wiley: New York, 1973.

(22) *International Critical Tables, Vol. 3*; McGraw-Hill: New York and London, 1928.

(23) Henderson, P. Z. *Phys. Chem.* **1908**, *63*, 325–345.

(24) Kakiuchi, T.; Senda, M. *Bull. Chem. Soc. Jpn.* **1984**, *57*, 1801–1808.

(25) Kakiuchi, T.; Obi, I.; Senda, M. *Bull. Chem. Soc. Jpn.* **1985**, *58*, 1636–1641.

(26) Kakiuchi, T.; Tsujioka, N. *J. Electroanal. Chem.* **2007**, *599*, 209–212.

Chapter 7

Conclusions

A liquid junction potential (LJP) always exists at the interface between two solutions of different compositions.[1–6] In potentiometric measurement of pH, one needs to eliminate the LJP or maintain it constant. A concentrated KClSB has been employed for this purpose over a century.[7,8] However, the function of the KClSB is not always ideal.[9] First, the LJP is not cancelled out by a KClSB, particularly when the ionic strength of a sample solution is low. The intrinsic problems caused by flowing of a concentrated KCl solution in a sample solution are remained unsolved.[10–29] In this work, the author examined fundamental properties of the ILSBs and determined by use of an ILSB the activities of hydrogen ions in the aqueous solutions which are not determined accurately with a KClSB . However, many problems still remain unsolved. In this chapter, the fundamental properties of ILSBs and the results of pH determination by use of the ILSB are summarized and the remaining problems in the determination of single-ion activity of H^+ by use of an ILSB are discussed.

7.1 Fundamental Properties of ILSB and pH Determination by Use of an ILSB

As already mentioned, it is difficult to determine the activities of hydrogen ions in low ionic strength solutions by use of a KClSB. In chapter 1, the activities of hydrogen ions in dilute sulfuric acid solutions were estimated by use of TBMOEPC_2C_2N salt bridge within precision

of ± 0.03 pH unit (±95 % confidence interval) and with accuracy that the difference between the experimental and calculated pH values is 0.005 pH unit. The source of the remaining difference between experimental and calculated pH values can be explained by the residual diffusion potential due to the dissolution of TBMOEPC_2C_2N in the H_2SO_4 solution (W) and the resultant increase in the ionic strength of W. This results will give the solution to the problem which have not solved for a long time in geochemistry and environmental science. The results showed the LJP between sufficiently low ionic strength solution to apply D-H limiting law and higher ionic strength solutions can be canceled out and opened the way to determine accurately single-ion activity at higher ionic strength solutions.

Moreover, the activities of hydrogen ions in dilute sulfuric acid solutions were estimated by use of a glass combination electrode equipped with TBMOEPC_2C_2N salt bridge within precision of ± 0.004 pH unit (±95 % confidence interval) and with accuracy that the difference between the experimental and calculated pH values is 0.015 pH unit. The glass combination electrode equipped with an ILSB allows us to obtain accurate pH values of low ionic strength solutions with the same procedure as has been used in conventional glass electrodes with KCl-type reference electrode.

pH values of primary standard buffer solutions are determined by use of the Harned cell[30] . This pH determination includes the uncertainty associated with the estimation of ion size parameter of chloride ion. The author showed the possibility of a new pH scale by use of an ILSB. Our method is based on the activity in the sufficient low ionic strength solution to apply D-H limiting law. Therefore, this method based on an ILSB has the potential to determine exactly single-ion activity, once thought to be elusive and the subject of argumentation to date.[31–39]

The problem that the LJP between the IL and the sample solution shifts when the sample solution includes hydrophobic ions was examined experimentally, and then the range in application of ILSBs was revealed quantitatively.

7.2 Remaining Problems and Scope for Future Studies

The cell voltage of the electrochemical cell with the ILSB sandwiched by two hydrogen electrodes varied widely. The variation amounted to 0.6 - 1.2 mV (equal to 0.01 - 0.02 pH unit). However, the dispersion of pH values measured by use of a glass combination electrode equipped with a gelled ILSB was less than 0.01 pH unit. A possible reason for the variation of the cell voltage is the change of the standard Gibbs energy of transfer of ions constituting the IL due to the dissolution of water into the IL. In the gelled IL, the dispersion may be decreased because the solubility of water decreases due to the hydrophobicity of a PVdF-HFP. The improvement of dispersion of the cell voltage is expected by revealing the influence of the dissolution of water into the IL.

The difference between the experimental and calculated pH values at 0.025 mol kg^{-1} phosphate buffer solutions which is primary buffer recommended by IUPAC is about 0.01 pH unit. We need to illuminate the reason for the difference and design new ILSB. Moreover, in order to apply the ILSB to determination of single-ion activity in the wide range of concentrations, we need to clarify the reason for the difference between the experimental and theoretical pH values at higher ionic strength solutions.

For the inescapable dilemma between the single-ion activity and the LJP,[40–44] an ILSB showed the way to escape from the dilemma in pH determination of low ionic strength solutions. However, many problems remain unsolved in high ionic strength solutions and the aqueous solutions in which hydrophobic ions exist. We need to design the suitable ILSB to each fields.

References

(1) Nernst, W. *Z. Phys. Chem.* **1888**, *2*, 613–637.

(2) Nernst, W. *Z. Phys. Chem.* **1891**, *8*, 129–181.

(3) Planck, M. *Ann. Physik [3]* **1890**, *39*, 161–186.

(4) Planck, M. *Ann. Physik [3]* **1890**, *40*, 561–576.

(5) Negbauer, W. *Ann. Phys. Chem.* **1891**, *44*, 737–758.

(6) Helmholtz, H. *Ann. Phys. Chem.* **1878**, *3*, 201–216.

(7) Tower, O. F. *Z. Phys. Chem.* **1895**, *18*, 17–50.

(8) Bjerrum, N. *Z. Phys. Chem.* **1905**, *53*, 428–440.

(9) Kakiuchi, T. *J. Solid State Electrochem.* **2011**, *15*, 1661–1671.

(10) Galloway, J. N.; Cosby, B. J.; Likens, G. E. *Limnol. Oceanogr.* **1979**, *24*, 1161–1165.

(11) Midgley, D.; Torrance, K. *Analyst* **1979**, *104*, 63–72.

(12) Tyree, S. Y. *Atmos. Environ.* **1981**, *15*, 57–60.

(13) Brezinski, D. P. *Anal. Chim. Acta* **1982**, *134*, 247–262.

(14) Brezinski, D. P. *Analyst* **1983**, *108*, 425–442.

(15) Mcquaker, N. R.; Kluckner, P. D.; Sandberg, D. K. *Environ. Sci. Technol.* **1983**, *17*, 431–435.

(16) Johnson, C. A.; Sigg, L. *Chimia* **1985**, *39*, 59–61.

(17) Covington, A. K.; Whalley, P. D.; Davison, W. *Pure Appl. Chem.* **1985**, *57*, 877–886.

(18) Davison, W.; Woof, C. *Anal. Chem.* **1985**, *57*, 2567–2570.

(19) Davison, W.; Gardner, M. J. *Anal. Chim. Acta* **1986**, *182*, 17–31.

(20) Koch, W. F.; Marinenko, G.; Paule, R. C. *J. Res. Natl. Bur. Stand (U.S.)* **1986**, *91*, 23–32.

(21) Metcalf, R. C. *Analyst* **1987**, *112*, 1573–1577.

(22) Davison, W.; Covington, A. K.; Whalley, P. D. *Anal. Chim. Acta* **1989**, *223*, 441–447.

(23) Durst, R. A.; Davison, W.; Koch, W. F. *Pure Appl. Chem.* **1994**, *66*, 649–658.

(24) Ozeki, T.; Tsubosaka, Y.; Nakayama, S.; Ogawa, N.; Kimoto, T. *Anal. Sci.* **1998**, *14*, 749–756.

(25) Bates, R. G.; Vega, C. A.; D. R. White, J. *Anal. Chem.* **1978**, *50*, 1295–1300.

(26) Maas, A. H. J. *J. Appl. Physiol.* **1971**, *30*, 248–250.

(27) Maas, A. H. J. *Clin. Chim. Acta* **1970**, *28*, 373–390.

(28) Khuri, R. N.; Merril, C. R. *Phys. Med. Biol.* **1964**, *9*, 541–550.

(29) Dickson, A. G. *Mar. Chem.* **1993**, *44*, 131–142.

(30) Buck, R. P.; Rondinini, S.; Covington, A. K.; Baucke, F. G. K.; Brett, C. M. A.; Camoes, M. F.; Milton, M. J. T.; Mussini, T.; Naumann, R.; Pratt, K. W.; Spitzer, P.; Wilson, G. S. *Pure Appl. Chem.* **2002**, *74*, 2169–2200.

(31) Malatesta, F. *Fluid Phase Equilib.* **2005**, *233*, 103–109.

(32) Wilczek-Vera, G.; Vera, J. H. *Fluid Phase Equilib.* **2005**, *236*, 96–110.

(33) Malatesta, F. *Fluid Phase Equilib.* **2006**, *239*, 120–124.

(34) Malatesta, F. *AIChE J.* **2006**, *52*, 785–791.

(35) Wilczek-Vera, G.; Rodil, E.; Vera, J. H. *Fluid Phase Equilib.* **2006**, *244*, 33–45.

(36) Malatesta, F. *Chem. Eng. Sci.* **2010**, *65*, 675–679.

(37) Malatesta, F. *Fluid Phase Equilib.* **2010**, *295*, 244–248.

(38) Wilczek-Vera, G.; Arce, A.; Vera, J. H. *Chem. Eng. Sci.* **2010**, *65*, 2263–2264.

(39) Zarubin, D. P. *J. Chem. Thermodyn.* **2011**, *43*, 1135–1152.

(40) Harned, H. S. *J. Phys. Chem.* **1926**, *30*, 433–456.

(41) Taylor, P. B. *J. Phys. Chem.* **1927**, *31*, 1478–1500.

(42) Guggenheim, E. A. *J. Phys. Chem.* **1929**, *33*, 842–849.

(43) Guggenheim, E. A. *J. Am. Chem. Soc.* **1930**, *52*, 1315–1337.

(44) MacInnes, D. A.; Belcher, D.; Shedlovsky, T. *J. Am. Chem. Soc.* **1938**, *60*, 1094–1099.

List of publications

Chapter 1: **Determination of the Activity of Hydrogen Ions in Dilute Sulfuric Acids Using an Ionic Liquid Salt Bridge Sandwiched by Two Hydrogen Electrodes**
Manabu Shibata, Hideaki Sakaida, and Takashi Kakiuchi
Anal. Chem. **2011**, *83*, 164-168.

Chapter 2: **Potentiometric Determination of pH Values of Dilute Sulfuric Acids with Glass Combination Electrode Equipped with Ionic Liquid Salt Bridge**
Manabu Shibata, Makoto Kato, Yasukazu Iwamoto, Satoshi Nomura, and Takashi Kakiuchi
submitted for publication

Chapter 3: **Reexamination of the pH Values Assigned to Aqueous Phosphate Buffers for a Primary Standard of pH Determination**
Manabu Shibata and Takashi Kakiuchi
in preparation.

Chapter 4: **Determination of the Activity of Hydrogen Ions in Phosphate Buffer by Use of Ionic Liquid Salt Bridge at 5 - 60 °C**
Manabu Shibata and Takashi Kakiuchi
in preparation.

Chapter 5: **Stability of a Ag/AgCl Reference Electrode Equipped with an Ionic Liquid Salt Bridge Composed of 1-Methyl-3-Octylimidazolium Bis(trifluoromethanesulfonyl) amide in Potentiometry of pH Standard Buffers**
Manabu Shibata, Mikito Yamanuki, Yasukazu Iwamoto, Satoshi Nomura, and

Takashi Kakiuchi

Anal. Sci. **2010**, *26*, 1203-1206.

Chapter 6: **Determination of the Activity of Hydrogen Ions in Buffers Used for pH measurement of Physiological Solutions by Use of Ionic Liquid Salt Bridge**

Manabu Shibata and Takashi Kakiuchi

in preparation.

Acknowledgements

The author would like to express his sincere gratitude to Professor Takashi Kakiuchi for his valuable advice and many helpful suggestions throughout the course of this work.

The author is deeply grateful to Professors Takeshi Abe, Masashi Inoue, Masahiro Yamamoto, and Nobuaki Ogawa for their kind advice and useful comment and discussion.

Sincere thanks are expressed to Drs. Naoya Nishi, Ryoichi Ishimatsu, Yuki Kitazumi, and Satoshi Nomura for their kind support and fruitful discussion.

The author is thankful to Yasukazu Iwamoto, Mikito Yamanuki, and Makoto Kato for their valuable suggestions and advice and their technical support.

Finally, the author is indebted to all members of Professor Kakiuchi's research group and co-workers of HORIBA Ltd. for their many contributions to this work.